Quantitative proteomic and phospho-proteomic analysis of human DLD1 cells differing in ploidy and chromosome stability

Inauguraldissertation

zur Erlangung der Würde eines Doktors der Philosophie vorgelegt der Philosophisch-Naturwissenschaftlichen Fakultät der Universität Basel von

Cristina Viganò

Von Italien

Italy, 2019

Genehmigt von der Philosophisch-Naturwissenschaftlichen Fakultät

auf Antrag von

Prof. Dr. Erich A. Nigg

Prof. Dr. Michael N. Hall

Basel, 19 September 2017

The Dean of Faculty Prof. Dr. Martin Spiess

The experiments displayed in this thesis have been performed from May 2014 to October 2017 in the laboratory of Prof. Erich A. Nigg, at the Biozentrum (Growth & Development), University of Basel. I herewith declare that I am primarily responsible for the work described in this publication.

Parts of this thesis have been published in:

- Viganó C, Schubert v C, Ahrné E, Schmidt A, Lorber T, Bubendorf L, Venner d J, Zaman G, Storchova Z and Nigg EA. *Quantitative proteomic and phospho-proteomic comparison of human DLD-1 cells differing in ploidy and chromosome stability.* Mol Biol Cell*. 29(9):1031-1047. Doi: 10.1091/mbc. E17-10-057.*

- Ahrné E, Glatter T, Viganò C, Schubert Cv, Nigg EA, Schmidt A. (2016) *Evaluation and Improvement of Quantification Accuracy in Isobaric Mass Tag-Based Protein Quantification Experiments.* J Proteome Res. 15(8): 2537-47. doi: 10.1021/acs.jproteome.6b00066.

- Domingues PH, Nanduri LS, Seget K, Venkateswaran SV, Agorku D, Viganó C, von Schubert C, Nigg EA, Swanton C, Sotillo R, Bosio A, Storchová Z, Hardt O. *Cellular prion protein PRPC and ecto-5'-nucleotidase are markers of a cellular stress response to aneuploidy.* Cancer Res. 2017 Apr 4. pii: canres.3052.2016. doi: 10.1158/0008-5472.CAN-16-3052.

Figure 12 has been performed in collaboration with Prof. Dr. Zuzana Storchova from Max Planck Institute for Biochemistry (München); and Figures 20 and 21 have been performed with Dr. Thomas Lorber from the Pathology Institute, University of Basel (Basel); and Figures 48 and 51 have been performed with Dr. Guido Zaman and Judith de Venner from Netherlands Translational Research Center (Oss).

Proteomic and phospho-proteomic experiments were performed at the proteomic core facility (PCF) of the Biozentrum, with great help of Dr. Erik Ahrné (for data analysis) and Dr. Alex Schmidt (for mass spectrometry). FACS experiments were performed at the FACS core facility (FCF) of the Biozentrum,

under the supervision of Janine Bögli. Dr. Conrad von Schubert (Prof. Dr. Erich Nigg laboratory) helped me for extensive data discussions throughout the course of this study.

This thesis was supported by the Marie Curie Network **Ploidynet**, funded by the European Union Seventh Framework Programme (FP7/2007-2013) under Grant Agreement n° 607722.

Table of contents

1. Summary

Aneuploidy is a state in which cells harbor a chromosome number that is not a whole multiple of the haploid chromosome set. This condition is poorly tolerated during embryogenesis and it the cause of developmental disorders such as Down syndrome (trisomy 21). Beside, aneuploidy is often associated with whole chromosomal instability (CIN), a constant chromosome mis-segregation ongoing from one cell division to the next. Aneuploidy and CIN are a common hallmark of many cancers, even if to date, the cellular processes involved in aneuploidization and tumorigenesis are poorly understood. This raises the questions of how CIN originates, how it is tolerated at the cellular level, and which cellular pathways are involved in this tolerance. In order to try to solve these questions, I performed a comprehensive proteomic analysis of cancer cell lines with different karyotypic and chromosome stability states. I have compared stable isogenic diploid and tetraploid colon cancer cell lines with descendant unstable aneuploid post-tetraploid (PTAs) and engineered trisomic clones. By applying quantitative mass-spectrometric approaches, I was able to identify the relative abundance of around 7'500 and 6'000 proteins across PTAs and trisomic clones, respectively. Analysis of proteomic data allowed me to conclude that most changes of protein abundance and phosphorylation, present in aneuploid clones, already occur after chromosome mass increase, i.e. the transition to the tetraploid state, rather than the presence of CIN. In particular I observed the deregulation of pathways involved in protein folding, proteolysis and response to oxidative stress. Additionally, in order to identify possible modifications in protein activity, I performed phospho-enrichment analysis in the generated cell lines, and this resulted in the identification of 13'500 and 9'000 phospho-peptides in PTAs and trisomic clones, respectively. Importantly, while a large number of proteins previously associated with CIN and cell cycle remained largely unaltered in their expression levels (compared with the parental diploid line), their phosphorylation levels showed substantial difference. Most interestingly, I observed a higher phosphorylation state at specific activation sites of key mitotic protein kinases, notably Aurora A and Plk1. Consequentially, tetraploid and post-tetraploid clones showed similar sensitivity profiles in a chemotherapeutic drug screen, notably increased sensitivity to several Plk1 and Aurora A inhibitors.

These results suggest that in transformed cancer cells, a gain in chromosome number, rather than an increased chromosome mis-segregation rate, triggers a clonal stress response at the protein level. Moreover, these results indicate that chromosome gains lead to activation or deactivation of pathways involved in cell division and mitosis primarily through hyper- or hypo-phosphorylation, rather than massive changes in protein expression. Being able to identify deregulated pathways in response to chromosome mass increase or instability may provide new opportunities to specifically targets cancer cells and block disease progression. Results from our drug screening approach, although preliminary, support this notion. They suggest that a common sensitivity profile may exist across aneuploid and polyploid cells, raising the prospect of new treatment strategies for tumors harboring a large excess of chromosomes.

2. Introduction

Each time that a cell divides the whole genome has to be precisely duplicated and faithfully segregated into the daughter cells. If this process fails, the two resulting cells may carry too many or too few chromosomes, a condition called aneuploidy. Chromosome segregation is monitored by the mitotic checkpoint; also known as spindle assembly checkpoint (SAC) that ensures the faithful and correct chromosome segregation in mitosis.

2.1 Chromosomal abnormalities

The eminent biologist T. Boveri reported more than a century ago the detrimental effects of aneuploidy in sea urchin organogenesis [1] and the deleterious effects of additional chromosomes has subsequently been confirmed in many different organisms [2-4](Eduardo M. Torre, 2007)(Williams et al 2008)(Segal and Mc Coy, 1974). In yeast, aneuploid strains show a series of chromosome dependent specific phenotypes, but share as well numerous common features, such as a reduction of cell proliferation and cell fitness, increased glucose uptake, increased sensitivity to conditions interfering with protein synthesis and protein folding [2](Eduardo M. Torres, 2007). Mouse embryonic fibroblasts (MEFs) from trisomic mice (trisomy 1, 13, 16, 19) show similar results [3](Williams et al 2008). To date, aneuploidy in humans is considered as the primary cause of miscarriage and mental retardation. For example, primary fibroblasts from Down syndrome patients (trisomy 21) show growth defects and premature aging [4](Segal DJ and Mc Coy, 1974). The collectivity of all these shared phenotypes across species, related to aneuploidy condition, has been called by several authors “aneuploidy stress response” [5](Torres, Cold Spring Harb. Symp Quant Biol 2010).

Although aneuploidy interferes with proliferation of normal cells, it is an almost universal feature in cancer cells and contributes to the tumor heterogeneity and thus to tumor evolution. Moreover, aneuploidy often correlates in cancer cells with the presence of CIN, described as dynamic changes in chromosome number during propagation [6-8](Haruki et al., 2001) (Lengauer et al., 1997) (Yoon et al., 2002). However, whether aneuploidy and CIN are a cause or a consequence of tumorigenesis remains debated. Clinical studies show that CIN is associated with resistance to cancer drug treatment and poor prognosis, most likely due to the formation of new karyotypes that

confer a selective advantage under specific conditions [9-11](Carter et al., 2006) (Duesberg et al., 2000) (Walther et al., 2008). However, other studies indicate that extreme CIN is associated with better clinical outcomes. It has been suggested that an excess of instability may surpass a threshold compatible with cell viability, thus impairing tumor fitness and growth [12](Nicolai J. Birkbak, 2011 Cancer Research). Therefore, aneuploidy may have tumor-suppressor as well as tumor-promoting effects, which could differ depending on the genetic background [13-15](Silk AD Proc Natl Acad Sci USA 2013) (Weaver BA 2009 J Cell Biol) (Weaver BA 2008 Cancer Cell) (Weaver BA Cancer Cell 2007). In conclusion, it is clear that the effects of aneuploidy on cells and organisms are complex, and further studies are required to fully understand their impact.

2.2 Roads to aneuploidy

In order to better understand the different ways that can lead to aneuploidy, it appears necessary to distinguish between whole chromosome aneuploidy and structural aneuploidy. Whole chromosome aneuploidy reflects both gains and losses of entire chromosomes, whereas non-balanced rearrangements of chromosomes, such as deletions, amplifications or translocations of large regions of the genome result in structural aneuploidy [16](Bernardo Orr, 2015 current Biol). Structural aneuploidies likely result from errors in DNA replication and repair, even though the mechanisms are not yet fully understood. (Fig 1). It is important to mention that these processes do not happen in a mutual exclusivity but in a duality relation. For example, structural aneuploidy may cause whole chromosome aneuploidy and *vice versa*.

In this section I will focus on the processes that lead to whole chromosome aneuploidy, such as SAC defects, errors in kinetochore-microtubule (k-MT) attachment, cohesion defects, supernumerary centrosomes and tetraploidy (Fig 1).

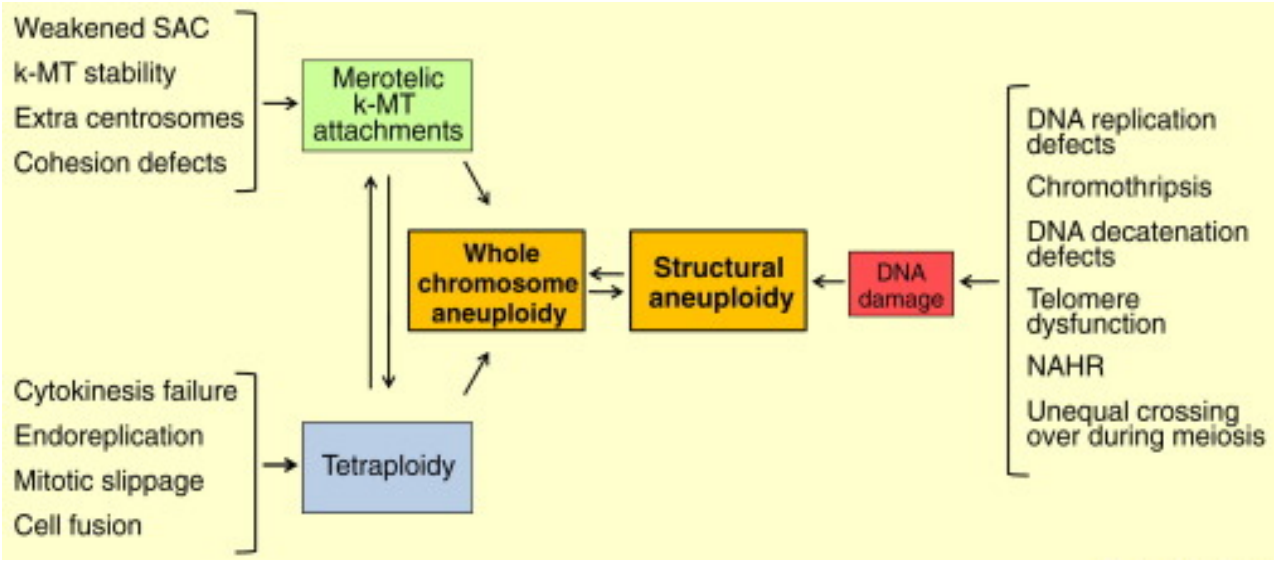

Figure 1. Mechanisms that generate aneuploidy. Schematic representation of the cellular mechanisms that generate whole chromosomal aneuploidy and structural aneuploidy. Bi-directional arrows illustrate the duality relation between events. For example, the formation of merotelic k-MT attachments and the induction of tetraploidy (from [16]Bernardo Orr, 2015 current Biol).

2.2.1 Mitotic checkpoint defects

Proper chromosomes segregation depends on various mitotic processes, notably spindle formation, bi-polar attachment of all chromosomes on the spindle apparatus and successful cytokinesis. I will discuss k-MT attachments in some detail in the next section, but, in brief, chromosomes attach to spindle microtubules at specialized protein structures known as kinetochores (KT), which are assembled on centromeric chromatin early in mitosis. Microtubules can coordinate plus-end dynamics in order to generate the forces required for both chromosome movements and to silence the spindle assembly checkpoint, allowing mitotic exit [17](DeLuca J, Curr Opin Cell Biol 2012).

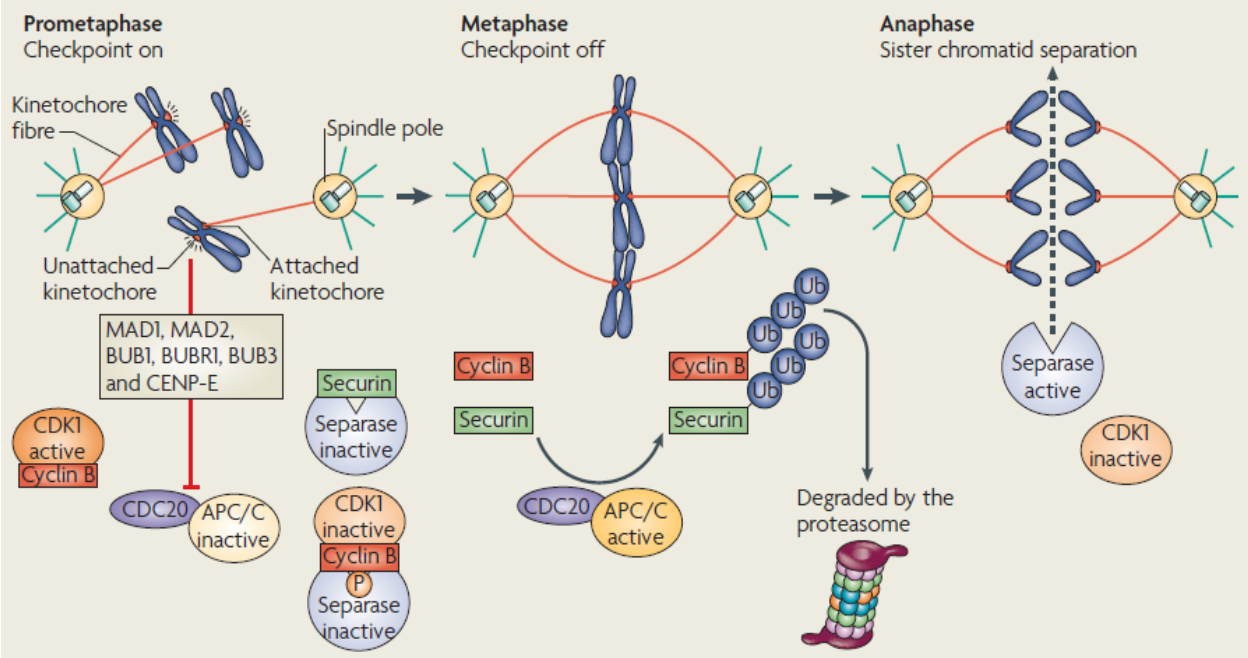

Figure 2. The mitotic checkpoint: a safeguard to protect against aneuploidy. Microtubules nucleated by the centrosomes form bilaterally symmetrical mitotic spindle. The bi-orientation process makes sure that sister chromatids are pulled in opposite directions, through the attachment of kinetochores to the microtubules arising from the opposite spindle poles. Errors in this process lead to the mis-segregation of chromosomes and the production of aneuploid daughter cells. The SAC supervises these all processes and makes sure that correct chromosome segregation occurs and it delays the onset of anaphase if even only one single chromosome is not properly attached and bi-oriented (from [1]Andrew J. Holland and Don W. Cleveland July 2009 Nature Reviews).

The key player of the SAC is the microtubule checkpoint complex (MCC), formed by mitotic-arrest deficient homologue-2 (MAD2), budding uninhibited by benzimidazole related protein 1 (BUBR1), BUB3, and cell division cycle 20 (CDC20). This complex acts together with other core components, such as BUB1, multipolar spindle-1 (Mps1), MAD1, Aurora B and centromere protein E (CENP-E). When the SAC is turned on, these proteins are enriched at the unattached or incorrectly orientated kinetochore and catalytically generate a diffusible signal that inactivates an E3 ubiquitin ligase, the anaphase promoting complex/cyclosome (APC/C), and its co-activator CDC20 (Fig 2). The SAC inhibits the ability of CDC20 to activate the APC/C-mediated polyubiquitylation of two key substrates, cyclin B and securin, thereby preventing their destruction by the 26S proteasome. Sister chromatids are kept together by cohesin rings and premature separation is avoided by the chaperone securin and the complex cyclin-dependent kinase 1 (CDK1)-cyclin B

that keep the separase inactive. When the correct attachment and alignment of all the chromosomes at the metaphase plate is reached, the spindle assembly checkpoint signal is silenced. Only after the ubiquitylation of securin and cyclin B by APC/C and consequentially their proteasome–mediated degradation, separase is activated and anaphase can initiate. At the same time, the progressive degradation of cyclin B inactivates CDK1, thereby promoting exit from mitosis (Fig 2) [18](Musacchio and Salmon 2007).

Consequently, deregulation of the SAC as well as the spindle architecture can lead to chromosome segregation defects and aneuploidy. An impaired capacity to sustain the SAC, due to deregulation of mitotic proteins, can lead to aneuploidy as observed in several tumors (Table 1) [19](Beth AA Weaver, Current Opinion in Cell Biology 2006). In agreement, both *in vivo* and *in vitro* experiments, confirm an impaired checkpoint and a consequent aneuploidy formation in mice and human cells. In detail, Bub3 null mice show embryonic lethality at day 8.5, whereas heterozygous mice are viable and show increased rates of premature sister chromatid separation and chromosome mis-segregation [20](J.R. Babu, J Cell Biol, 2003). Similar results were obtained with mice heterozygous for BubR1 [21](D.J. Baker, 2003 Nat Genet,) or overexpressing Mad2 [22](Sottillo R. 2007 Cancer Cell).

Genes preventing aneuploidy that are mutated and/or misregulated in human cancers.

Gene	Primary function	Mutated in, frequency, reference	Upregulated in, frequency, reference	Downregulated in, frequency, reference
BUB1	Mitotic checkpoint	Colorectal, 2/19, [16] Colorectal, 1/31, [78] Colorectal, 1/1, [76] Leukemia (ATLL), 4/10, [79] Leukemia (T lymphoblastic), 2/2, [80] Lung, 1/60, [81] Lung, 1/88, [82] Thyroid, 1/27, [77]	Barrett's oesophagus (precancercous), 12/33, [48] Breast, 20/21, [83] Gastric, 36/43, [84] Gastric, 8/20, [84,85] Melanoma, 21/30, [86] Leukemia, (t-AML), not specified, [87] Oesophageal, 1/4, [48]	Barrett's oesophagus (precancerous), 9/33, [48] Colorectal, 10/110, [78] Gastric, 4/20, [85] Oesophageal, 1/4, [48]
BUBR1	Mitotic checkpoint	Colorectal, 2/19, [16] Lymphoma, 1/8, [79] MVA[a], 5/8, [56] MVA, 6/6, [57]	Breast 20/21, [83] Gastric, 29/43, [84] Lung, 8/8, [88]	Colorectal, 10/116, [78] Thyroid, 3/8, [77]
BUB3	Mitotic checkpoint		Breast, 18/21, [83] Gastric, 34/43, [84] Lung, 5/18, [89]	Breast, 2/21, [83] Lung, 7/18, [89]
MAD1	Mitotic checkpoint		Breast, 16/17, [83] Lung, 13/14, [90]	Nasopharyngeal, 3/5, [74] Leukemia (ATL), 6/6, [66]
MAD2	Mitotic checkpoint	Breast, 1/22, [91] Breast, 1/1, [68] Gastric, 23/54, [92]	Barrett's oesophagus (precancerous), 8/33, [48] Bladder, not specified, [93] Breast, 3/13, [83] Breast, 15/21, [83] Colorectal, not specified, [94,95] Neuroblastoma, not specified, [93] Oesophageal, 1/4, [48]	Barrett's oesophagus (precancerous), 8/33, [48] Breast, 5/21, [68,83] Hepatocellular carcinoma, 5/10, [96] Hepatoma, 6/11, [71] Leukemia (ATL), 2/6 [66] Nasopharyngeal, 3/5, [74] Oesophageal, 2/4, [48] Ovarian, 3/7, [75]

Table 1. Frequent impairment of the mitotic checkpoint in human cancers [19](Beth AA Weaver, Don W Cleveland Current Opinion in Cell Biology 2006).

In human cells, it has been shown that overexpression of Mad2 leads to the hyperstabilization of k-MT attachments, decreasing the efficiency of error correction, thus leading to chromosome mis-segregation and aneuploidy [23](Kabeche L. 2012 Curr Biol). Similar results were reported for human breast cancer tumors overexpressing Mad1 [24](Ryan et al., 2012). All these results suggest that levels of every spindle component must be tightly regulated to prevent aneuploidy and transformation and that de-regulation may promote tumors.

By contrast, complete inactivation of the SAC is lethal in different cell lines and homozygous deletion of key checkpoint components causes embryonic lethality in mice [25,26](Janssen A, 2009, Proc Natl Acad Sci USA) (Thompson et al., 2010). Moreover, even though mutations of SAC components, leading to checkpoint inactivation, have been found in different tumor types, these mutations are not commonly seen, probably because massive chromosome mis-segregation triggers cell death [19](Beth AA Weaver, Current Opinion in Cell Biology 2006). Contrarily, some CIN cancer cell lines show a rather robust SAC response to spindle poisons [27](Tighe A, EMBO 2001); moreover, in CIN cell lines, anaphase onset is blocked in the presence of misaligned chromosomes [28](Gascoigne and Taylor, 2008). All these indications show that upon mutation in SAC proteins that lead to checkpoint defects, the cell fates and the raising of aneuploidy are not predetermined.

Therefore aneuploidy is not necessarily associated with SAC impairment and the role of the SAC response in the common occurrence of CIN and cancer is largely debated in the field.

2.2.2 Microtubule attachment defects

As mentioned before, in order to segregate correctly the duplicated chromosomes, the sister KTs must be attached to microtubules from opposing spindle poles. The bi-oriented attachment is called amphitely. However, the initial attachment of microtubules to KTs is stochastic and error prone. During this process different incorrect attachments can be generated, such as monotelic, syntelic and merotelic, and these need to be solved (Figure 3). Monotelic attachments are a normal condition during prometaphase before bi-orientation. In syntelic attachments, both sister chromatids attach to the same

pole. In these two cases, cells experience a lack of tension between sister chromatids that generate a "wait signal" and the consequent SAC activation. Merotelic attachments occur quite frequently as well, but in this case the SAC is unable to detect them, due to the presence of tension between chromatid sisters. Activated SAC arrests cells in prometaphase to allow correction of the attachment.

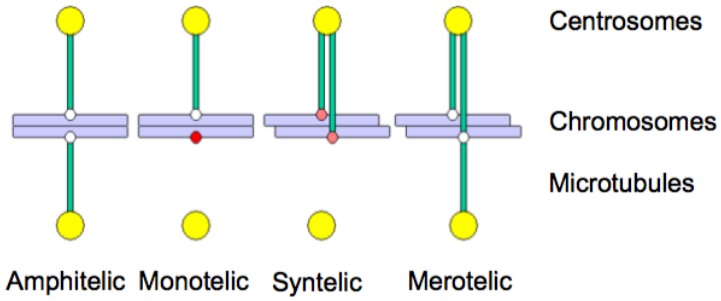

Figure 3. Scheme showing different attachment configurations between chromosomes and microtubules. (From Maiato, H 2004 The Journal of Cell Biology)

The KT is a large macromolecular structure assembled at sites of centromeric heterochromatin and composed by an inner and outer part (Fig 4). The inner KT proteins, called Centromeric Proteins (CENPs), are associated with the centromeric chromatin containing the histone H3 variant centromere protein A (CENP-A) [29-31](Earnshaw WC. 2015 Nature Reviews Molecular Cell Biology) (Bungo Akiyoshi 2012 Chromosoma) (Musacchio A. 2017 Biolosy). The outer KT components are 10 highly conserved proteins forming the KMN "network", composed of the KNL1 complex, formed by kinetochore null protein 1 (Knl1) and ZW10 interacting protein (Zwint-1); the MIS12 complex including Mis12, Dsn1, Nsl1, and Nnf1; and the NDC80 complex with Ndc80/Hec1, Nuf2, Spc24, and Spc25 (Fig 4) [17,32](DeLuca J. Curr Opin Cell Biol 2012) (Godek K, Nature Reviews Molecular Cell Biology 2015). In addition to core KT components, many regulatory proteins also localize to kinetochores, such as spindle checkpoint proteins, microtubule-associated proteins (MAPs), motor proteins, mitotic kinases and phosphatases.

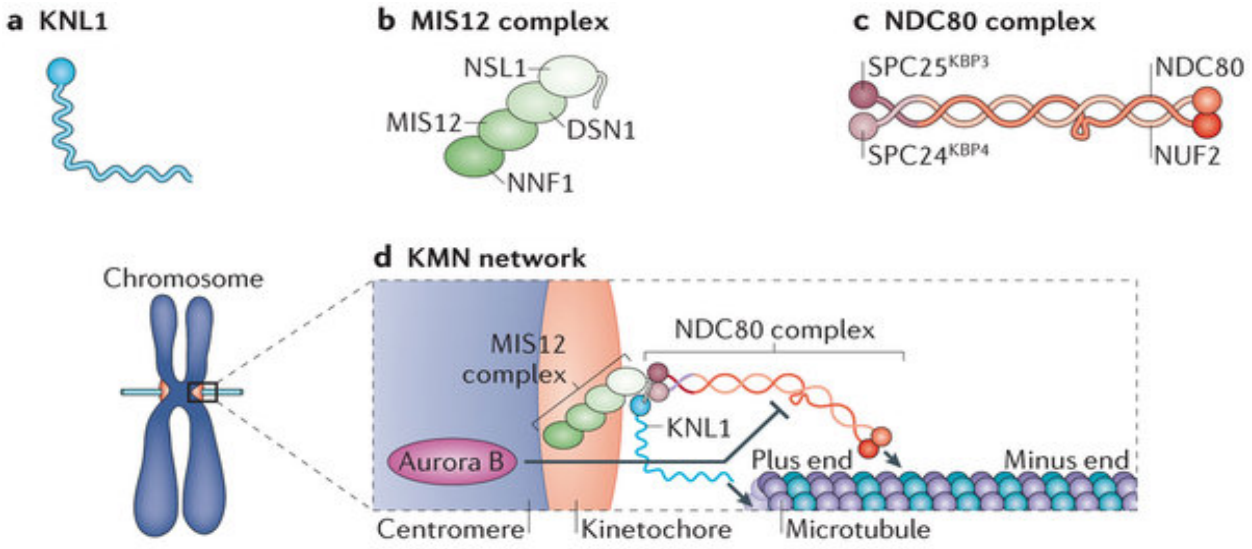

Figure 4. Scheme showing KT structure. Some components are direct targets of Aurora B kinase phosphorylation as indicated (DSN1, KNL1 and NDC80), while arrows indicate the direct k-MT binding site (from Godek K, DA Compton. Nature Reviews Molecular Cell Biology 2015).

Erroneous attachments are corrected through repeated cycles of microtubule attachments/detachments at KTs. Only when correct attachment is achieved is the SAC satisfied and the cell can progress through anaphase. A key complex responsible of k-MT attachment correction is a group of proteins forming the Chromosome Passenger Complex (CPC), with Aurora B as its catalytic component. Once released, the unattached KT triggers the SAC response that in turn delays mitotic progression until the error is corrected. CPC is composed of Aurora B, together with Survivin, Borealin and inner centrome protein (INCENP) [33](Ruchaud et al., 2007). A common concept is that Aurora B, a serine-threonine kinase, phosphorylates proteins localized in the outer KMN network (Fig 4) to destabilize and facilitate the release of erroneous attachments [34](Welburn J.P.I. 2010 Mol Cell). According to one plausible model, Aurora B creates a gradient of phosphorylation at the inner KT, thus in the absence of tension, KT substrates are phosphorylated because they are in close proximity to Aurora B at the inner centromere [35](Liu Dan 2009 Science). The released KT can eventually be reattached by a microtubule fiber from the correct pole and tension is restored, thereby satisfying the SAC and allowing progression toward anaphase. Sister KTs are thus pulled toward opposite directions, away from the inner centromere, so that KT substrates are dephosphorylated and the attachment is stabilized [35,36](Liu Dan 2009 Science) (Wang E 2011 JCB).

Thus, Aurora B deregulation leads to defects in chromosome segregation. It has been shown that cells down-regulating this protein undergo premature anaphase onset without proper alignment [37](Martin-Luesma S. 2002 Science). Moreover, overexpression of Aurora B it has been observed in many tumors showing CIN [38](Lin et al 2010).

However, the SAC does not always detect improper k-MT attachments, and if these are not corrected by anaphase onset, the probability of chromosome mis-segregation increases, resulting in whole chromosome aneuploidy. Furthermore, during cell division chromosomes with unresolved merotelic attachments frequently get trapped in the cleavage furrow, leading to chromosome breakup and consequentially structural chromosome aberrations.

In summary, alterations in the k-MT errors correction machinery and KT defects, in particular through Aurora B kinase deregulation, are frequently linked to CIN [39](Giet et al., 2005; Katayama et al., 1999). However, the role of Aurora B and CPC proteins in carcinogenesis remains elusive, as mutations in this machinery are rather rare in cancer.

2.2.3 Chromosome cohesion defects

Sister chromatids are kept together by a protein complex which is known as the cohesin complex, established during DNA replication [40](Michaelis, C. *Cell* 1997). Its ring structure is composed of a pair of rod-shaped proteins, structural maintenance of chromosomes protein 1 (Smc1) and Smc3, that form V-shaped heterodimers with ATP-binding cassette (ABC) -like nucleotide-binding domains, at the end of each arm, interconnected by a subunit called Scc1 (also known as Mcd1 or Rad21) and Scc3 (known in mammalian cells as SA1 and SA2) [41](Gruber, Stephan 2003 *Cell*.) (Fig 5). Several other proteins are essential for cohesion's association with chromosomes, but not for its maintenance after DNA replication, such as Scc2 (known as Nipbl in mammalian cells) and Scc4 [42](Kim Nasmyth and Christian H. Haering 2009 Annual Review of Genetics). In addition, many other proteins are necessary to regulate cohesion efficiency, such as polo-like kinase 1 (Plk1), Aurora B and Serine/threonine-protein phosphatase 2A (PP2A) [43-46] (Waizenegger et al. 2000) (Losada et al. 2002) (Sumara et al. 2002) (Gimenez-Abian et al. 2004).

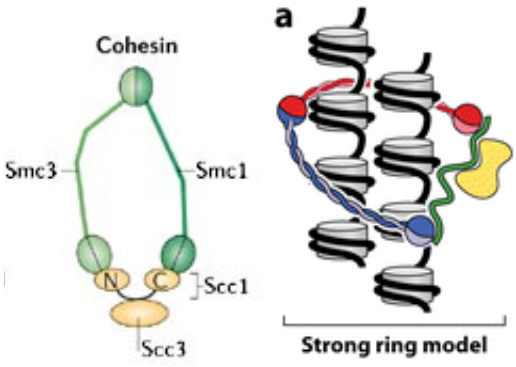

Figure 5. Scheme showing Cohesin structure [47](Raquel A. Oliveira, Kim Nasmyth. 2010 Biochem Soc Trans).

As mentioned above, sister chromatids are held together starting from the time of DNA duplication in S phase until the SAC is satisfied and cohesin are cleaved to allow anaphase onset. By keeping sister chromatids together, cohesin prevents premature sister chromatid separation and extensive chromosome mis-segregation. Moreover, by counteracting the spindle pulling forces, cohesion between the two sisters generates the tension necessary to stabilize k-MT attachments [47](Raquel A. 2010 Biochem Soc Trans). An important player required to protect centromere cohesion is shugoshin that in vertebrates counteracts cohesin dissociation [48](Clift D 2011 Cytogenet Genome Res). Thus sister chromatid cohesion is indispensable for chromosome segregation and defects in this system are potential causes of mis-segregation. For example, CIN cell lines show often impairment in the integrity of the conserved inner centromere-shugoshin network [49](Tanno Y, 2015 Science) and SGO1 haploinsufficiency causes enhanced CIN, pre-neoplastic lesions and tumorigenesis in mice [50](Yamanada HY 2012 Cell Cycle). Moreover mutation in STAG2/Scc3 promotes chromatid cohesion defects and aneuploidy [51,52](Solomon DA 2011 Science) (Djos A, BMC Med Genet. 2013). Besides, Scc1-deficient cells frequently fail to complete metaphase chromosome alignment and show chromosome segregation defects [53](Morrison C 2003 Biochem Soc Trans). Taken together, the levels of cohesin complex proteins and their cofactors should be tightly regulated to ensure chromosome segregation fidelity.

2.2.4 Supernumerary centrosomes

Centrosomes are responsible for the assembly of cilia and the formation

of the mitotic bipolar spindle. Each centrosome comprises two centrioles, barrel-shaped structures that, in humans, are composed by microtubule triplets assembled in a typical nine-fold symmetry. Centrosomes are surrounded by an amorphous mass of dense material, called pericentriolar material (PCM). The correct centriole number in proliferating cells is guaranteed at several levels: the centriole duplicates once and only once in every cell cycle and exactly one new centriole forms next to every pre-existing centriole. Thus, different mechanisms can be the source of centrosome amplification: centrosome overduplication, abortive cell division, cell fusion and *de novo* centriole formation [54](E.A. Nigg, Nat. Cell Biol. 2011). It is important to note that while the presence of extra centrosomes is a serious problem during cell division, centrosomes are not strictly required for mitosis in many cell types, even though they are often active participants in the process [55](Basto, R. et al. Cell 2006).

Independently from the cause, centrosome overduplication can result in massive chromosome mis-segregations due to the increased probability to form multipolar spindles that often lead to aneuploid daughter cells [56](EA Nigg 2002). Possible outcomes of a multipolar spindle are the balanced or unbalanced chromosome repartition. In the first case cells can progress through anaphase in a tripolar manner (the most frequent type of multipolar anaphase), where each of the daughter nuclei gets nearly a third of parental DNA material, thus resulting in severely compromised viability [57-60](Ganem et al. 2007) (Genem et al 2009) (Kwon et al. 2008) (Gisselsson et al., 2010). Meanwhile, in the second case the unbalanced multipolar chromosome segregation is often followed by an asymmetric cytokinesis, resulting in overall diploid daughter cells carrying many trisomies and monosomies. Moreover daughter nuclei formed during unbalanced multipolar division frequently displayed sister chromatid non-disjunction and poorly viable nullisomies [60,61](Sansregret, 2017 Cold Spring harb perspect med) (Gisselsson et al., 2010). For this reason is not surprising that centrosomes clustering mechanisms operate in cancer cells to suppress the multipolar cell division. The clustering leads to the reduction of spindle pole numbers, resulting in pseudo bipolar spindle formation, which then decreases the probability of nullisomies, monosomies or trisomies [62,63](Brinkley BR. 2001 Trends Cell Biol.) (Drosopoulos K 2014 Nat Commun). In this way progeny after multipolar mitosis could limit the detrimental effects of a multipolar division [64](Basto R 2008 Cell). Finally, even if bipolar clustering and cytokinesis are at

the end successful, transient multipolar spindles formed during mitosis greatly increase the formation rate of merotelic k-MT attachments, resulting in increased chromosome mis-segregation rates (Fig 6.) [58,65](Ganem et al., 2009) (Silkworth et al., 2009).

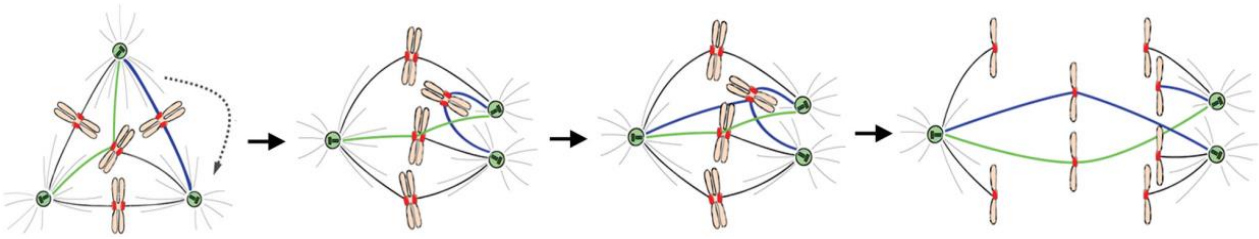

Figure 6. The formation of lagging chromosomes in anaphase could be due to an accumulation of unresolved merotelic k-MT attachments due to the extra centrosome [58](Ganem et al., 2009).

Thus, supernumerary centrosomes and multipolar spindles are observed early in the development of many tumors and often correlate with advanced tumor grade and poor clinical outcome [66-69](Godinho and Pellman, 2014) (Nigg and Raff, 2009) (Nigg, 2006) (Oncol Rep. 2015 Telentschak S) (Figure 6). Moreover centrosome abnormalities correlate with chromosome aberrations even though a relation of causality has not yet been proven.

Since a long time, the relation between loss of p53, a transcription factor that causes cell-cycle arrest or apoptosis in response to DNA damage, and centrosome aberrations has attracted great interest [70](Fukasawa, Science 1996). Originally, it has been proposed that loss of p53 could directly cause centrosome overduplication [71](Tarapore, P. Oncogene 2001), but more likely is an involvement of p53-dependent checkpoints in the elimination of cells that emerge from aborted divisions [63,72](Borel, F. Proc. Natl Acad. Sci 2002) (Drosopoulos K 2014 Nat Commun.) Supporting this idea, analysis of brains in p53–/– mice revealed that these animals have normal centrosome numbers [73](Marthiens V, 2013 Nat. Cell Biol.). A good example of how loss of p53 could enhance centrosome amplification is represented by high-risk human papillomavirus (HPV)-associated tumors. HPV-16 E7 protein disrupts normal centriole duplication, inducing centrosome amplification through a process that involves increased mRNA levels of the key centriole duplication factor Plk4 [74](Korzeniewski N, mol cancer 2011). At the same time Plk4 mRNA levels are negatively regulated by p53, thus, loss of p53 could potentially contribute to centrosome amplification through increased levels of Plk4 [75](Li J, Neoplasia

2005).

To summarize, centrosome amplification represents one of the common mechanisms of CIN generation/induction. However, the fact that increased centrosome number is not maintained for a long period after formation argues against the role of extra centrosomes as the exclusive triggers of CIN.

2.2.5 Tetraploidization

Polyploidy (triploidy, tetraploidy and so on) occurs very frequently in plants and fungi and is thought to generate mutations that would favor adaptations to environmental changes [76](Aleza et al 2011). Polyploidy also appears to be frequent during evolution; genome sequencing suggests that many contemporary genomes, including genomes of higher vertebrates, evolved from ancient genome duplications [77](M.Kellis Nature 2004). In animals, polyploidy occurs mainly in lower forms, such as flatworms and rarely in higher forms such as *Xenopus laevis* [78](Gallardo et al 1999). In humans, polyploidy occurs in some somatic cells and it mostly takes place during developmentally programmed processes, notably in trophoblasts, hepatocytes, human heart muscle cells and megakaryocytes [79](Guidotti et al 2003).

A duplication of the genome can also occur aberrantly and, even if unscheduled polyploidy is poorly tolerated by mammalian organisms, it is frequently observed in human cancers [80](Storchova and Kuffer, 2008). As mentioned before, abortive cell division or cell fusion, both resulting in genome doubling, can cause supernumerary centrosomes. Yet, supernumerary centrosomes then promote aberrant mitotic divisions and chromosome mis-segregation. Thus, tetraploidy is an unstable state that can potentially promote further aneuploidy and instability. Tetraploidy is found in early stages of several tumors, and documented in 37% of cancers, moreover a significant proportion of solid tumors (11-64%) show evidence of genome duplication events [81](2013 Nat Genetics Zack TI, et al.). A further link comes from the observation that tetraploid cells lacking p53 can initiate tumors in mice, while diploids do not [82](Fujiwara T, et al. Nature. 2005). Notably these tumors displayed near-tetraploid aneuploidy with chromosome gains and losses as well as structural chromosome rearrangements, implying that tetraploidization can initiate chromosomal instability [57](Ganem Neil J 2007 Current opinion in Genetics & development). A later study further confirmed

the role of tetraploidy in tumorigenesis in mice: upon prolonged cell passaging *in vitro*, diploid mouse ovarian surface epithelial cells (MOSEC) underwent cytokinesis failure with a high frequency, forming tetraploid cells and, subsequently, aneuploid cells [83](Lv et al., 2012). The intraperitoneal injection of aneuploidy cells (late passages) into C57BL/6 mice induced tumor formation on the intestinal surface, whereas injection of diploids (early passages) did not. Of note, the p53 status in the cells from resulting tumors was not investigated. Thus, possible p53 pathway deregulation likely allowed the proliferation in an aneuploid state and tumor growth.

Experimentally generated tetraploid cells often fail to propagate, as these cells arrest in G1 in a p53-dependent manner [26,84](P.T. Stukenberg J Cell Biol. 2004) (S.L. Thompson, D.A. Compton J.Cell Biol. 2010). A recent study supports the concept that changes in p53 regulation could favor the capacity of tetraploid clones to proliferate after chromosome mis-segregation. In particular colon cancer microsatellite instable (MIN) HCT116 cells, upon tetraploidization, exhibit a CIN positive phenotype, as well as deregulation of p53 signaling. Even though the idea of a "tetraploidy checkpoint" is appealing, studies suggest that there might not be a ploidy-sensing checkpoint that necessarily arrest tetraploidy cells in G1 [57,85,86](Ganem Neil J. 2007 Cell) (Mar Soto 2017 Cell reports) (Santaguida S 2017 Dev cell). Supporting this idea is the fact that normal hepatocytes for instance are capable of proliferation, [79](Guidotti et al 2003). Moreover, Uetake and Sluder found that upon treatment with low doses of DCB (dihydrocytochalasin B) tetraploid cells did not necessarily undergo to cell cycle arrest or delay in G1 [87](Y.Uetake J cell biol 2004). In the next section I will present the role of p53 response to chromosome mis-segregation and aneuploidy in more detail.

In summary, evidence suggests an oncogenic potential of transient tetraploidy and an association of transient tetraploidy with complex aneuploidy and CIN, even if little is known about the molecular mechanisms underlying this transition.

2.3.1 Short and long term consequences of chromosome mis-segregation and aneuploidy.

Aneuploidy in somatic cells is a rare event but, when it occurs, the effects on health are dramatic. Below, I summarize the current understanding of the immediate and long-term effects of chromosome mis-segregation and

aneuploidy. I will explore in particular the effect of the *aneuploidy-associated stresses*, a mixture of common features and traits, such as transcriptional and post-transcriptional responses and proteotoxic stress, that collectively are responsible for the effects on cellular fitness [88-90](Santaguida S et al. Genes Dev. 2015) (Dominigues PH Cancer Res 2017) (Torres EM 2008 Genetics).

2.3.1 DNA damage

Chromosome mis-segregation can impact on chromosome integrity. In fact, chromosomes that mis-segregate are frequently damaged during cytokinesis (Fig 7). As defined above, merotelic attachments are formed when microtubules, from opposite spindle poles, attach to the same KT. This incorrect attachment can cause the chromosomes to lag in the midzone during anaphase. Similarly, lagging chromosomes can be trapped in the cytokinetic furrow and broken during cytokinesis, or enclosed within micronuclei. In either case, the mis-segregated chromosome is going to be damaged. The cytokinesis-induced DSBs can cause the separated parts of the broken chromosomes to end up in distinct daughter cells, providing a platform for an unbalanced translocation event [91](A. Janssen 2011 Science). Moreover, DSBs can trigger DNA double-strand break responses in the respective daughter cells, involving ATM, Chk2, and p53. Besides, new-formed micronuclei undergo defective and asynchronous DNA replication, resulting in DNA damage and often in an extensive fragmentation of the chromosome in the micronucleus. Finally, the micronuclei persist normally during several generations, but they can be reintegrated as well into one of the daughter cell [92](K. Crasta 2012 Nature).

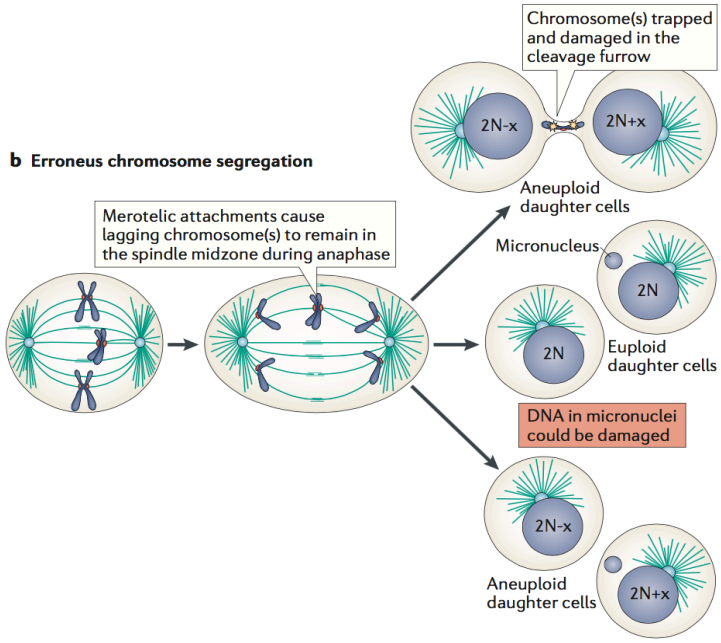

Figure 7. Merotelic attachments lead to lagging chromosomes, which can be trapped in the cytokinetic furrow and break during cytokinesis or, alternatively, form their own micronucleus, which is either accurately segregated (middle) or mis-segregated (bottom). Adapted from *S. Santaguida and A. Amon* 2015 Nature Review.

The complex chromosomal rearrangements that form in micronuclei are reminiscent of chromothripsis, a process in which entire chromosomes become fragmented and then are repaired in a seemingly random manner, leading to dozens (sometimes even hundreds) of rearrangements within a single chromosome [93](Liu P 2011 Cell). Chromothripsis has been observed in approximately 3% of cancers and is prevalent in osteosarcomas (35%) and aggressive neuroblastomas (18%) and might provide the fuel for rapid genome evolution.

2.3.2 Transcriptional and post transcriptional responses

The first attempt to find a conserved gene expression response to environmentally stressful changes, such as temperature shock, oxidative stress and starvation, was already performed several years ago [94](Gasch A.P. 2000 Molecular Biology of the Cell). More recently, gene expression analyses in aneuploid budding yeast strains and plants, as well as aneuploid primary, untransformed mouse and human cells, have revealed a conserved gene expressions response to the aneuploid state across species [95,96](Sheltzer J.M. 2012 PNAS) (Durrbaum M. 2014 BMC Genomics). In particular, analysis of a

collection of different yeast strains carrying an extra copy of one of almost all yeast chromosomes revealed a gene expression signature characteristic of the environmental stress response (E.M. Torres 2007 Science). Furthermore, the stress and growth related transcriptional signature was found to be conserved, independently of the identity of the extra chromosome [95](Sheltzer J.M. 2012 PNAS). Consistently with this observation, different aneuploidies in human cells trigger common and uniform transcription profiles, such as consistent upregulation of stress and acute inflammatory responses, and downregulation of genes associated with the cell cycle, cell proliferation and DNA replication [96](Durrbaum M 2014 BMC Genomics). Finally, lymphoma cells of engineered mice, with heterozygous-deletion p53 background, showed changes in the expression of metabolic, splicing and DNA-synthesis genes after induction of chromosome instability [97](F. Foijer 2014 PNAS). Notably, these changes were very similar to the ones previously found after the introduction of an extra chromosome into mouse embryonic fibroblasts (MEFs) [3](Williams B.R. Science 2008).

An important question is if, and how, the presence of an extra chromosome affects mRNA levels, and what is the physiological response to these changes. Of particular interest was the recent finding that transcription levels in human trisomic and tetrasomic cells reflect the chromosome copy number changes. Contrarily, quantitative proteomic data revealed generally a reduction of proteins, and in particular subunits of protein complexes, toward diploid level, even if not completely [98](Stingele S. 2012 Mol Syst. Biol). This reduction was observed simultaneously with the hyperactivation of the proteasome, through inactivation of the proteasome-associated deubiquitylating enzyme ubiquitin carboxyl-terminal hydrolase 6 (UBP6), raising the interesting possibility that proteotoxicity is a hallmark of the aneuploid state (discussed below). On the other hand, transcriptome profiling from *in vitro* generated aneuploidy in yeast, mouse, human cells, pathogenic *Candida* strains and plants, suggests that mRNA levels derived from genes encoded on the extra chromosomes, mostly scale up proportionally with the gene copy numbers [2,3,99-101](Upender et al, 2004) (Torres et al, 2007) (Williams et al, 2008) (Selmecki et al, 2006) (Makarevitch et al, 2008). In conclusion, studies supported both the idea that the presence of extra chromosomes can directly affect the mRNA levels of the unbalanced genes, and at the same time the existence of feedback control that buffers the mRNA levels of amplified or underrepresented genes.

Several studies report a correlation between aneuploidy gene expression profiles and clinical prognosis in human cancers. Of particular interest is the work proposed by Carter and Szallasi [9](S.L. Carter 2006 Natuer Genetics) that identified some transcripts to be more abundant in cancers with a high level of aneuploidy. This list, known as CIN70, was described as a marker for intrinsic CIN, its overexpression in patients being correlated with a poor clinical outcome. Lately, however, it has been suggested that this list correlates better with the cell proliferation rate rather than with the CIN tumor level [102](J.M. Sheltzer 2013 Cancer Res).

Finally, it is important to mention that the aneuploidy stress related transcripts are not found in all types of aneuploidy. In particular, when comparing highly aneuploidy breast tumor cells with (almost) diploid breast tumors, it has been observed that transcriptional patterns are different. This has led to the idea of two "types" of aneuploidy that are common to cancer cells. The first one is clonally selected and stable aneuploidy, which is present in the bulk of a tumor but arises due to the selective advantages that it gives. The second type is a spontaneous aneuploidy, resulting from chromosome mis-segregation and decreasing cellular fitness, that changes continuously the karyotypes, [102] (J.M. Sheltzer 2013 Cancer Res). In this perspective, aneuploidy cannot always be deleterious for fitness, as some chromosome aberrations confer a proliferative advantage and then become predominant. Thus, tumors with a high grade of aneuploidy, like the ones investigated by Carter and Szallasi, could have acquired more growth-promoting genetic alterations, explaining the tight link between CIN70 and cell proliferation.

2.3.3 Proteotoxic stress

Proteotoxic stress is another aspect of the *aneuploidy-associated stresses*. Proteostasis is defined as a complex regulatory network that maintains cellular proteins functional and at the appropriate level [103](Balch W.E. 2008 Science). This regulatory network is maintained by several processes: the chaperone-mediated folding pathway is responsible of protein folding, while autophagy and the ubiquitin proteasome system make sure that the misfolded proteins are degraded [104](Tyedmers J. 2010 Nat. Rev. Mol. Cell.). When this equilibrium is disturbed, unfolded and misfolded proteins accumulated and generate proteotoxic stress. In aneuploid cells the stoichiometry of protein complex subunits is altered. Every protein encoded by an unbalanced

chromosome that functions in a protein complex and lacks its binding partner (or partners) risks to form aggregates and be insoluble. Thus, cellular chaperones and proteases have extra work to keep the unbalanced proteins soluble and eventually degrade them. Consistent with this idea, proteome analysis of disomic budding yeast revealed that most of the proteins scale with the gene dosage, and the those that do not are indeed subunits of protein complexes [98,105,106](Stingele S. Mol Syst Miol 2012) (Dephoure N eLife 2014) (Torres E.M. Cell 2010). This effect is even more pronounced in haploid cells as compared with diploid ones. Indeed, in haploid cells the addition of a single chromosome results in the doubling of gene expression, while in a diploid background the relative increase is only 50%. Moreover, aneuploid budding yeast strains reveal an increased sensitivity to high temperature and to inhibitors of protein synthesis and folding, as well as to chemical and genetic perturbation of proteasomal degradation [2,106](Torres 2007 Science) (Torres 2010 Cell). A recent study confirms that aneuploid strains are more prone to form proteins aggregates, most likely due to the defective heat shock protein 90 (HSP90) [107](Oromendia A.B. Genes Dev 2012). In line with these findings in yeast, aneuploidy in murine and human cells also showed profound changes in proteostasis. In particular, heat shock factor 1 (HSF1) transcription is compromised in the aneuploid colon cancer cells HCT116 [108](Donnelly N EMBO J 2014). Moreover, human trisomic cells show an accumulation of cytoplasmic foci positive for ubiquitin and autophagy markers [98](Stingele S Mol Syst Biol.2012). In agreement with this finding, chromosomally unstable aneuploid cancer cell lines are more sensitive to HSP90 inhibition than chromosomally stable cell lines. Furthermore, primary trisomic MEFs are sensitive to chemical inhibition of the chaperone HSP90 as well as to the inhibitor of autophagy chloroquine [109](Tang et al, 2011). Proteomic analyses in aneuploid human cells further revealed an altered metabolism and redox homeostasis. Even if the reason for this is not completely clear, results indicate that disruption of protein homeostasis may be responsible of the redox stress and the generation of reactive oxygen species (ROS), whose levels are indeed increased in aneuploid cells [105](Dephoure eLife 2014).

To summarize, aneuploidy unbalances the expression of proteins encoded by the additional chromosomes and thus increases burden on protein quality control processes. This finding is potentially significant, because proteotoxic stress becomes an important target for cancer therapy and could represent a way to kill aneuploid cancers selectively.

2.3.4 Inhibition of cell proliferation

Aneuploidy has been shown to be profoundly detrimental at both the cellular and organismal levels in all species investigated to date [110](Gordon et al., 2012). One consequence of aneuploidy, originally observed in fibroblast from Down syndrome patients, is the inhibition of cell proliferation [3,4](Segal and McCoy, 1974) (Williams B.R. 2008 Science). This phenotype is now well described for different species, such as yeast [2](Torres et al., 2007), where progenies from triploid meiosis delay in G1 [111](Niwa O 2006 Yast). Furthermore, experiments in mice, carrying an extra copy of one of four different chromosomes, revealed impaired proliferation independently from the identity of the extra chromosome [3](Williams et al., 2008). Finally, in mammalian cells, mutations in spindle assembly checkpoint components, such as BubR1, lead to chromosome mis-segregation, aneuploidy and a variety of features such as proliferation defects [21](Baker D.J. 2004 Nature Genetics). Notably, however, not all mutations that cause mis-segregation lead to defects in proliferation [15,20](Weaver B.A. 2007 Cancer Cell) (Babu J.R. J. Cell Biol. 2003). This could be explained by the fact that the percentage of cells showing mis-segregation events is low, and so the proliferation defects could be missed in the total population.

A fundamental question regards the reason why aneuploidy would cause proliferation defects. One possible explanation could be that copy number changes of few deleterious genes, or the cooperation of many genes that cause no growth defects if altered alone, could be responsible. The most likely answer is that a mixture of both situations causes proliferation defects. Moreover, the proliferative disadvantage might be explained in several ways since, as just described in the previous sections, aneuploid cells exhibit a variety of stress-related phenotypes (DNA damage, transcriptional response, proteotoxic stresses) [109](Y.C. Tang Cell 2011).

2.3.5 Chromosome mis-segregation and p53 response

It has been shown that chromosome mis-segregation leads to p53 activation and cell cycle arrest in G1; moreover in human cells the deletion of p53 leads to the accumulation of non-diploid cells [26](Thompson S & Compton D.A. J.Cell Biol. 2010). Similar effects were observed in vivo. Mutant mice lacking MAD2 are embryonic lethal, similarly the derived blastocysts die in

culture after a short time. But when p53 is deleted, blastocysts manage to survive for several weeks [112](Burds A.A. Proc Natl Acad Sci 2005). To date, the reason why chromosome mis-segregation leads to p53 activation and cell cycle arrest is not fully understood. It has been proposed that DNA damage might be an upstream activator of the p53 pathway. In this scenario, lagging chromosomes, frequently produced during mitosis of aneuploidy cells, can be damaged during cytokinesis by cleavage furrow [91](Janssen et al., 2011) or can be exposed to conflicting forces generated by microtubules from multiple poles and finally form DNA double-strand breaks (DSBs) [113](Guerrero et al., 2010). Alternatively, other studies point towards the increase of ROS after mis-segregation as a cause of p53 arrest. In this case, the elevated amount of ROS causes an activation of the DNA damage checkpoint, dependent on ataxia-telangiectasia mutated (ATM) and p53 [114](Li M. 2010 Proc. Natl. Acad. Sci.).

Interestingly, some recent studies proposed that not all types of mis-segregation induce p53 dependent cell cycle arrest [85,86](Soto M. 2017 Cell Reports) (S. Santaguida Cell Dev 2017). In particular, a clear distinction has been proposed between cells presenting structural aneuploidy, and those displaying a whole numerical aneuploidy. RPE1 cells, presenting structural aneuploidy (induced by Mps1 inhibition), continued to proliferate only in p53 deficient background even after mis-segregation events. Contrarily, in whole aneuploidy (obtained by combining a low dose of Mps1 inhibitor with CENPF inhibition), at least a fraction of cells continued to proliferate also in a p53 proficient genetic background. This would suggest that the degree of aneuploidy is an important determinant factor: mild whole-chromosome aneuploidies can be tolerated and propagated even in a p53 proficient background. A parallel study confirms that cells with complex karyotypes do not proliferate anymore, and instead increase p53 levels and senescence markers. Moreover, these non-proliferating cells with complex karyotypes show an increase in a pro-inflammatory gene expression profile, such as the phosphorylation of STAT3 and the secretion of interleukin. Together, these findings indicate that aneuploid p53 arrested cells could elicit an immune response [86,115](S. Santaguida Dev Cell 2017) (Karen J Mackenzie Nature 2017).

To date the prevailing thinking is that the aneuploid state per se does not lead to p53 activation and G1 arrest, whereas events associated with chromosome mis-segregation such as DNA damage and aneuploidy-associated stresses do. Thus, p53 activation is a potential but not an obligatory outcome of aneuploidy.

2.4 Ambivalent role of aneuploidy in transformation

2.4.1. Aneuploidy in cancer

The presence of aneuploidy in cancer it has been observed since a long time ago [1](Boveri T 1902, Boveri T. 1014). Around 90% of solid tumors and 50% of blood cancers present aneuploidy [116](Mitelman F. 2014 Chromosomes) (Beroukhim R. Nature 2010). This notwithstanding, the relation between aneuploidy and cancer has not yet been fully clarified, and whether aneuploidy is a consequence or a cause of tumorigenesis is still debated. It has been shown, in different organisms, that aneuploidy could sometimes fuel CIN [117,118](Storchova Z, et al. 2006 Nature) (Li R. et al 1997 Proc Natl Acad Sci U S A). Moreover, it has been shown in human cells that the presence of a single extra chromosome appears to be sufficient to initiate chromosome mis-segregation events [119,120](Nicholson, et al. 2015) (Passerini, et al. 2016). On the other hand, as mentioned in the previous section, induction of aneuploidy in diploid systems can lead to multiple cellular changes, including cell cycle arrest [121](Santaguida and Amon 2015). Thus, it becomes more and more clear that aneuploidy can both promote and inhibit tumorigenesis. For example, patient from Down syndrome have less chances to develop solid tumors compared with the rest of diploid population [122](Hasle H. 2001 Nature), and mice carrying chromosome 16 in three copies are resistant to cancer-inducing APC mutations [123](Sussan T 2008 Nature). Contrarily, a different trisomy 8 has been frequently found in a high percentage of chronic and acute leukaemias [124](Paulsson K. Path. Biol 2007).

Adding another level of complexity in the relation between aneuploidy and tumorigenesis, is CIN. Cancer cells are also often associated with CIN, which involves loss or rearrangement of partial or entire chromosomes during cell division, resulting in even further whole and structural aneuploidy [7,125](Lengauer, et al. 1998) (McGranahan, et al. 2012). Again, the positive or negative contribution of CIN to tumorigenesis is still discussed. The best example of this dual nature of CIN in cancer development is CENPE. As discussed before, CENPE is a motor protein that participates in making/maintaining the kinetochore-microtubule attachment. When CENPE is reduced by 50% in heterozygous MEFs, aneuploidy and mis-segregations are increased, as is the apparition of spontaneous lung tumors in vivo. However, at the same time, mice are less prone to develop liver tumors and chemically

induced tumors [15](Weaver B.A.A. Cancer cell 2007). These findings indicate that low rates of chromosome mis-segregation can promote tumorigenesis by increasing the odds to generate a tumor-promoting karyotype. However, when chromosome mis-segregation is too high, tumor cells cannot sustain such tumorigenesis-promoting karyotypes. Finally, in a CIN genetic background, unviable karyotypes are constantly generated and those lead to cell death and eventually tumor suppression.

Positive or negative contributions of CIN represent also a clinical problem. It has been proposed that instability can predict the drug resistance and poor prognosis [126-128](Swanton C. 2009) (Jamal Hanjani 2017 N Engl J Med) (Murugaesu 2015 Cancer Discov). Tumors that show chromosomal instability are more resistant to cancer drugs, thus more difficult to treat. For example, cells derived from tumors, or after Mad1 deregulation, show CIN and are more resistant to chemotherapy [26,129](Thompson and Compton 2010) (Rutledge 2016 Sci Rep). Several reasons have been indicated behind the increase of drugs resistance. In particular, it has been proposed that cells could acquire resistance due to the massive genomic variation caused by CIN. There is also evidence that chromosomal instability can act as an adaptive mechanism to allow cancer cells to survive during periods of stress, promoting advantageous karyotypes. In this model CIN can lead to intra-tumor heterogeneity that upon selective pressure like cancer therapy, promote the 'ideal' genetic configuration to survive [26,129](Thompson and Compton 2010) (Rutledge 2016 Sci Rep). At the same time, as already presented, CIN and aneuploidy can have a negative impact on cellular fitness. In particular, some studies analyzed the CIN70 gene expression signature [9](Carter SL. Nat Genet 2006) in relation with tumor outcome, proposing the interesting finding that extreme levels of CIN70 signature are associated with better outcomes, compared with tumors with intermediate CIN70 scores [130](Birbak NJ 2011 Cancer Res). However, in the same study, examples of ovarian, gastric and lung cancers showing an intermediate level of CIN70 expression, presented the poorest outcome, suggesting a non-linear relation between survival and presence of instability [130](Birbak NJ 2011 Cancer Res).

These studies open more unresolved questions. For example, what is the action of CIN during tumor evolution? Does it act constantly or just during a short period/window of time. Moreover, is CIN increased upon specific types of cancer therapy? Answering these questions could potentially help cancer treatment by finding the weak points of chromosomally instable cells and thus

providing information for the drug discovery process. This could also provide inputs for the development of personalized and targeted therapies, with the aim to avoid the rapid adaptation of tumors after treatments and eventually further relapses.

3. Introduction

Aneuploidy is detrimental in embryonic cells, interfering with cell proliferation and cell fitness; on the other hand, it is an almost universal feature in cancer cells. Moreover, aneuploidy often correlates in cancer with the presence of CIN, defined as dynamic changes in chromosome number and structure during cell propagation. Mechanisms that lead to CIN have been studied, but the link between aneuploidy, CIN, and tumorigenesis remains to be fully understood. In particular, the question of whether aneuploidy is a cause or consequence of the transformation process is still without definitive answer.

The aim of my study was to find a proteomic and/or phospho-proteomic signature associated with CIN, in order to begin dissecting the deregulated processes and pathways that make cells tolerant to aberrant karyotypes. To pursue this goal I performed the following steps:

1. Generation of cell lines carrying various karyotypic states that have the same parental source. These lines included:
    - diploid (microsatellite instable) colon cancer cell line DLD-1
    - derived tetraploid line, obtained by inhibition of cytokinesis;
    - spontaneously derived post-tetraploid aneuploidy single clones (PTAs) with a near-triploid or hyper-triploid ploidy content;
    - cell lines carrying a single extra chromosome (chromosome 7), generated by microcell fusion.
2. Cell biology characterization, including:
    - confirmation of chromosome and ploidy content;
    - determination of chromosome segregation fidelity and rate of instability.
3. Comparison of protein expression, applying a state-of-art quantitative mass spectrometry technique Tandem Mass Tag labeling (TMT) to identify deregulated cellular processes or pathways in DLD-1 derived cells of different ploidy states.
4. Comparative phospho-proteomic analysis by phospho-enrichment mass spec analysis in DLD-1 derived cells of different ploidy states.
5. Determination of sensitivity of the DLD-1 derived cell lines to a panel of mitotic anti-cancer drugs.

With this study I was hoping to shed some light on the changes in cellular processes and pathways that lay behind the presence of aneuploidy and the rising of CIN.

4. Results

4.1. Establishment of DLD-1-derived cell lines harboring various levels of ploidy and aneuploidy

The current proteomics study aims to clarify events responsible for and/or associated with CIN, as well to provide information about proteins and pathways potentially conferring tolerance to CIN. The identification of deregulated pathways in different cancer cell lines associated with CIN is difficult due to the continuous karyotypic reshuffling and the high inter-line variation caused by clonal, tissue origin or cancer type differences [131,132](Rebecca R. Beach Cell 2017)(McGranahan N Cell 2017). Using multiplexed tandem mass tag (TMT) labeling, I nevertheless tested if the quantification of relative protein levels in a well-described panel of karyotypically stable and unstable human adenocarcinoma cell lines (Fig. 8) [28](Gascoigne KE, Taylor S. Cancer Cell 2008) would allow to discriminate the two groups based on proteome data.

	Name	Ploidy	Chromosome Number
hTERT	RPE1	Diploid	46 (90%)
MIN	HCT116	Diploid	46 (62%)
	DLD1	Diploid	46 (86%)
	RKO	Diploid	46-50
CIN	SW480	Aneuploid	Hypotriploid
	HT29	Aneuploid	71 (68-72)
	Hela-S3	Aneuploid	76-80
Other	Sw837	Hypodiploid	40

Figure 8: Table listing ploidy and chromosome numbers for 8 human cancer cell lines used in the pilot experiment, including diploid telomerase-immortalized (hTERT) RPE1 cells, diploid microsatellite instable (MIN) and aneuploid chromosomally instable (CIN) cells. Chromosome counts were obtained from the American Tissue Culture Consortium (ATCC).

I found the differences in global protein expression between cell lines to be too profound to distinguish between karyotypically stable und unstable cell lines, since hierarchical cluster analysis did not group the cell lines based on their karyotypic stability (Fig. 9).

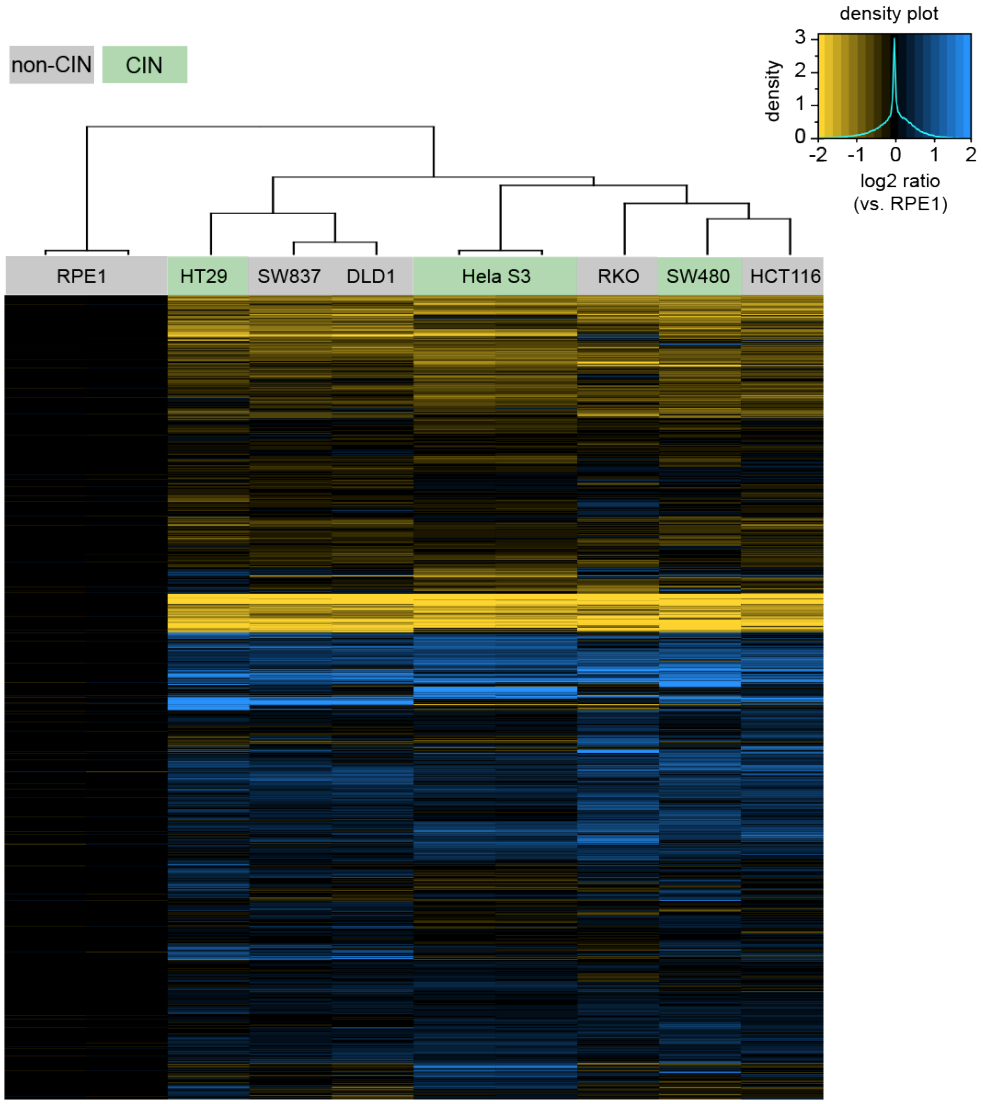

Figure 9: Hierarchical clustering based on the LC-MS/MS results for the cell lines listed in table 8 using the tandem mass tag (TMT)-labeling approach. The vertical dimension depicts ~7.500 proteins detected in the indicated cell lines. The heat map shows the degree of deregulation versus the diploid control cell line hTERT-RPE1.

Thus, in order to reduce inter-line variation due to tissue origin, cancer type or clonal variation, I decided to generate cell lines carrying various karyotypic states that have the same parental genetic source. By comparing chromosomally stable diploid, tetraploid and trisomic cells with chromosomally unstable aneuploid cells, I aimed at dissecting the effects of

chromosome mass gains from the influence of chromosomal instablility (CIN) (Fig. 10).

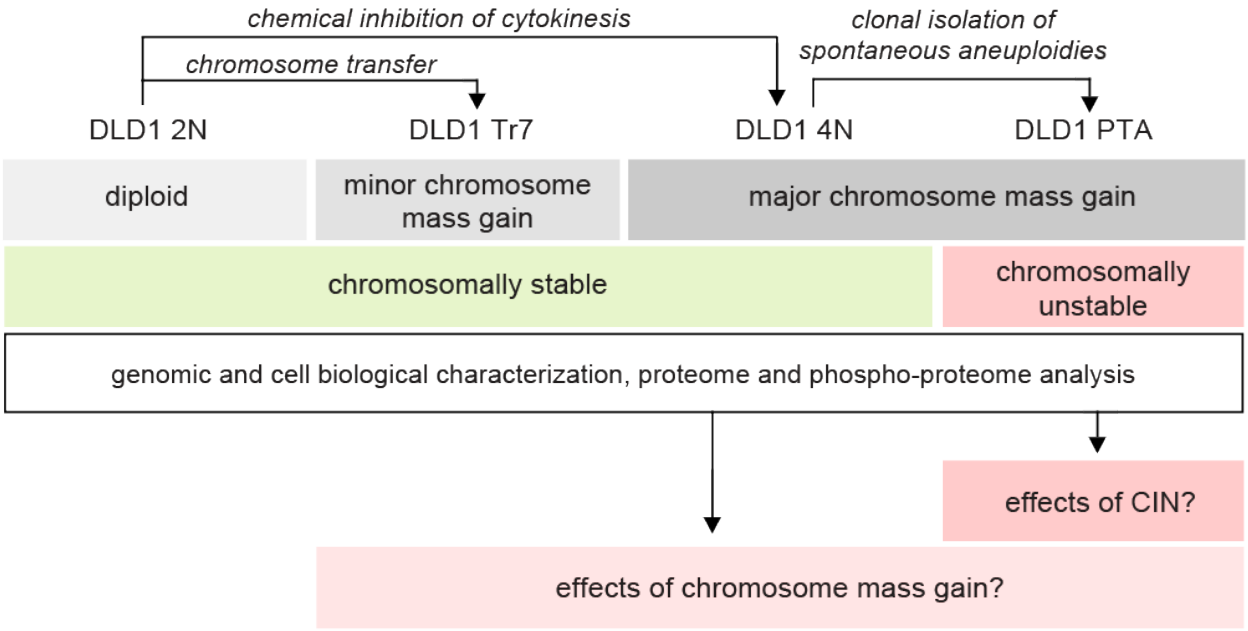

Figure 10: Schematic showing the approach to human DLD-1 colon cancer cell line generation and analysis. From a diploid (2N) parental culture, tetraploid (4N) cells were obtained by inhibition of cytokinesis. These were then used for the clonal isolation of post-tetraploid aneuploid (PTAs) descendants. Clones harboring trisomies of chromosome 7 (Tr7) were generated from the diploid parental culture by microcell fusion.

I used the microsatellite instable (MIN) diploid colon cancer cell line DLD-1, which has been described to remain viable after chromosomal gains due to its p53 deficiency [7](Lengnauer, Nature 1997). As discussed in the introduction, aneuploidy is often preceded by tetraploidy in early stage cancers, which correlates with the loss of p53 functionality [26,57,133](Galipeau et al., 1996) (Thompson S & Compton D.A. J.Cell Biol. 2010) (Ganem Neil J 2007 Current opinion in Genetics & development). It is believed that a polyploid karyotype provides a protective buffer against gene loss or haploinsufficiency and thus offers a breeding ground for spontaneously arising aneuploid clones [76,77](Aleza et al 2011) (M.Kellis Nature 2004). I made use of a culture of tetraploid DLD-1 cells that was previously generated through inhibition of cytokinesis, obtained by the actin inhibitor dihydro-cytochalasin B (DCB). This cell line was shown to have largely lost super-numerary centrosomes [63](Drosopoulos et al Nat. Comms 2014), thus providing a stable reference line for polyploidy and a

potential source for aneuploid descendants. Next, I performed single cell FACS sorting from this tetraploid culture to select for spontaneously arisen aneuploid cells showing a DNA content shift, hereafter referred to as post-tetraploid aneuploid cells (PTAs). After almost one month of clonal expansion I obtained 4 clones, presenting near triploid and near-tetraploid DNA content (Fig. 11). These 4 lines are considered to represent highly complex aneuploidy states.

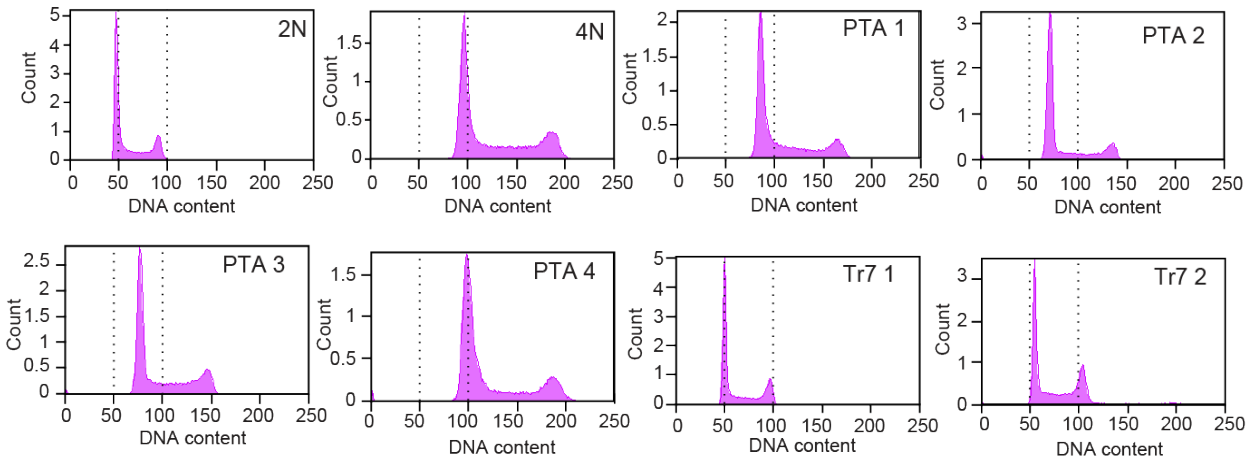

Figure 11: Histograms represent flow cytometric results the cell lines generated and used in this study. Cells were stained with propidium iodine to verify DNA content. Dotted lines indicate G1 and G2/M peaks expected for a diploid culture.

I also sought to generate a cell line with a defined chromosome gain that would serve as a control for low-complexity and defined aneuploidy. Thus, in collaboration with Dr. Zuzana Storchova's laboratory at the Max-Planck institute for Biochemistry in Martinsried (DE), I applied microcell-mediated chromosome transfer to the diploid parental DLD-1 [120](Passerini V. et al Nat. Comms 2016), in order to obtain trisomic clones (Fig. 12).

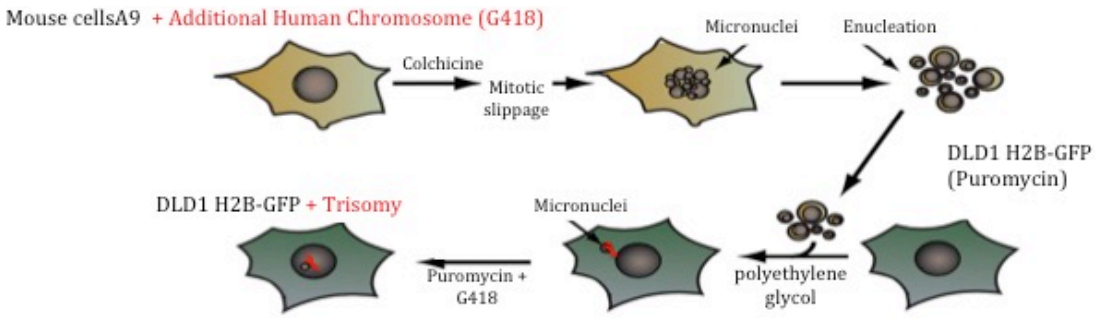

Figure 12: Microcell Fusion workflow. Adapted from [98]Stingele S. et al. 2012 Mol Syst Biol. Micronucleation was induced in mouse A9(Neo5) donor cells, containing an additional human chromosome with an antibiotic resistance gene, through colchicine. Micronuclei were separated by several centrifugation and filtration steps and then added to the recipient cell line.

I had originally planned to generate clones carrying chromosomes 4, 7 and 21 in three copies (Tr 4, Tr 7 & Tr 21), but few single clones survived the double antibiotics selection and chromosome painting often revealed only partial trisomies. (Most likely, the chromosome part integrated into recipient cells contained the antibiotic resistance, thus allowing these cells to survive with a partial trisomy). Importantly, however, two viable clones carrying trisomies of chromosome 7 (Tr 7) were obtained successfully (Fig. 11 and 13).

For all generated cell lines (diploid, tetraploid, PTAs and Tr 7), DNA content was confirmed by chromosome counting and chromosome painting in spread cells (Fig. 13 upper and lower panels). While the parental cell line presents typical diploid DNA content, the derived tetraploid cells show the double amount of chromosomes, PTAs show mainly a triploid karyotype and, finally, Tr 7 clones show a chromosome number that resembles the parental one (Fig. 13 upper panel).

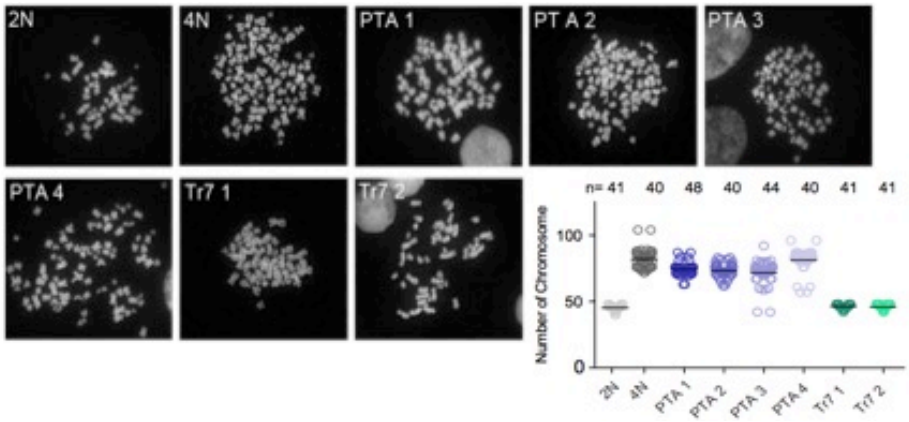

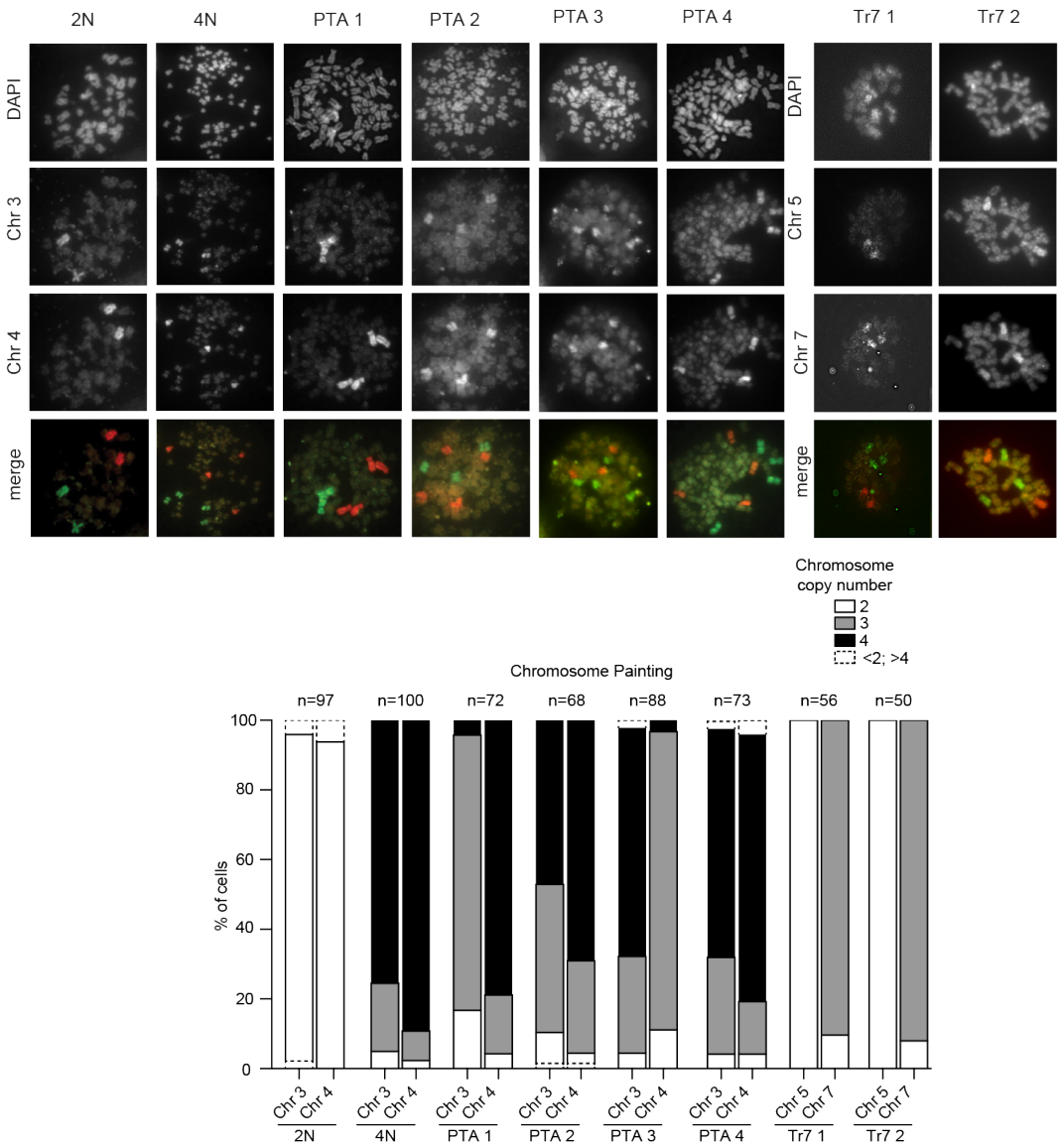

Figure 13: Upper panel: micrographs depict mitotic spreads of indicated cell lines; chromosomes were stained with DAPI. The dot plot panel shows chromosome numbers for each cell line; bars represent mean values, numbers refer to counted cells. Data represent results from three biological replicates. Lower panel: whole FISH in diploid, tetraploid, PTAs and Tr7 clones. Cells were stained for chromosome 3 and 4 in 2N, 4N and PTAs; stainings for chromosomes 5 and 7 were performed in Tr7 clones. Below histograms show chromosome numbers for each cell line, and the color code represents chromosome copy numbers (as indicated). Values were normalized for the number of counted cells (n).

Chromosome painting further confirm the chromosome copy numbers in all the cell lines (Fig. 13 lower panel). In particular, diploid culture reveal two copies for the two investigated chromosomes (Chromosome 3 in green and 4 in red). Around 80% of tetraploid cells show 4 copies of the above mentioned chromosomes. Notably, the PTA clones present high intra-cell line variability,

which is in line with the presence of aneuploidy and instability. Specifically, PTA2 and PTA4 show extensive intra-line variation, with cells presenting 4 copies of chromosome 4 or 3, but also a high percentage of cells showing 3 copies of the same chromosomes. Very nicely, PTA1 and PTA3 show a reduction of chromosome 3 and 4 respectively, in line with a corresponding reduction revealed by array chromosome genomic hybridization (aCGH) (Fig. 20). Finally 90% of trisomic clones reveal 3 copies of chromosome 7 and only 2 copies of the control chromosome 5, as expected.

In conclusion, I successfully created cell lines with different karyotype and stability states, setting the stage for proteomic studies aimed at identifying pathways that are deregulated by changes in karyotypes and CIN.

4.2. Analysis of chromosome segregation fidelity, mitotic duration and cell fate in DLD-1 derived cells

I next verified the occurrence of chromosomal instability in post-tetraploid and trisomic cells by microscopy. As discussed in the introduction, formation of micronuclei, anaphase bridges and lagging chromosomes, and as well multipolar spindle, are signs of a chromosome instability phenotype. When compared to the diploid culture, the rates of chromosomal mis-segregation and micronuclei formation were significantly elevated in most PTA clones, but not in the tetraploid parent-culture nor in the trisomic clones (Fig. 14). Specifically, in PTAs the percentage of anaphase bridges, multipolar spindles, lagging chromosomes and micronuclei increased up to 25%. Notably in trisomic clones I observed a trend towards similar increases, but these were not significant and accompanied by high standard deviations.

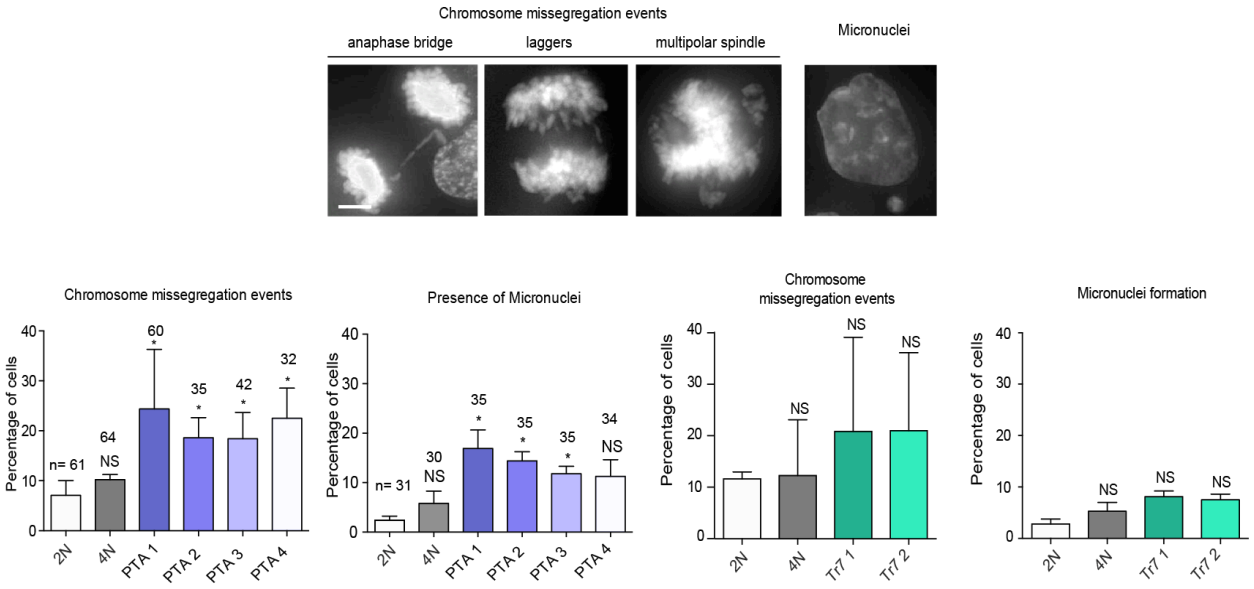

Figure 14: Top panel: representative images of chromosome mis-segregation events and micronucleation. Lower panel: histograms showing the frequency of chromosome mis-segregation events and micronucleation observed in the indicated cell lines. Scale bar represents 5 µm. All fixed cells were stained with DAPI. Error bars indicate standard deviation (SD), numbers refer to counted cells. Data represent results from three biological replicates. Two-tailed *t*-test: **P*<0.05, ***P*<0.01, ****P*<0.001 and *****P*<0.0001.

In agreement with the presence of a CIN phenotype, I observed an increase also of structural aberrations in post-tetraploid clones and, in line with a previous report [120](Passerini V. et al Nat. Comms 2016), in trisomic clones as well. Specifically, I observed increases of chromosome arm breaks and chromosome constrictions. In contrast, frequencies of such aberrations were low in diploid and tetraploid cultures (Fig. 15).

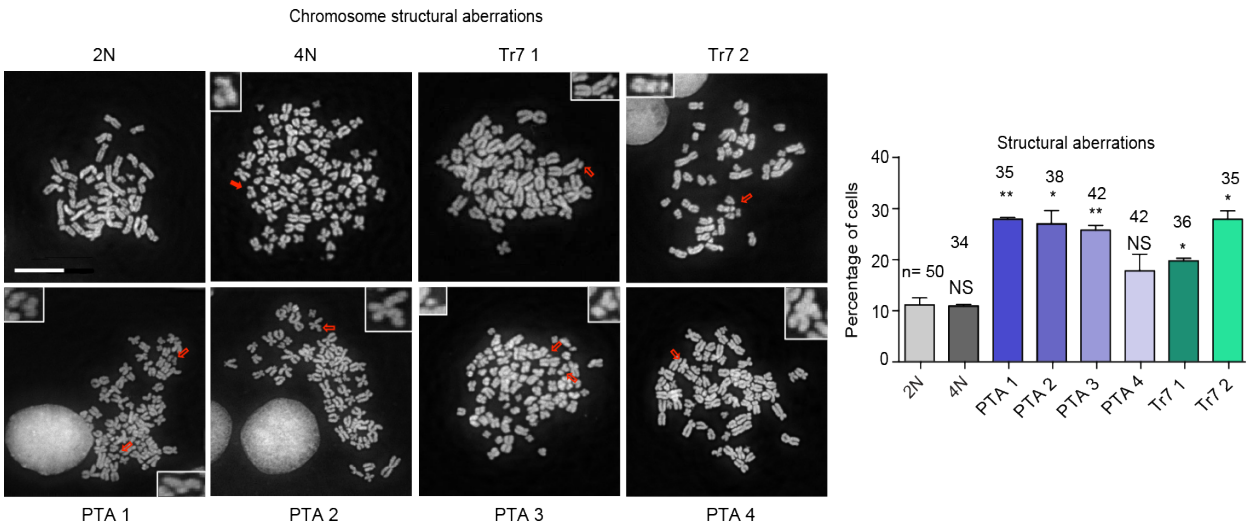

Figure 15: Micrographs show mitotic spreads prepared from the indicated cell lines, and arrows point at structural chromosome aberrations depicted in inlays. Scale bar represents 10 μm. Right panel: histogram shows the frequency of chromosome structural aberrations observed for the indicated cell lines. Error bars indicate standard deviation (SD), numbers refer to counted cells. Data represent results from two biological replicates. Two-tailed *t*-test: **P*<0.05, ***P*<0.01, ****P*<0.001 and *****P*<0.0001.

From these results I conclude that PTAs present different types of aneuploidy: whole chromosome aberrations (Fig. 13 and Fig. 20), as well as structural aberrations (Fig. 15). In principle, both could contribute to the observed increase of an instability phenotype. Together, these findings support the notion that the unbalanced gain of chromosomes leads to an increase in chromosome segregation stress and/or genetic instability [120,134](Passerini V. et al 2016 Cell Cycle) (Dodgson SE et al 2016 Genetics).

In order to see if any other signs of instability were present in PTAs I thus decided to also investigate the presence of alterations in spindle morphology. However, mitotic spindle angle, which was considered an indicator of proper spindle geometry, was not significantly altered in either of the cell lines (Fig. 16). However, tetraploid and PTAs cultures presented a bigger spindle apparatus, represented by the increased width and length, most likely reflecting the fact that these cells have to deal with an substantical increase in chromosome mass.

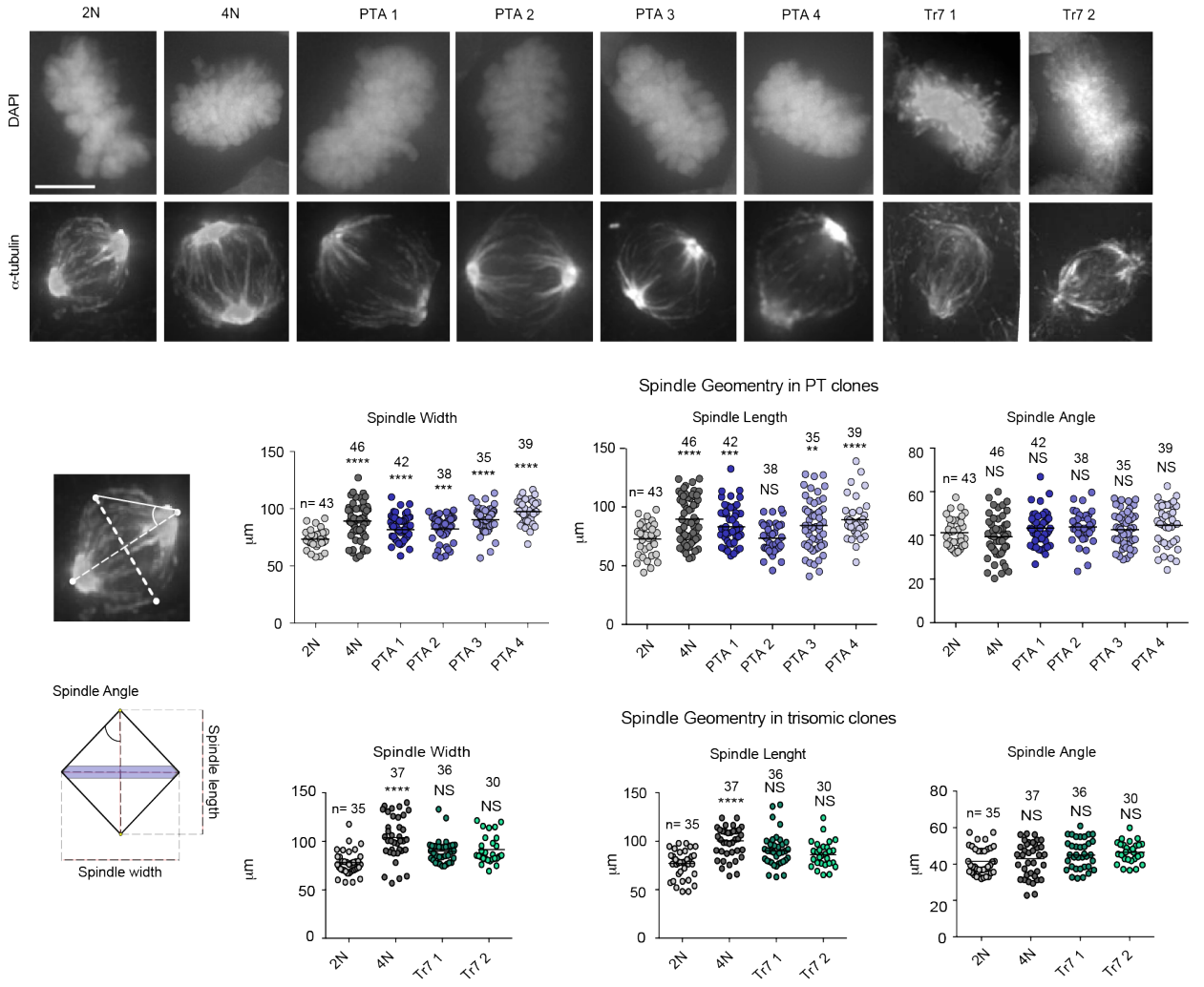

Figure 16: Upper panel, representative α-tubulin staining used for spindle geometry measurements in metaphase cells. Scale bar represents 5 µm, DNA was stained with DAPI. Lower left panel: schematic showing approach used for spindle geometry measurements. Lower right panels: dot plots showing mitotic spindle length, width and angle measurements for the indicated cell lines. Horizontal bars indicate mean values. Data represent results from two biological replicates, two-tailed *t*-test: **P*<0.05, ***P*<0.01, ****P*<0.001 and *****P*<0.0001.

Next, I investigated the possibility that sister chromatid cohesion might be attenuated in the post-tetraploid cell lines, which, as previously discussed, in turn results in chromosome mis-segregation and merotelic attachments. Specifically, I measured the distance between the sister chromatid centromeres, as marked by the centromere antibody calcinosis, Raynaud's syndrome, esophageal dysmotility, sclerodactyly, telangiectasia (CREST) (Fig. 17). Analysis of primary constrictions in mitotic spreads from diploid control cells and PTA cells did not reveal an elevated frequency of cohesion defects.

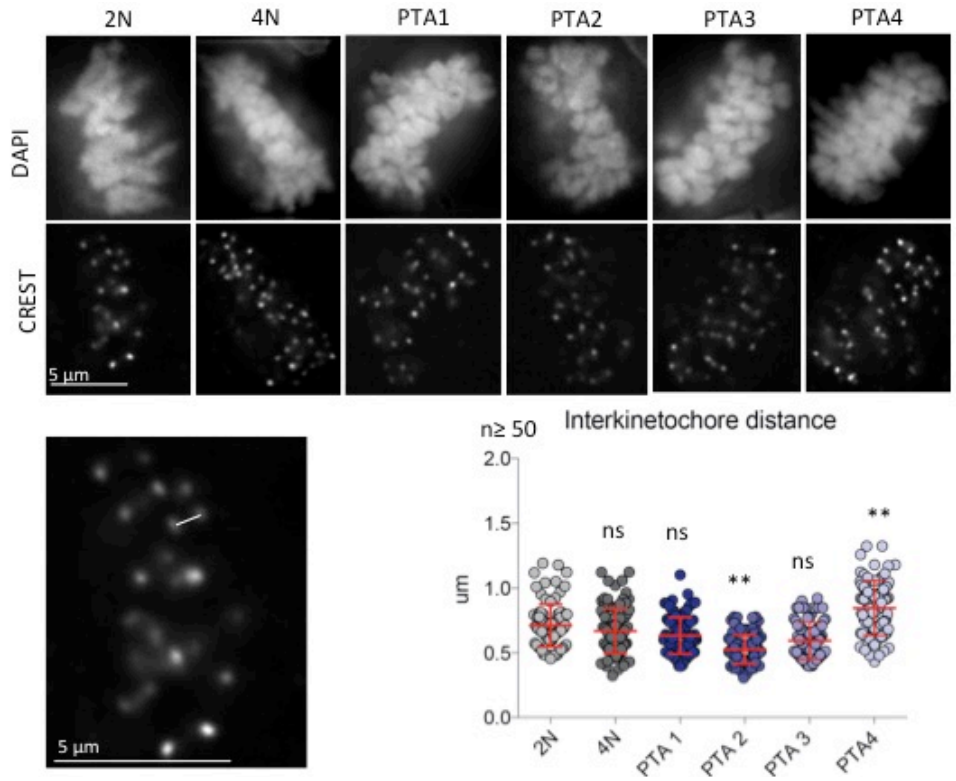

Figure 17: Upper panel: micrographs of fixed cells stained with CREST antibodies, marking centromeres. Scale bar represents 5 µm, DNA was stained with DAPI. Lower left panel: schematic showing the approach used for measurements of inter-kinetochore distances. Lower right panel: model dot plots showing inter-kinetochore distance in the indicated cell lines. Horizontal bars indicate mean values and numbers refer to counted cells. Data represent results from two biological replicates, two-tailed *t*-test: **P*<0.05, ***P*<0.01, ****P*<0.001 and *****P*<0.0001.

Measurements of inter-kinetochore distances revealed no significant differences between diploid cells, 4N and PTA1 and PTA3; the measured distances in fixed cells were 0.71±0.16 (mean±SD) for 2N and between 0.53±0.11 and 0,85±0.021 for PTA2 and PTA4 respectively (Fig. 18). These data indicate that inter-kinetochore distance does not appear to be the leading cause in all post-tetraploid cells.

Cytokinesis failure induces not only formation of binucleated tetraploid cells but also results in the gain of an extra centrosome. As discussed in the introduction, duplication of centrosomes in the following cell cycle can then lead to the formation of multipolar spindles, causing severe chromosome mis-segregation. The tetraploid culture used in this study had essentially lost the supernumerary centrosomes, and only 5.8% of the cells still showed centrosome amplification at 25 days after DCB release [63](Drosopoulos K. Nat Commun 2014). Thus, I investigated for the eventual presence of

abnormalities in centrosome and centriole numbers, using typical markers for these organelles, such as CP110 and CEP135, respectively. The large majority of mitotic figures in all cell lines contained the diploid equivalent of centrosomes and centrioles (Fig. 18), which is in agreement with the low percentage of multipolar spindle in tetraploid culture (Fig. 14) and with data shown in the literature [63] (Drosopoulos K.Nat.Commun 2014). This notwithstanding, it remains possible that very few cells in the tetraploid culture presented an aberrant centrosome number, and these could have been generating the various PTA clones. In agreement with this hypothesis, FACS profiles of the tetraploid culture showed the presence of a small population with a decreased DNA content, after one month of culturing [63] (Drosopoulos K. Nat. Commun 2014).

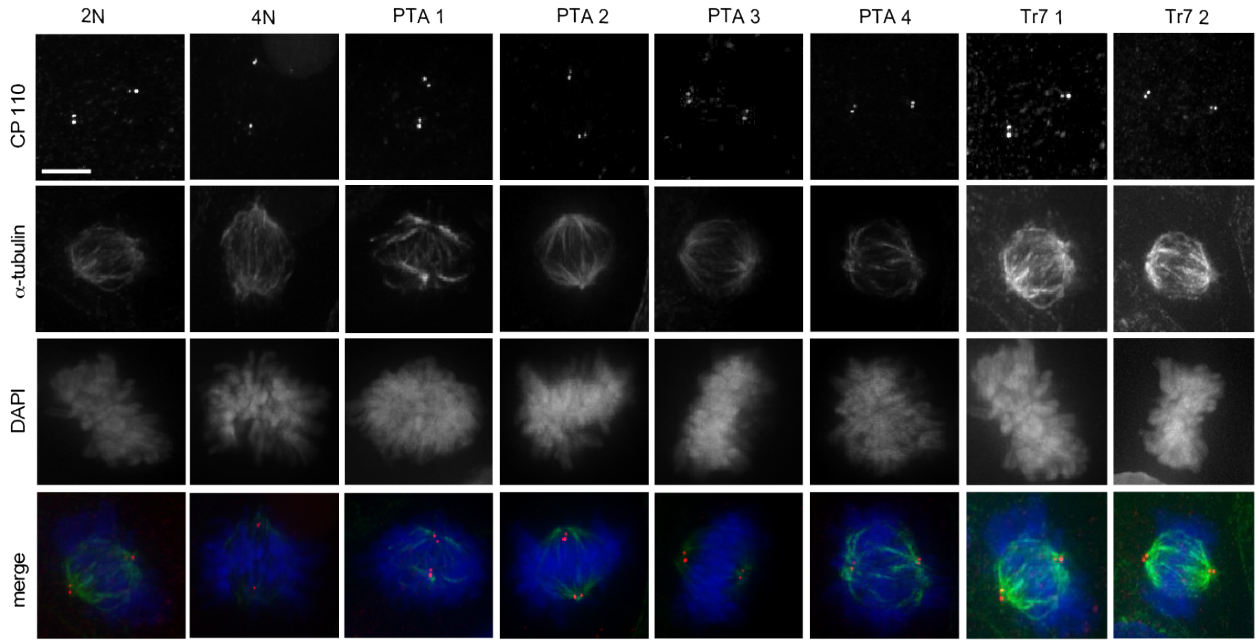

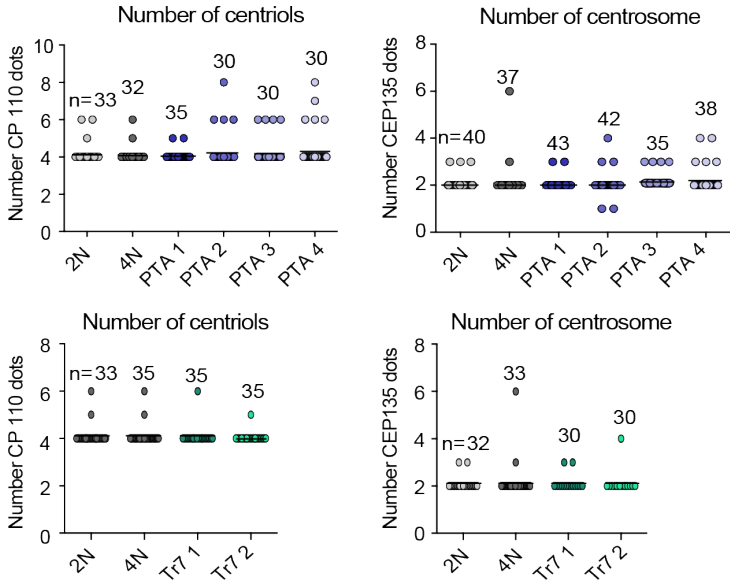

Figure 18: Upper panel: micrographs of fixed cells stained with antibodies raised against the centriole maker CP110 and α-tubulin. Scale bar represents 5 μm, DNA was stained with DAPI. Lower panel: dot plots showing centrioles and centrosomes numbers in the indicated cell lines. Horizontal bars indicate mean values and numbers refer to counted cells. Data represent results from two biological replicates, two-tailed *t*-test: **P*<0.05, ***P*<0.01, ****P*<0.001 and *****P*<0.0001.

Since extra chromosomes are likely to prolong the time required for proper chromosome alignment on the mitotic spindle, I next used live cell imaging to perform a cell fate analysis. Specifically, I used histone H2B-GFP transfected cells and scored cell fates (notably division with/without chromosome mis-segregation, mitotic checkpoint slippage, death in interphase/mitosis) after the completion of a cell division displaying a chromosomal mis-segregation event (Fig. 19).

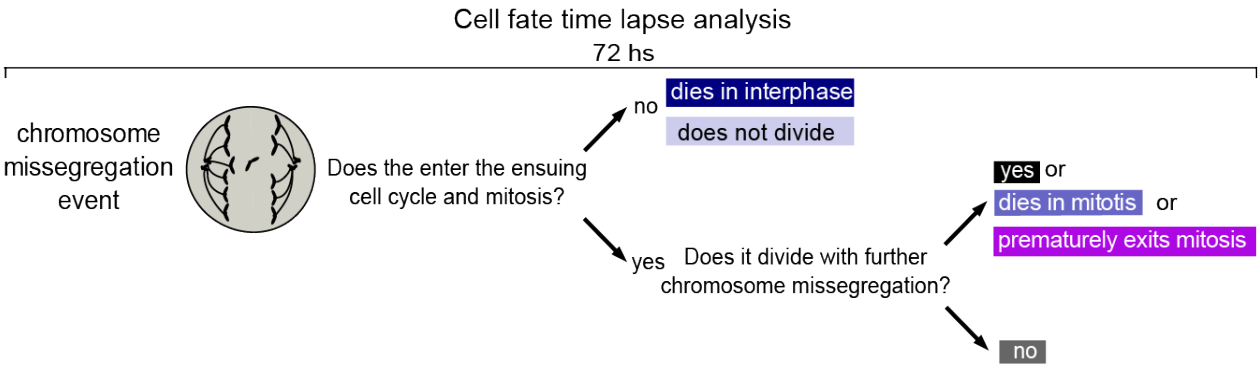

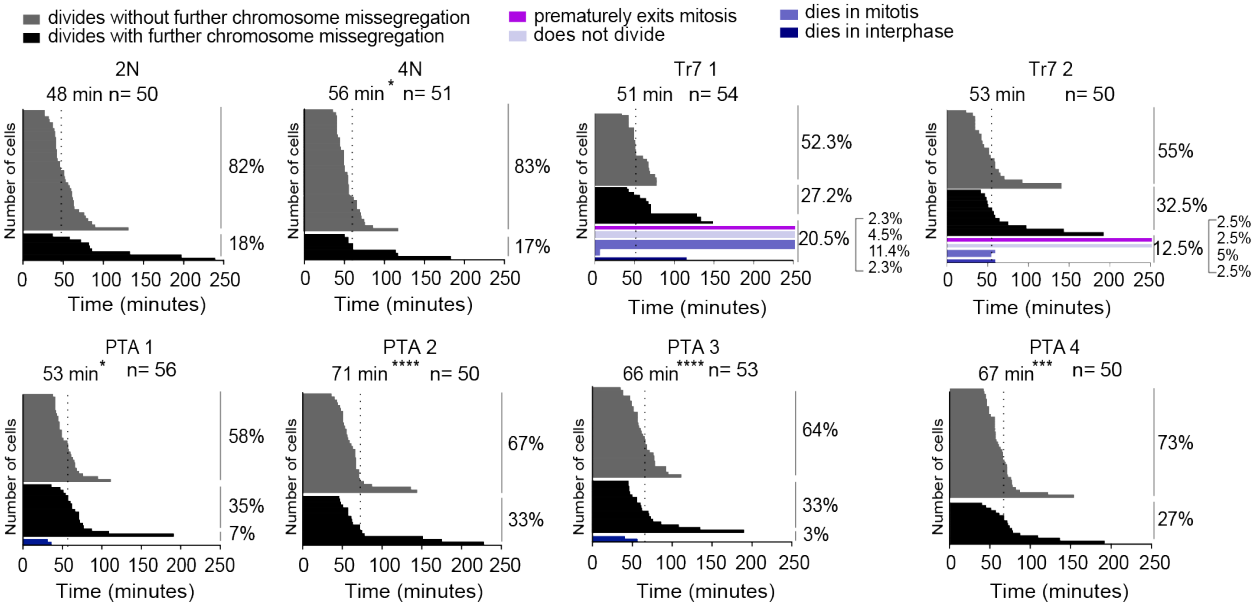

Figure 19: Upper panel: schematic showing the approach to cell fates analysis by time-lapse microscopy of asynchronously growing cultures stably expressing GFP-tagged histone H2B. Lower panel: dashed lines indicate mean mitotic duration. Frequencies of cell fates are shown to the right of each histogram. Two-tailed *t*-test: **P*<0.05, ***P*<0.01, ****P*<0.001 and *****P*<0.0001. Data represent results from two biological replicates.

While in the diploid culture chromosomal mis-segregation was largely followed by error free cell division in the ensuing cell cycle, I observed an elevated rate of chromosomal mis-segregation and a significant prolongation of mitotic duration in all post-tetraploid clones. In the tetraploid culture, mitotic length was significantly increased but it was not accompanied by an elevated rate of mis-segregation, whereas trisomic clones only responded with a non-significant prolongation of mitosis and increased cell death. These observations indicate that a gain in chromosome number provokes increased mitotic duration and occasional chromosome aberrations, but not necessarily a rampant increase of chromosomal mis-segregation. The latter was only observed in post-tetraploid clones that display CIN, i.e. a persistently increase rate of mis-segregation. Thus, the PTAs display an increased frequency of abnormal mitoses, but, remarkably, this mis-segregation is not associated with an accumulation of non-proliferating cells (Fig. 19). In this context, it is relevant that DLD-1 cells lack a functional p53 gene [135](Nanda R Rodrigues Proc Natl Acad Sci USA 1990) and, as already discussed in the introduction, mis-segregating cells have previously been observed to proliferate in p53 deficient cells [82](Fujiwara et al., 2005). Thus, it seems reasonable to conclude

that the lack of functional p53 allowed the proliferation of mis-segregating PTA cells.

Having characterized the different cell lines, I was hopeful that a comparison of karyotypically stable diploid, tetraploid and trisomic cells with karyotypically unstable post-tetraploid clones might allow me to study the effects of altered chromosome mass *versus* altered chromosome stability on protein expression and protein phosphorylation (see also Fig. 10).

4.3. Comparison of chromosome copy number and corresponding protein expression

To test the impact of chromosome copy number on protein levels, I teamed up with Dr. Thomas Lorber (University Hospital Basel) to submit all cell lines to aCGH (Fig. 20,). In parallel, taking advantage of the Proteomics Core Facility at the Biozentrum, I subjected all cell lines to quantitative proteome analysis using tandem mass tag (TMT) labeling (Fig. 22). Array hybridization assays showed that, firstly, prominent whole-chromosome copy number reductions, notably of chromosomes 3, 4 and 9, were detected in only two post-tetraploid clones (Fig. 20 and 13). The latter observation can be rationalized by the assumption that post-tetraploid clones were subjected to selective pressure that resulted in near-triploid or hyper-triploid karyotypes prior to clonal isolation from the tetraploid culture, except for chromosomes 3, 4 and 9 which had possibly undergone copy number losses prior to clonal isolation by FACS and are thus present in most sub-clones. Less frequent copy number alterations in post-tetraploid clones were likely masked by clonal heterogeneity due to increased chromosome mis-segregation rates of post-tetraploids and were thus not readily detectable by this assay. This result is in agreement with the increased frequency of structural aberrations in PTAs that would be expected to cause rearrangements, amplifications and deletions of small DNA portions.

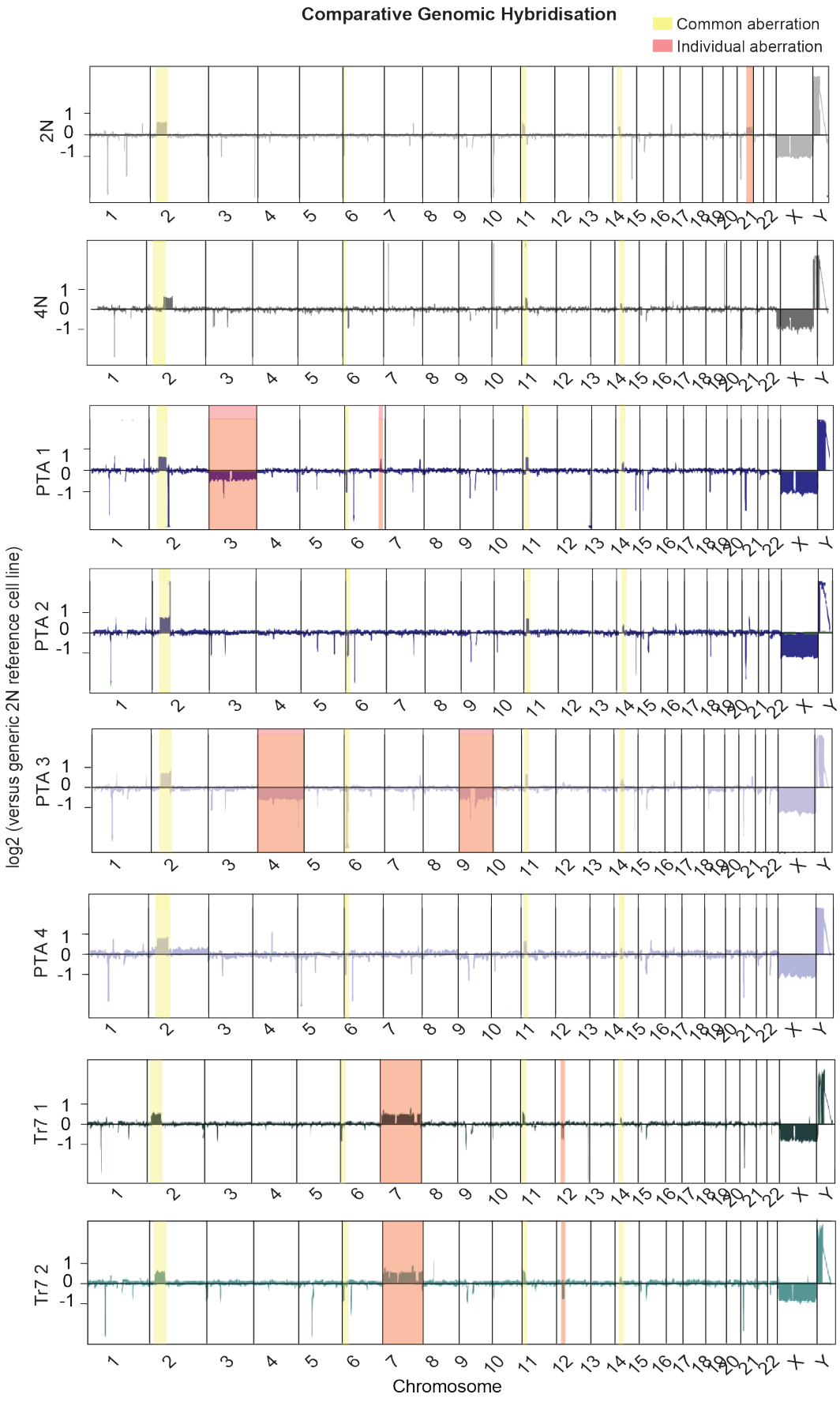

Figure 20: aCGH assay showing chromosome copy number changes relative to the generic

diploid (2N) DLD-1 reference cell line for the indicated cell lines and chromosomes. Copy number variations that remained largely unchanged in all cell lines are highlighted in yellow, individual variations are highlighted in red.

In contrast, single chromosome gains could be readily observed in the karyotypically stable trisomy 7 clones (Fig. 20), further confirming the presence of one extra copy of chromosome 7 (Fig. 13). Secondly, most small structural aberrations present in the diploid parental cell line were propagated to the cells harboring tetraploid, post-tetraploid and trisomic karyotypes (Fig. 20), and they were also detected in a diploid DLD-1 cell line originating from a different laboratory [99](Madhvi B. U. et al 2004 Cancer Research) (Fig. 21). These regions are likely to be typically aberrant in DLD-1 colon cancer cells.

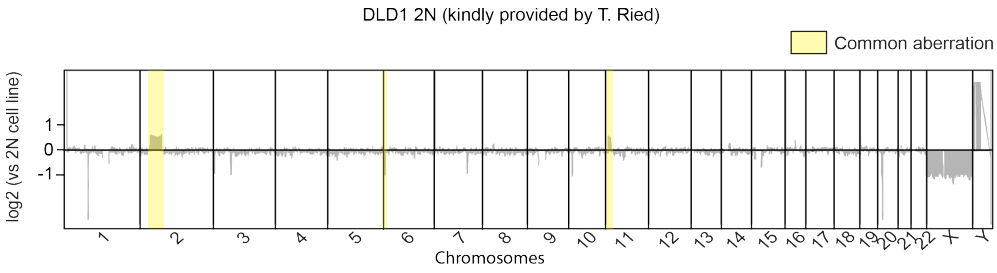

Figure 21: aCGH assay in DLD-1, from a different lab, showing chromosome copy number changes relative to a generic diploid (2N) reference cell line for indicated cell lines and chromosomes. Copy number variations that remained largely unchanged, compare with other DLD-1 used in this study, are highlighted in yellow.

As discussed in the introduction, analyses of genome, transcriptome and proteome changes in response to aneuploidy in human cells, and other species, have yielded contradictory results [2,103,131,136](Torres at al 2007) (William et al 2008) (Kvitek et al 2008) (Stenberg et al 2009). In particular, both positive and negative correlations between extra chromosomes and corresponding protein levels have been reported [98,106,131,137](Torres et al 2010) (Pavelka et al 2010) (Stingele et al 2012 Mole Syst Biology) (Rebecca R. Beach Cell 2017). This being said, it is generally agreed that the expression of subunits of protein complexes is generally compensated in order to maintain correct stoichiometry [106](Torres et al 2010).

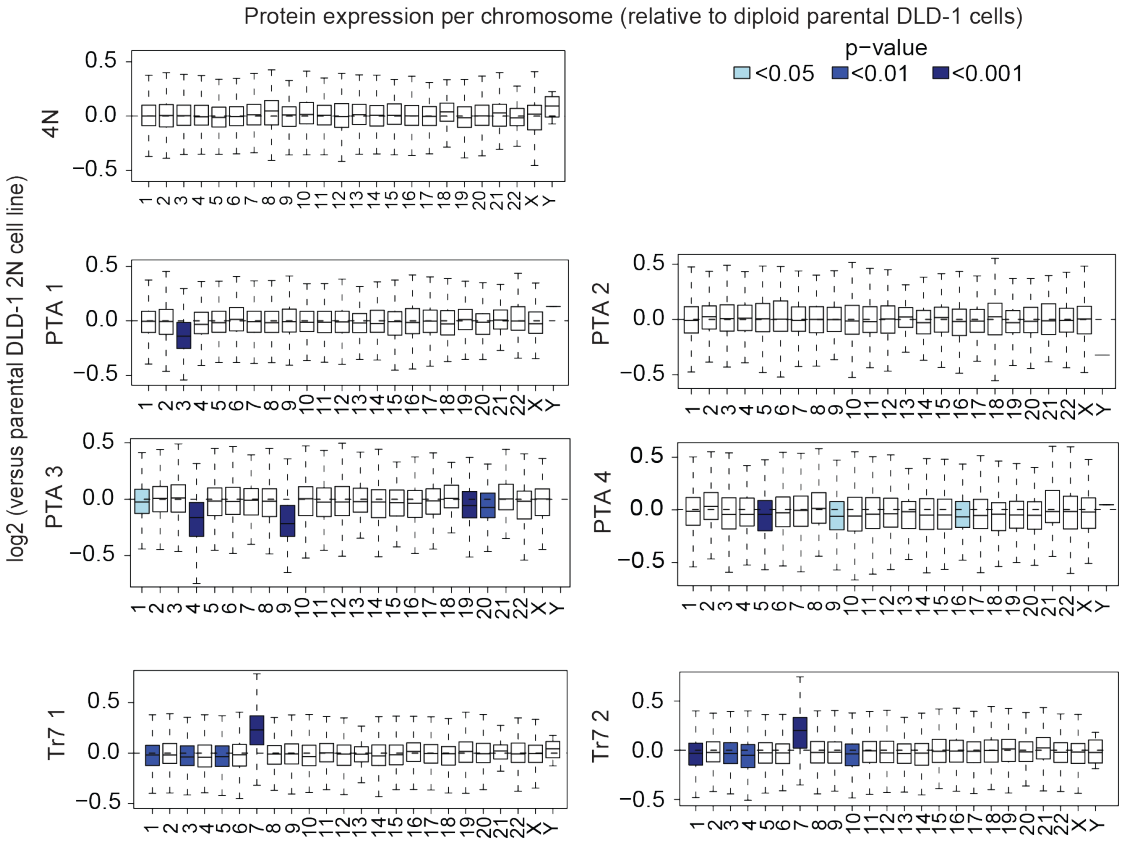

Figure 22: LC-MS/MS analysis using the tandem mass tag (TMT)-labeling approach. Box-whisker plots show protein abundance relative to the parental diploid (2N) DLD-1 culture for the indicated cell lines. Proteins are ordered by chromosome origin, blue shading indicates the level of significance. Data are from three biological replicates.

Comparison of data from array hybridization with data from proteomic analyses indicates that chromosomal copy number alterations positively correlated with the average relative expression levels of the genes encoded by the respective chromosomes in 2 PTAs and both trisomic clones (Fig. 22). In comparable expression analyses, the tetraploid line and one PTA clone (PTA2) did not show chromosome-specific deregulations, likely due to a balanced karyotype (in the case of 4N) or mild and clonally heterogeneous aneuploidy (in the case of PTA2). Supporting this hypothesis is the fact that in PTA4 presented small, but significant, proteomic deregulations in proteins encoded by chromosome 5-9 and 16 (Fig. 20), meanwhile no corresponding aberration could be detected by the aCGH in the same chromosomes (Fig. 22,). These results lead me to speculate that in PTA4 the aneuploidy may be modest and more heterogeneous when compared to PTA1 or PTA3, and that the gene aberrations are likely buffered by clonal variability. In any case, it is important to bear in mind that the sensitivities of the two experimental techniques

(aCGH and TMT proteomics) are not the same. In fact, in two PTAs and both trisomic clones, I identified further statistically significant reductions in protein expression for chromosomes that did not show deviations in copy number in the array hybridization assays (Fig. 22). On the other hand, in PTA1, PTA3 and trisomic clones the comparative genomic hybridization showed a chromosome copy number reduction (PTA1 and PTA3) or increase (Tr 7) of 0.5 log2, corresponding to one fold change. However, the corresponding protein abundance analysis showed a less pronounced reduction/increase in protein content (log2 around 0.25). This discrepancy is likely to be explained by the technical ratio compression in the Tandem Mass Tag labeling technique [131,138](Erik Ahrné 2016 Journal of Proteome research) (Rebecca R.Beach Cell 2017). In conclusion, the above observations confirm the high sensitivity of proteomic analyses and that gene dosage can directly impact on corresponding protein expression levels [106,131](Torres et al 2010) (Rebecca R. Beach Cell 2017).

4.4. Comparative proteomic analysis of DLD-1 derived cells

Data from proteomic TMT experiments, presented in the previous section, were next subjected to detailed analysis in order to identify specific protein expression patterns across stable and unstable cell lines. Notably, comparative proteomics analyses were performed independently in three biological replicates, using the 6- plex (for 2N, 4N and trisomic clones) and 10-plex (for 2N, 4N and PTAs) TMT labeling approach [138](Ahrné E. 2016 J Proteome Res.). These studies identified a total of 6'000 and 7'500 proteins across the DLD-1 trisomic and PTA cells, respectively. It is important to notice that even when a stringent q-value cut off was applied (False discovery rate (FDR) score 0.05) I was able to identify many proteins that were significantly deregulated (Fig. 23 left and right panel). (For information on the meaning of q-values, p-values, and false-discovery rates in data analysis, please refer to http://www.nonlinear.com/progenesis/qi-for-proteomics/v3.0/faq/pq-values.aspx).

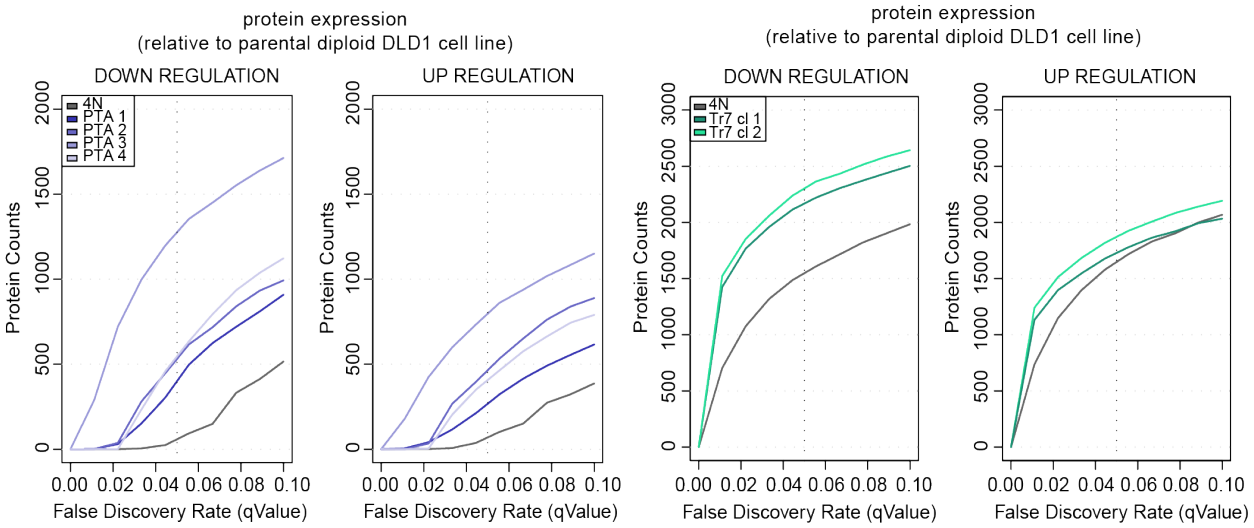

Figure 23: Left and right graphs showing the number of significant down- and up-regulations of protein expression in relation to the false discovery rate. Dashed lines indicate a false discovery rate of 5%. Proteomic data are from three biological replicates. It should be noted that the two experiments were performed separately, resulting in independent results/numbers of identified hits. Importantly, the two experiments presented here were done independently, using in one case a 6-plex tag system (trisomic clones; right graph) and in the other a 10-plex assay (PTAs; left graph), resulting in the identification of 6'000 and 7'500 proteins, respectively. This likely explains why the two curves for the tetraploid cell cultures are not identical between the two dataset.

As discussed in the introduction, it has been reported that aneuploidy-induced stresses promote global proteolytic activity, mainly due to unbalanced protein expression (due to additional chromosomes) and the consequently increased burden on protein quality control processes [88,108](Santaguida et al. 2015) (Donnelly N, Storchova Z. Mol Cell Oncol. 2015). Thus I tested if stress response proteins, including proteins regulating proteolysis, folding and/or oxidative stress, were upregulated in the various cultures. To this end, I created a list of gene ontology (GO) terms associated with these processes (Fig. 24 lower panel) and analyzed the relative abundance of proteins associated with these GO terms (Fig. 24 upper panel).

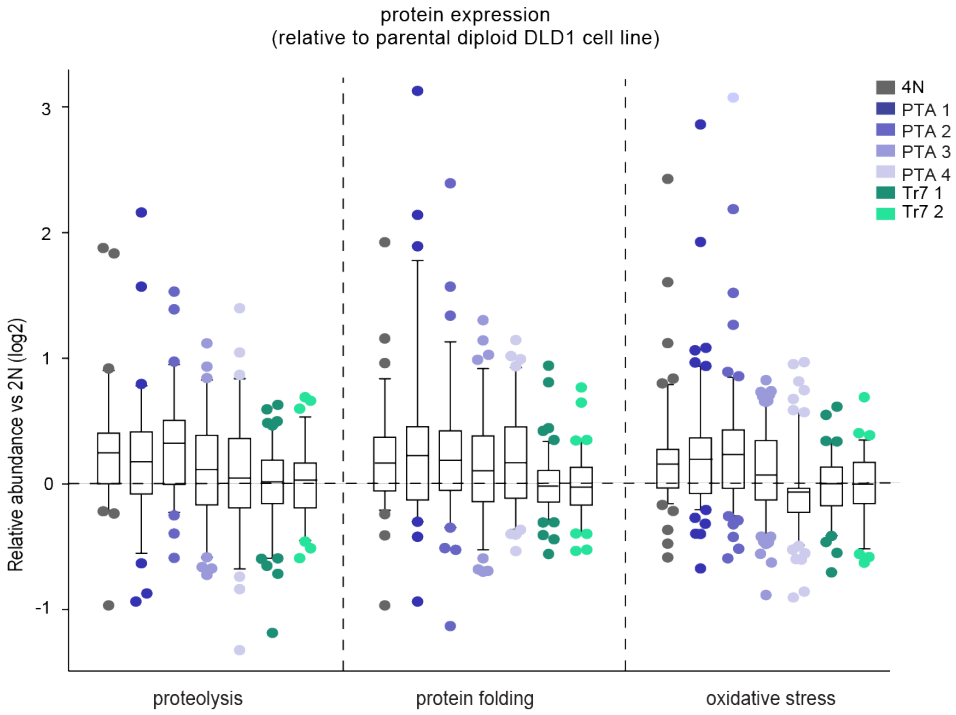

goTerm Proteolysis	
GO:0006508	proteolysis

goTerm Protein Folding	
GO:0006457	protein folding
GO:0034975	protein folding in endoplasmic reticulum

goTerm Oxidative Stress	
GO:0006979	response to oxidative stress
GO:0034599	cellular response to oxidative stress
GO:1902882	regulation of response to oxidative stress
GO:1902883	negative regulation of response to oxidative stress
GO:1902884	positive regulation of response to oxidative stress
GO:0008631	intrinsic apoptotic signaling pathway in response to oxidative stress
GO:0043619	regulation of transcription from RNA polymerase II promoter in response to oxidative stress
GO:0032938	negative regulation of translation in response to oxidative stress
GO:0036475	neuron death in response to oxidative stress
GO:1900407	regulation of cellular response to oxidative stress
GO:0001306	age-dependent response to oxidative stress

Figure 24: Upper panel: box whisker plot showing relative abundance of proteins (versus parental diploid DLD-1 cells) functionally related to protein proteolysis, protein folding and oxidative stress response regulation for the indicated cell lines. Below panel: tables listing gene ontology (GO) terms that were used to select proteins associated with the mentioned processes.

I detected a moderate increase in the average expression of proteins relevant to all three processes in tetraploid cells and most PTAs, but not in trisomic clones (Fig. 24). These results suggest that a gain in chromosome mass *per se* provokes a deregulation of protein expression, which results in upregulation

of protein quality control processes, such as protein folding and protein lysis [88,139](Santaguida et al. 2015) (Donnelly N, Storchova Z. Mol Cell Oncol. 2015).

I next decided to perform an unbiased data analysis testing for the presence of deregulated protein expression that would correlate with chromosome mass gain (in tetraploid, PTA and trisomic clones) or the genetic imbalance present in CIN cells (in PTAs and, perhaps to a minor extent, also in trisomic clones). To this end, I examined the proteome datasets by comparing the 300 most deregulated proteins (based on an FDR of <10%, and in most of the cases less than 5%) (Fig. 25 table below) in each of the PTAs, trisomic and tetraploid samples. Surprisingly, I observed very few deregulations that correlated with the presence of extra chromosome mass (tetraploid, PTAs and trisomic clones) or the presence of CIN (only PTA clones) (Fig. 25 left and right panels). In particular, I found that only 12 proteins were commonly shared across unstable PTAs (Fig. 25 left). Of these 12 common proteins the great majority (11) correlated with the strong gain of extra chromosomes in stable tetraploid (Fig. 25 left panel), suggesting that most of the proteome changes occur already in response to chromosome mass gain, rather than the presence of CIN. Similar analyses in trisomic clones revealed that only 18 proteins were commonly deregulated across 4N and trisomic clones (Fig. 25 right). In contrast, when I considered proteins overlapping between the two trisomic clones, I observed a high number of share hits (Fig. 25 right panel), as expected. Indeed, these 100 shared proteins are likely explained by the fact that in trisomic clones I artificially introduced only one additional chromosome in a mostly diploid background. Thus, the amount of genetic heterogeneity is definitively less compared with the PTAs. Moreover trisomic clones showed a less pronounced level of chromosomal instability than PTAs (Fig. 14 and 15), which results in increased genetic complexity in the latter lines.

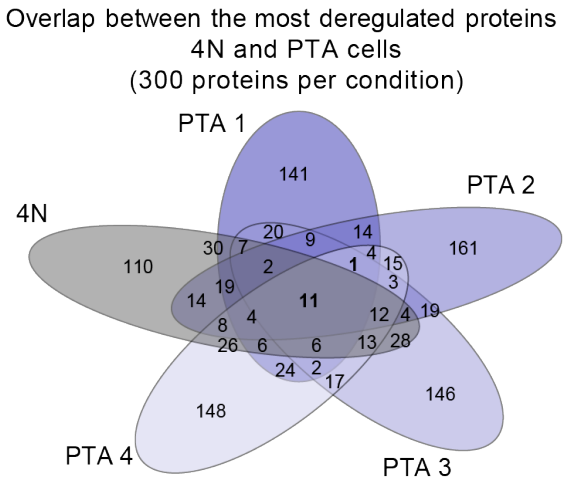

	FDR
DLD1 4N	0.0700
DLD1 PTA 1	0.0300
DLD1 PTA 2	0.0300
DLD1 PTA 3	0.0090
DLD1 PTA 4	0.0300

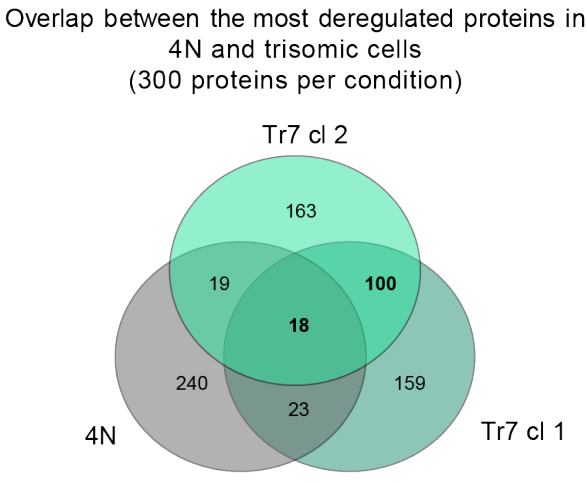

	FDR
DLD1 4N	0.0300
DLD1 Tr 7 cl 1	0.0030
DLD1 Tr 7 cl 2	0.0040

Figure 25: Left panel: Venn diagrams representing the number of shared protein deregulations across the indicated cell lines. Results were obtained by selecting the 300 most deregulated proteins per cell line (based on an FDR of <10%). Panel below: table listing the false discovery rates (FDR) for the analyzed cell lines.

Among the 11 proteins deregulated in 4N and PTAs, 5 proteins (IFIT2, IFIT3, OASL, STAT1 and DDX58) are annotated to be involved in the regulation of interferon signaling (Fig. 26 left panel), and these proteins were also functionally linked by STRING analysis (Fig. 26 right panel). This observation is reminiscent of a previous study that detected a deregulated expression of interferon signaling genes in human HCT116 colon cancer cells engineered to harbor trisomies/tetrasomies [96](Dürrbaum et al. BMC Genomics 2015).

Proteins commonly deregulated in 4N and all PTA clones

ID	geneName	proteinDescription
O14879	IFIT3	Interferon-induced protein with tetratricopeptide repeats 3
Q15646	OASL	2'-5'-oligoadenylate synthase-like protein
P42224	STAT1	Signal transducer and activator of transcription 1-alpha/beta
P09913	IFIT2	Interferon-induced protein with tetratricopeptide repeats 2
O95786	DDX58	Probable ATP-dependent RNA helicase DDX58
P63316	TNNC1	Troponin C, slow skeletal and cardiac muscles
P54803	GALC	Galactocerebrosidase
Q9NW13	RBM28	RNA-binding protein 28
P06703	S100A6	Protein S100-A6
P62760	VSNL1	Visinin-like protein 1
P07305	H1F0	Histone H1.0
Q9P2M7	CGN	Cingulin*

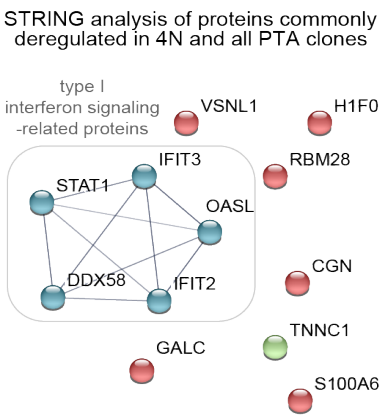

Figure 26: Left panel, list of the 11 proteins commonly deregulated across tetraploid and PTA clones as shown in Fig. 25. Asterisk demarks the single protein found to be deregulated across only PTA clones as shown in Fig. 25 Shaded area highlights proteins involved in type I interferon signaling. Right panel: STRING functional network analysis of the 11 proteins commonly deregulated in 4N and PTA clones. Nodal connections are based on a confidence value of 0.9 using experimental and database evidence.

Most recently, it has been shown that cells with complex karyotypes, generated by experimentally inducing chromosome mis-segregation, produce pro-inflammatory signals that promote their clearance by the immune system [86](Santaguida S. 2017 Dev Cell). Moreover, a cytosolic sensor of dsDNA, GMP-AMP synthase (cGAS), was recently found to be activated by DNA damage and, more importantly, localize to micronuclei arising from genome instability [115](Karen J Mackenzie Nature 2017). Our findings thus fall in line with these independent observations. On the other hand, none of the 18 genes commonly upregulated in chromosomally stable 4N and trisomic clones were annotated for interferon signaling (and they also did not show any other obvious functional relationships) (Fig. 27).

Proteins commonly deregulated in 4N and both Tr7 clones

ID	geneName	proteinDescription
P02774	GC	Vitamin D-binding protein
Q12864	CDH17	Cadherin-17
P07478	PRSS2	Trypsin-2
P62760	VSNL1	Visinin-like protein 1
P37268	FDFT1	Squalene synthase
Q9GZV4	EIF5A2	Eukaryotic translation initiation factor 5A-2
Q9Y223	GNE	Bifunctional UDP-N-acetylglucosamine 2-epimerase
P17482	HOXB9	Homeobox protein Hox-B9
Q9Y4C1	KDM3A	Lysine-specific demethylase 3A
Q6PEY2	TUBA3E	Tubulin alpha-3E chain
Q8IUZ5	PHYKPL	5-phosphohydroxy-L-lysine phospho-lyase
Q96QA5	GSDMA	Gasdermin-A OS=Homo sapiens
P15923	TCF3	Transcription factor E2-alpha
O95340	PAPSS2	Bifunctional 3'-phosphoadenosine 5'-phosphosulfate synthase 2
Q16555	DPYSL2	Dihydropyrimidinase-related protein 2
P14635	CCNB1	G2/mitotic-specific cyclin-B1
P63167	DYNLL1	Dynein light chain 1, cytoplasmic
O15231	ZNF185	Zinc finger protein 185

Figure 27: List of 18 proteins that are commonly deregulated across 4N and Tr7 clones. Relates to data shown in Fig. 24.

I hypothesized that the observed expression signature related to interferon signaling, in 4N and PTA clones, could be elicited by the increased presence of

cytoplasmic DNA. It could be that increased replication stress in tetraploid cells and the presence of more frequent chromosome mis-segregation in CIN cells result in higher abundance of chromosomal lesions, cytosolic shedding of DNA fragments and, consequently, an induction of type I interferon signaling [140-143](Samantha et al., Immunity, May 2016) (Weichselbaum et al. PNAS Nov 2008) (Erdal et al. Genes Dev March 2017) (Shen et al. Cell Reports 2015). In line with this possibility, I observed that tetraploid and post-tetraploid aneuploid clones showed upregulated expression of interfeon proteins (Fig. 28).

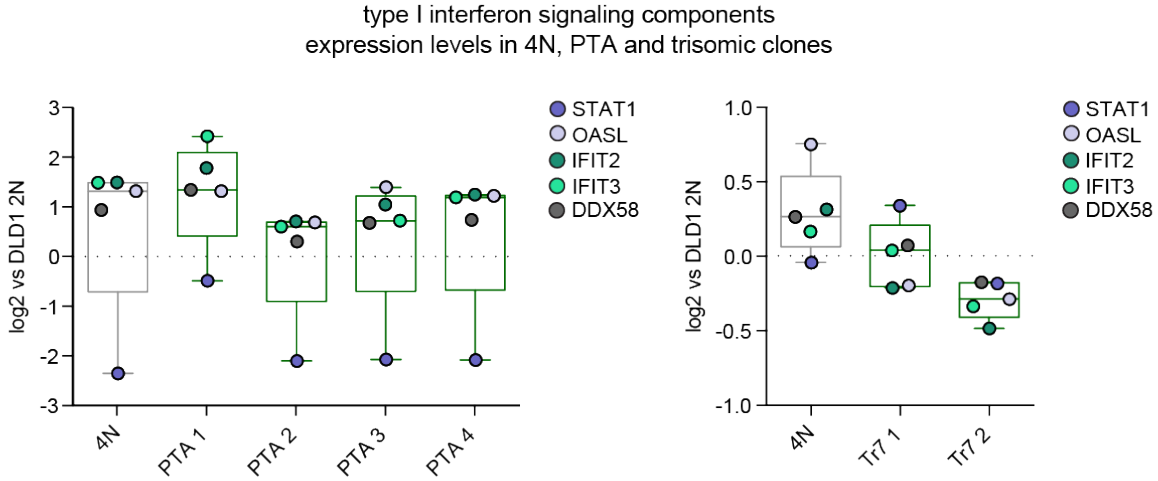

Figure 28: Box whisker plots showing the relative abundance of proteins involved in type I interferon signaling across tetraploid, post-tetraploid and trisomic cell lines.

Supporting this data is the observation that cell lines presenting extra chromosomes showed an elevated number of cytoplasmic ssDNA foci, as determined by BrdU incorporation and microscopic analysis in non-denaturing conditions (Fig. 29). These results indicate that DNA-damage, which is a common consequence of mis-segregation and aneuploidy, leads to the release of ssDNA fragments from the cell nucleus into the cytosol, engaging an innate immune response.

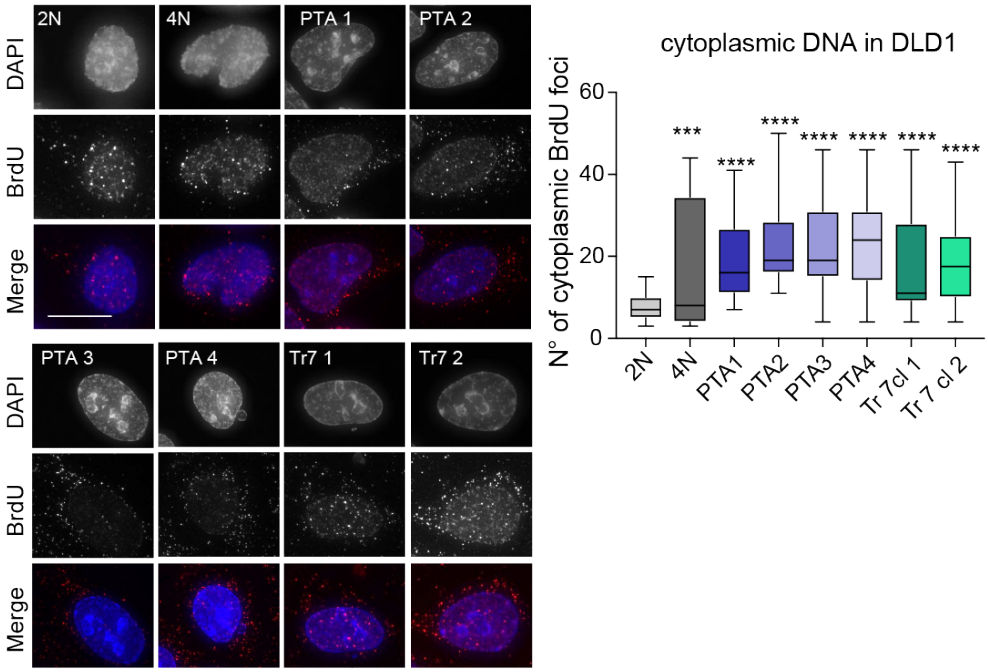

Figure 29: Left panel: micrographs of cells treated with BrdU and stained with anti-BrdU and DAPI. Acid denaturing of the DNA was omitted, extra-nuclear BrdU foci represent cytoplasmic DNA. Scale bar represents 10 μm. Right panel: box whisker plot showing the number of cytoplasmic BrdU foci for the indicated cell lines. Two-tailed *t*-test: **P*<0.05, ***P*<0.01, ****P*<0.001 and *****P*<0.0001. Data represent results from two biological replicates.

I next asked if I could detect an upregulation of these interferone genes in our dataset on established MIN and CIN cell lines (Fig. 8). While none of the diploid MIN cell lines, notably HCT116, RKO as well as diploid DLD-1 (from a distinct source), showed upregulated expression, 3 out of 4 tested CIN cell lines, including the near-triploid aneuploid HeLa and HT29 cells as well as the hypo-diploid SW837 cells, showed an elevated expression of interferon signaling genes (Fig. 30). Together this data indicates that a deregulated expression of genes associated with interferon signaling correlates with strongly altered chromosomal burden found in both chromosomally stable tetraploid cells and in chromosomally instable aneuploid cells.

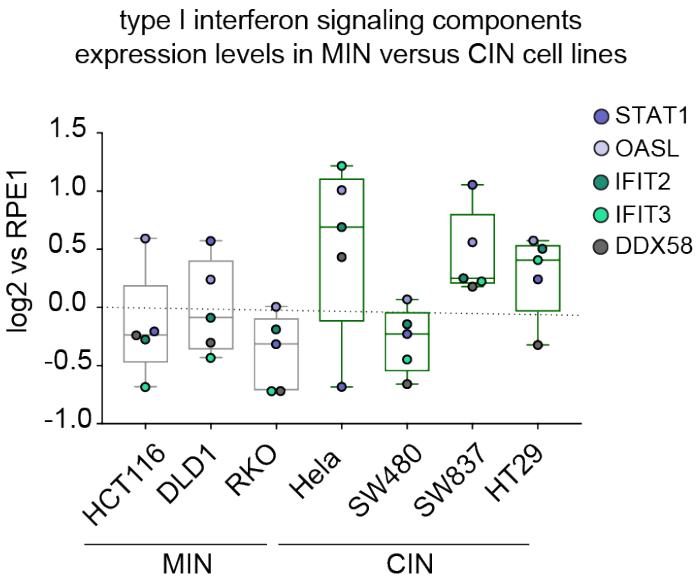

Figure 30: Box whisker plots showing the relative abundance of proteins involved in type I interferon signaling across microsatellite instable (MIN) and chromosomally instable (CIN) cell lines. The graph is based on experimental data shown in Fig. 8 and 9.

Interestingly, it has been recently shown that factors controlling DNA end resection during double-strand break repair, including the Bloom syndrome (BLM) helicase, could play a role in the generation of cytosolic and nuclear ssDNA [142](Erdal et al. Genes Dev March 2017). In particular, depletion of BLM brings about a reduction of both nuclear and cytoplasmic ssDNA in MCF7 cells. Thus, I analyzed the occurrence of ultrafine anaphase DNA bridges (UFBs), strand-like DNA structures that associate with the BLM protein and link the dividing DNA masses (Fig. 31). UFBs originate either from DNA catenae or from replication or recombination intermediates that form during double strand repair; thus, the occurrence of UFBs can be indicative of un-replicated or abnormal DNA structures [144](Chan, K 2011 Semin. Cell Dev. Biol). Staining with an antibody against BLM revealed an increased frequency of UFBs by up to 30% in the trisomic clones and by ca. 20% in tetraploid and PTA cells, compared with controls (Fig. 31).

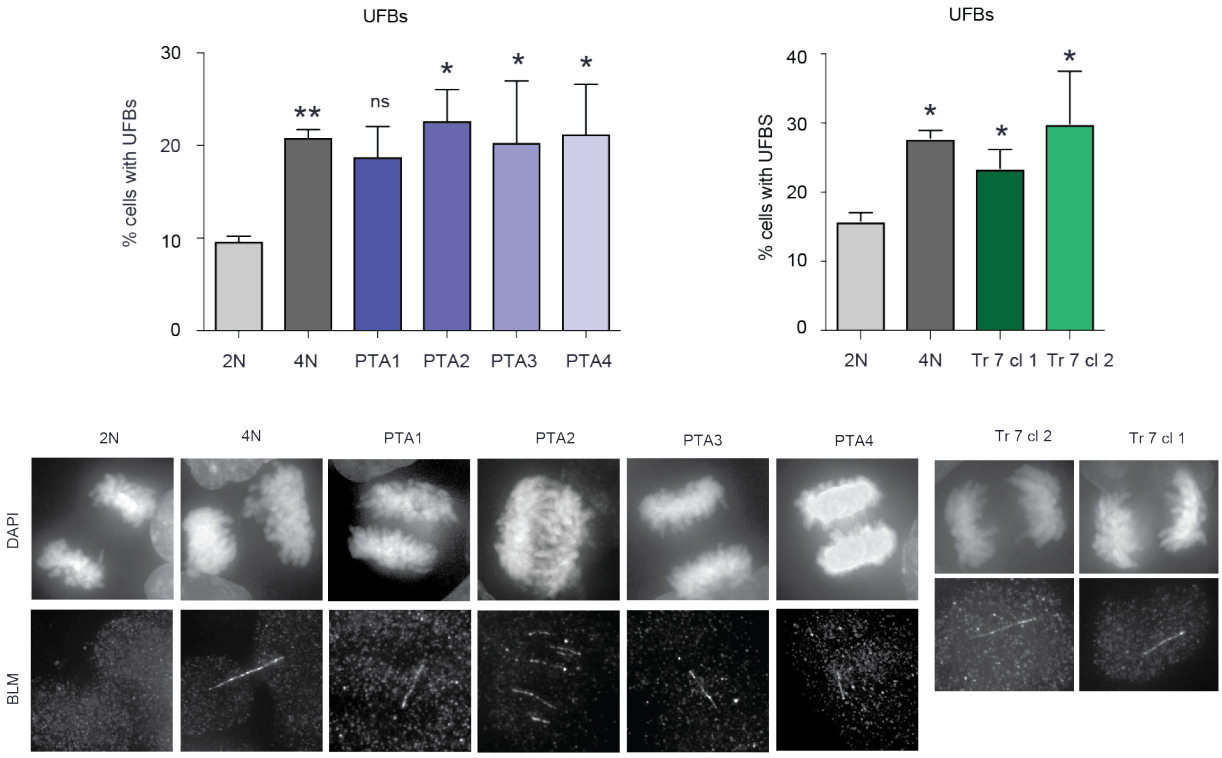

Figure 31: Upper panel: plot showing the percentage of cells showing UFBs marked by BLM staining. Below panel: micrographs of cells stained with anti-BLM and DAPI. Two-tailed *t*-test: **P*<0.05, ***P*<0.01, ****P*<0.001 and *****P*<0.0001.

All these results support the hypothesis that an increase in chromosome mass can lead to an increase in DNA damage (including double strand breaks), as discussed in the introduction, and, moreover, to the generation of ssDNA. Finally, the presence of ssDNA in aneuploidy cells could then trigger upregulation of an innate immune response in order to promote the clearance of damaged cells by the immune system [86](Santaguida S. 2017 Dev Cell).

4.5. Targeted analysis of protein expression in DLD-1-derived cells

In order to determine whether increases in chromosome mass or mis-segregation rate lead to effects on deregulation of cell cycle and mitotic proteins, I took advantage of past efforts and designed a targeted data analysis. Firstly, I made use of an inclusion list featuring 550 common tumor suppressor genes (TSGs) and oncogenes (OGs) [145](Davoli Science 2017) that encompasses 14 signaling pathways involved in cancer cell transformation (TSG/OG inclusion list, Table S1). Secondly, I generated an inclusion list of 737

proteins that was compiled from a CIN signature determined by meta-analysis of gene expression datasets [9](Carter SL, Nat Genet. 2006), from a list of genes that were associated with cell division by the MitoCheck project [146](Neumann et al. Nature 2010), as well as from a list of genes that were assigned gene ontology (GO) terms attributed i.e. to kinetochore-, centrosome-, microtubule-, cell cycle checkpoint-, cell division- and chromosome segregation-related processes (CIN/cell division inclusion list, Table S1). Thirdly, I generated smaller inclusion lists that contained hallmark genes of the spindle assembly checkpoint, the anaphase-promoting complex/cyclosome (APC/C), the kinetochore-microtubule interface as well as the DNA replication licensing and origin complexes MCM and ORC, representing pathways and protein complexes that have been previously linked to chromosomal mis-segregation [19-23](Beth AA Weaver, Current Opinion in Cell Biology 2006) (J.R. Babu, J Cell Biol, 2003)(D.J. Baker, 2003 Nat Genet,) (Sottillo R. 2007 Cancer Cell) (Kabeche L. 2012 Curr Biol) and genetic instability [120](Passerini et al 2016 Nature Communications). Analyzing the 300 most deregulated proteins in each cell line with the TSG/OG inclusion list, I could not detect a significant enrichment in tetraploid, post-tetraploid, nor trisomic samples (Fig. 32).

Tumour suppressor genes (TSG)

TSG enrichment analysis of proteins up-regulated in 4N and PTA cells

	signIList	totSign	nonSignIList	totNonSign	ftPValue
4N	6	145	175	5486	0.3374176
PTA 1	3	128	182	5479	0.7905782
PTA 2	3	143	181	5480	0.8425621
PTA 3	0	108	182	5479	1.0000000
PTA 4	2	156	181	5480	0.9593175

TSG enrichment analysis of proteins down-regulated in 4N and PTA cells

	signIList	totSign	nonSignIList	totNonSign	ftPValue
4N	4	145	175	5486	0.6771092
PTA 1	0	169	182	5479	1.0000000
PTA 2	1	153	181	5480	0.9920951
PTA 3	3	189	182	5479	0.9425012
PTA 4	2	140	181	5480	0.9387884

Oncogenes (OG)

OG enrichment analysis of proteins up-regulated in 4N and PTA cells

	signIList	totSign	nonSignIList	totNonSign	ftPValue
4N	1	150	87	5574	0.9011513
PTA1	1	131	88	5573	1.0000000
PTA 2	0	146	89	5572	1.0000000
PTA 3	0	108	89	5572	1.0000000
PTA 4	2	156	89	5572	0.7117185

OG enrichment analysis of proteins down-regulated in 4N and PTA cells

	signIList	totSign	nonSignIList	totNonSig	ftPValue
4N	4	145	87	5574	0.2099882
PTA1	4	165	88	5573	0.2815287
PTA 2	3	151	89	5572	0.4444776
PTA 3	3	189	89	5572	0.5862782
PTA 4	1	141	89	5572	0.8922519

Tumour suppressor genes (TSG)

TSG enrichment analysis of proteins up-regulated in 4N and trisomic cells

	signlList	totSign	nonSignlList	totNonSign	ftPValue
4N	3	157	213	7160	0.8381178
Tr7d1	1	155	213	7160	0.9882724
Tr7d2	2	132	215	7158	0.8997608

TSG enrichment analysis of proteins down-regulated in 4N and trisomic cells

	signlList	totSign	nonSignlList	totNonSign	ftPValue
4N	3	137	213	7160	0.7682216
Tr7d1	5	139	213	7160	0.4109171
Tr7d2	2	164	215	7158	0.9520510

Oncogenes (OG)

OG enrichment analysis of proteins up-regulated in 4N and trisomic cells

	signlList	totSign	nonSignlList	totNonSign	ftPValue
4N	4	156	104	7269	0.2017603
Tr7d1	4	152	105	7268	0.1946339
Tr7d2	4	130	105	7268	0.1353750

OG enrichment analysis of proteins down-regulated in 4N and trisomic cells

	signlList	totSign	nonSignlList	totNonSign	ftPValue
4N	1	139	104	7269	0.8612769
Tr7d1	0	144	105	7268	1.0000000
Tr7d2	0	166	105	7268	1.0000000

Figure 32: Tables showing an enrichment analysis of the 300 most deregulated proteins per cell line based on the TSG/OG. The number of inclusion list matches (signlList) and non-matches (totSign) were compared to random inclusion list matches (nonSignlList) and non-matches (totNonSign) in a human proteome background. Significance (ftPValue) was calculated using Fisher's exact test. Shaded areas highlight the most significant enrichments.

Unfortunately, use of the CIN/cell division inclusion list also failed to identify any intriguing hits, since none of the expression deregulations found in the generated cell lines showed significant enrichment of CIN- or cell division-related genes among the most deregulated expressions (Fig. 33). The only exception was an apparently significant enrichment in one of the two trisomic clones (Fig. 33 grey cluster and zoom in square). Unfortunately, STRING analysis of these 19 proteins, only yielded a small network composed by 8 proteins, which is unlikely to be a ubiquitous marker for aneuploidy.

CIN/Cell division inclusion list

Enrichment analysis of proteins up-regulated in 4N and PTA cells

	signlList	totSign	nonSignlList	totNonSign	ftPValue
4N	13	138	711	4950	0.9289159
PTA 1	15	116	699	4962	0.6477453
PTA 2	21	125	700	4961	0.2957998
PTA 3	9	99	706	4955	0.9108165
PTA 4	10	148	706	4955	0.9916212

Enrichment analysis of proteins down-regulated in 4N and PTA cells

	signlList	totSign	nonSignlList	totNonSIgn	ftPValue
4N	11	137	711	4962	0.4440535
PTA 1	22	147	699	4962	0.4440535
PTA 2	15	139	700	4961	0.8415546
PTA 3	21	171	706	4955	0.7450646
PTA 4	20	122	706	4955	0.3435905

Enrichment analysis
of proteins up-regulated in 4N and trisomic cells

	signlList	totSign	nonSignlList	totNonSign	ftPValue
4N	11	149	681	6692	0.8624752
Tr7d1	20	136	679	6694	0.1097800
Tr7d2	19	115	680	6693	0.0605936

Enrichment analysis
of proteins down-regulated in 4N and trisomic cells

signlList	totSign	nonSignlList	totNonSign	ftPValue
12	128	681	6692	0.6403011
5	139	679	6694	0.9959316
5	161	680	6693	0.9990127

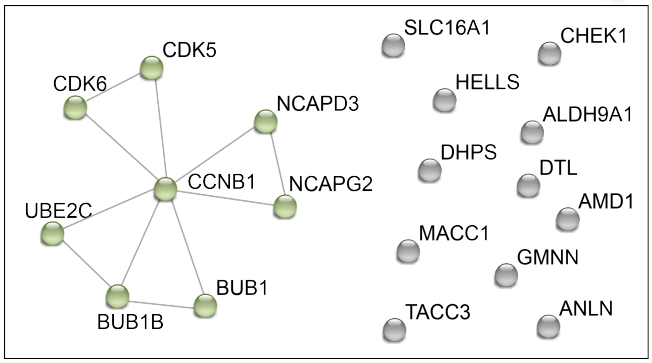

Figure 33: Tables showing an enrichment analysis of the 300 most deregulated proteins per cell line, considering tetraploid and PTAs, based on CIN/cell division inclusion lists. The number of inclusion list matches (signlList) and non-matches (totSign) were compared to random inclusion list matches (nonSignlList) and non-matches (totNonSign) in a human proteome background. Significance (ftPValue) was calculated using Fisher's exact test. Shaded areas highlight the most significant enrichments. STRING functional network analysis of the phospho-peptides is indicated in the zoom in square. Nodal connections are based on a confidence value of 0.9 using experimental and database evidence. Solid lines indicate intra-network connections.

Lastly, I could also not detect significant deregulation of genes involved in the spindle assembly checkpoint, APC/C complex, or kinetochore-microtubule interface that would have correlated with a gain in chromosome mass or the presence of CIN in most clones (Fig. 34).

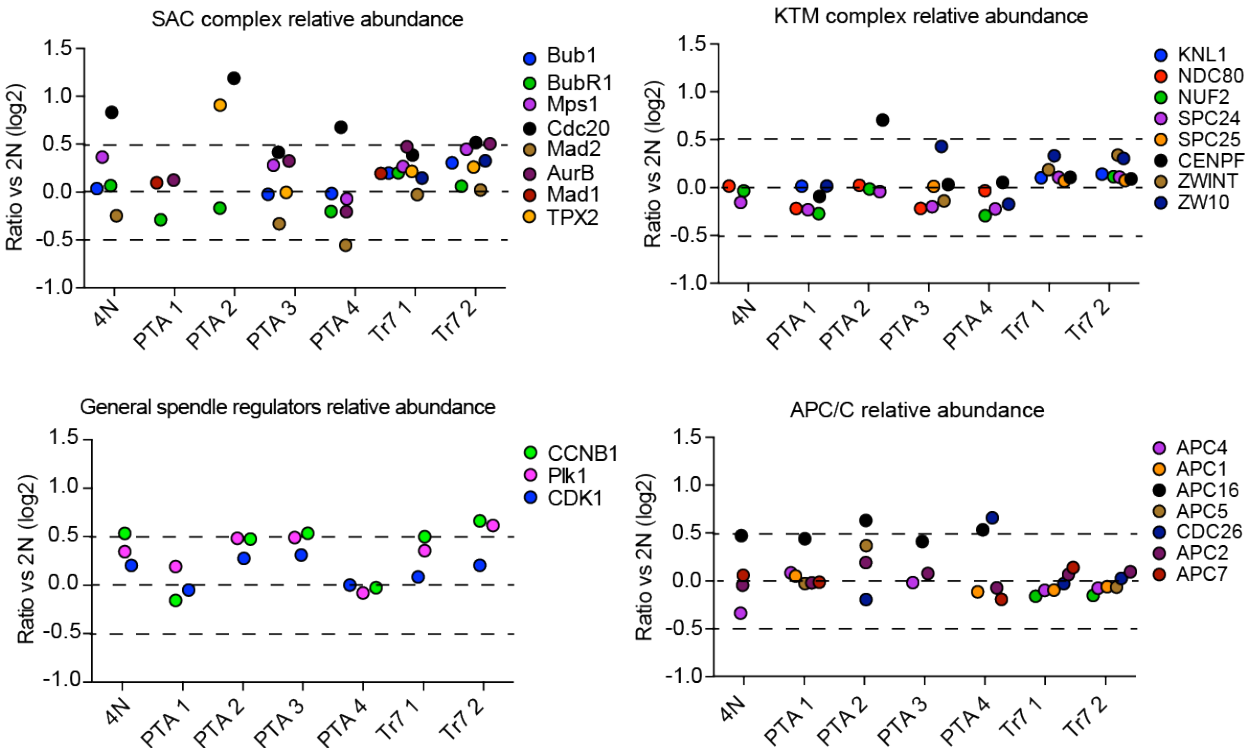

Figure 34: Dot plots showing the relative abundance of selected mitotic proteins in 4N, PTA and Tr7 clones. Note that a less stringent p-Value cut off 0.1 was applied.

I also tested the expression of the DNA replication-licensing complex MCM, for which low expression levels were previously described to drive genetic instability in low-complexity aneuploidy [120](Passerini et al., Nat Comms 2016), but while most MCM subunits were slightly down-regulated in one post-tetraploid clone, I found no marked deregulation in any of the other clones (Fig. 35, left panel). Furthermore, I could not detect a deregulation of the origin of replication complex (ORC) subunits (Fig. 35, right panel). Regardless of whether or not the observed change in MCM expression could be rate limiting for the licensing of DNA replication in an aneuploid cell (which a priori seems unlikely given the abundance of MCM proteins) [147,148](Debbie McIntosh & Blow JJ Cold Spring harb Perspect Biol 2012) (Stephanie A. Hills Current Biology 2014), deregulated MCM expression is unlikely to be a ubiquitous maker for aneuploidy. The most plausible explanation for the absence of common expression patterns in the analyzed cultures is that deregulations occur at a level that is easily masked by clonal heterogeneity, especially in aneuploid cultures that show elevated rates of chromosomal mis-segregation. Another plausible explanation is that, as previously discussed, there is a positive correlation between the presence of extra chromosomes

and the corresponding protein levels [106,131](Torres et al 2010) (Rebecca R. Beach Cell 2017), with the exception of subunits of protein complexes, where stoichiometry is generally maintained [106](Torres et al 2010). In line with this interpretation, MCM protein levels are close to Log2 0.0 in 4N, most of the PTAs and trisomic clones (Fig. 35).

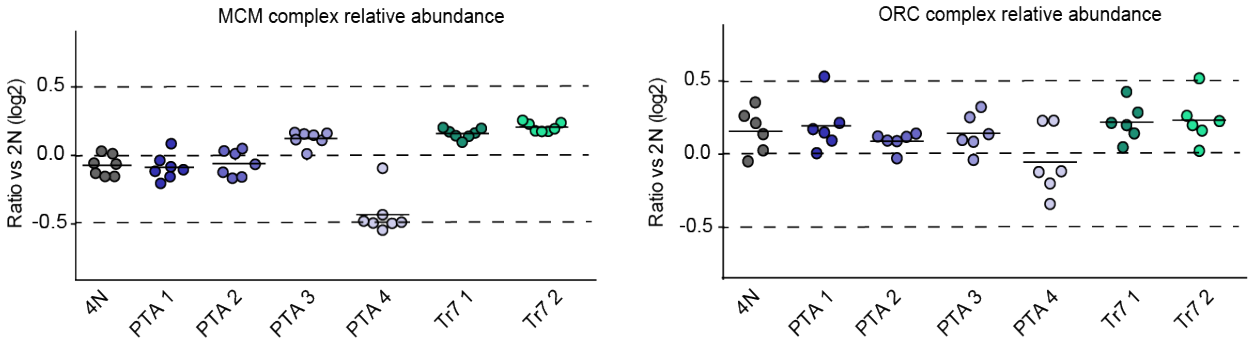

Figure 35: Dot plots showing the relative abundance of proteins belonging to the MCM and ORC complexes in 4N, PTA and Tr7 clones.

It is also possible that components associated with the occurrence of - or tolerance towards - chromosomal gains and CIN are less rate limiting in the transformed background found in the parental MIN cells. For instance, the lack of functional p53 alleles in DLD-1 cells [135](Rodrigues NR Natl. Acad. Sci 1990) could exert weaker selective pressure and could thus allow for a broader range of genetic variation. Yet, I reasoned that small expression changes could have synergistic effects on enzyme activity, especially in dynamic mitotic networks, and that polygenic phenotypes such as CIN might therefore be accompanied by detectable deregulation at the level of post-translational modifications. I therefore submitted all cell lines to phospho-proteome analysis in order to quantify possible correlations of phospho-occupancy with the gain of chromosome mass and elevated rates of chromosomal instability.

4.6. Comparative phospho-proteomic analysis of DLD-1 derived cells

Since the effects of aneuploidy and increased chromosome mis-segregation could be reflected at a post-translational level, I decided to perform TiO_2 phospho-peptide enrichment and HPLC-MS/MS. This resulted in the identification of 15'300 phospho-peptides from 3'192 proteins across biological triplicate samples of the diploid, tetraploid and three post-tetraploid

DLD-1 cell. Unfortunately, due to technical reasons, one post-tetraploid clone revealed poor FDR scores for most of the phospho-peptides found, and so I decided to not consider the corresponding data for further analysis. The same approach was applied in parallel to the trisomic cell lines, resulting in identification of 8'960 phospho-peptides from 2'553 proteins. As previously done for protein abundance analysis, when I set up a stringent q-value cut-off of 0.05, I observed a considerable number of phosphopeptides to be significantly deregulated in all cell lines (Fig. 36).

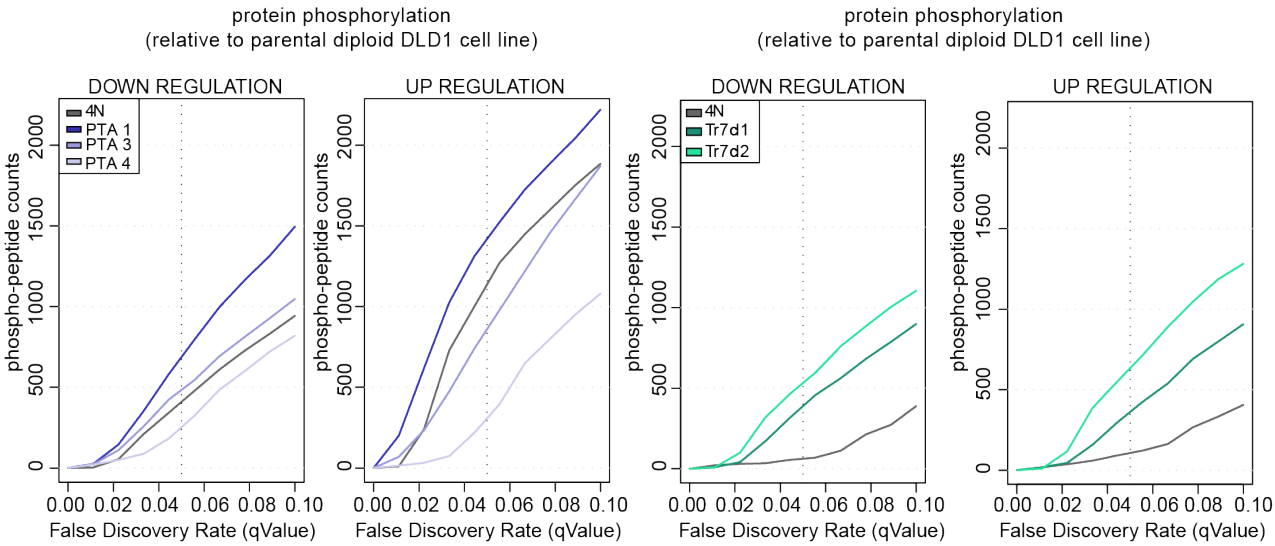

Figure 36: Graphs showing the numbers of significant down- and up-regulations of phospho-peptide counts in relation to the false discovery rate. Dashed lines indicate a false discovery rate of 5%. Data are from three biological replicates. It should be noted that the number of phospho-peptides identified in the trisomic clone experiments was lower than in the PTA experiment (because the two experiments were performed separately, resulting in independent results/numbers of identified hits).

To identify changes in protein phosphorylation that correlate with a gain in chromosome mass, I compared the 500 most deregulated phospho-peptides (based on an FDR of <10%, comprising both up and down regulation) in 4N, PTAs and trisomic clones (Fig. 37 left and right panel). I identified 63 proteins showing significantly deregulated phosphorylation across 4N and PTA clones (Fig. 37 right panel, Table S2) and 75 proteins across 4N and trisomic clones (Fig. 37 left panel, Table S2). These results indicate that changes in chromosome number not only have an impact on protein expression, as discussed above for the TMT data analyses, but also on protein phosphorylation.

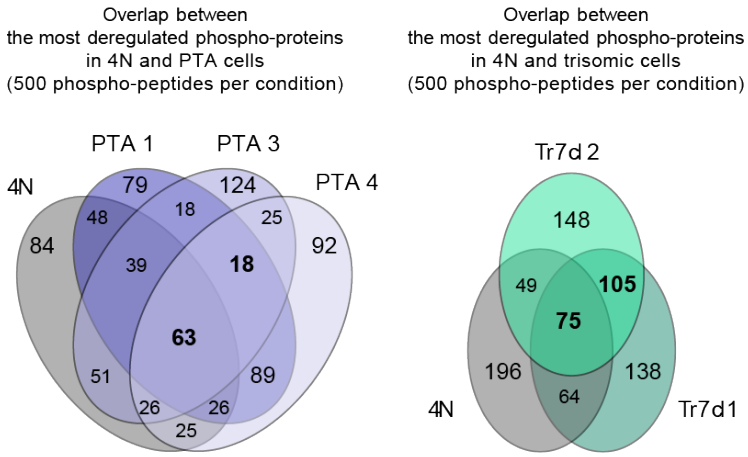

	FDR
DLD1 4N	0.03
DLD1 PTA 1	0.02
DLD1 PTA 3	0.03
DLD1 PTA 4	0.05

	FDR
DLD1 4N	0.08
DLD1 Tr 7 cl 1	0.04
DLD1 Tr 7 cl 2	0.03

Figure 37: Left panel: Venn diagrams representing the number of statistically significant shared phospho-protein deregulations across the indicated cell lines. Results were obtained by selecting the 500 most deregulated phospho-peptides per cell line (based on an FDR of <10%). Right panel: table listing the false discovery rates (FDR) for the analyzed cell lines.

Interestingly, as observed for the deregulation of protein expression (Fig. 25), I detected only few proteins that shared deregulated phosphorylation across only PTA clones (Fig. 37 left panel, S6), which would have been indicative of a correlation with the presence of CIN. This suggests that a big gain of chromosome mass is a stronger determinant for deregulated protein phosphorylation than frequent chromosome mis-segregation. To detect regulatory patterns that were shared among 4N and/or PTA clones, I submitted phospho-enrichment data to cluster analysis using the fuzzy C-means algorithm "MFuzz" [149](Futschik & Carlisle, J Bioinform Comput Biol. 2005). For cells that had gained a greater number of chromosomes, such as in 4N and PTA clones, I was able to identify only patterns of phopho-peptide up-regulation (Fig. 38, Table S6) but not down-regulation. Most likely this is due to the fact that increases in phosphorylation are technically less difficult to detect than decreases in phosphorylation.

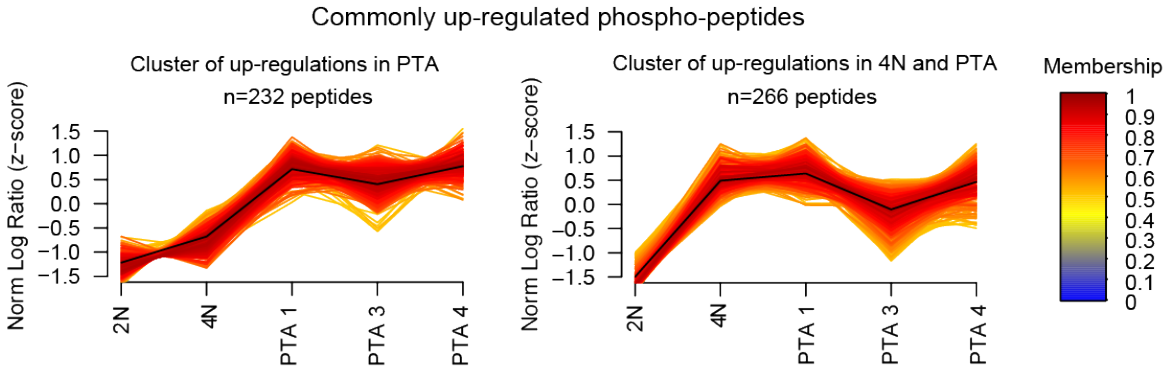

Figure 38: Cluster analysis based on the 500 most deregulated phospho-peptides (FDR of <10%, yielding a total of 1410 phospho-peptides from 807 proteins) per condition using the fuzzy C-means algorithm "MFuzz". Depicted clusters show phospho-peptide up-regulations common to PTA (left graph) or 4N and PTA (right graph) clones. Log2 ratios were normalized to have a standard deviation of 1 and a mean of 0 (z-score). Black lines indicate the optimal membership of 1, color-coding represents cluster membership values. Note that clusters were formed based on peptides that showed significant deregulation in at least one condition.

The single chromosome gains in trisomic clones, however, allowed me to detect common phospho-peptide up- (Fig. 39 upper left and right panels) as well as down-regulations (Fig. 39 Lower panel).

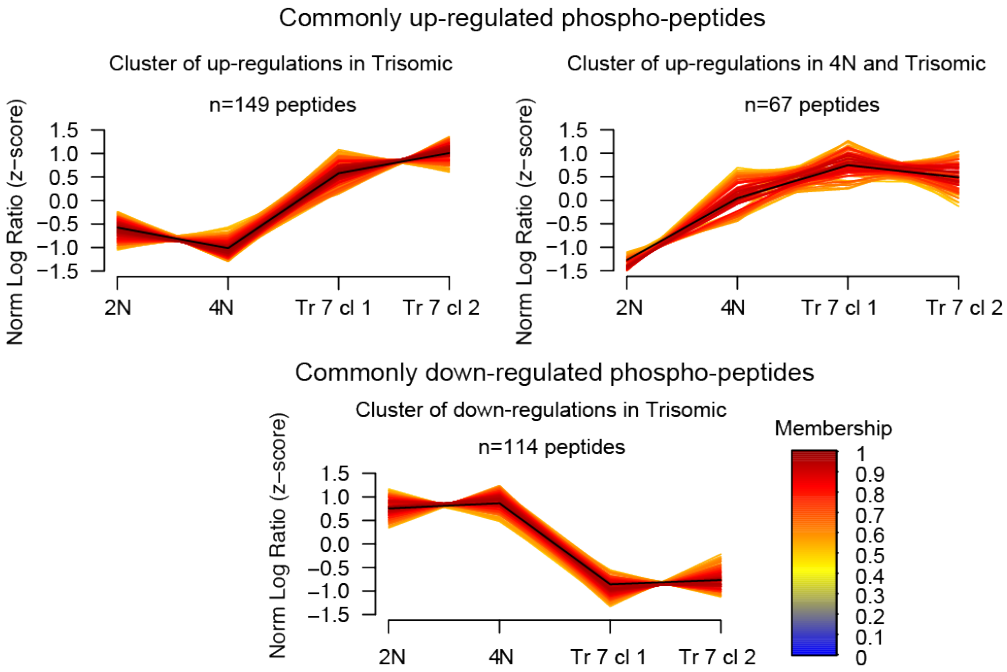

Figure 39: Cluster analysis based on the 500 most deregulated phospho-peptides (FDR of <10%, yielding a total of 1410 phospho-peptides from 807 proteins) per condition using the fuzzy C-means algorithm "MFuzz". Depicted clusters show phospho-peptide up-

regulations and down regulations common to Tr 7 (upper left graph and lower graph) and upregulations common to 4N and Tr 7 clones (upper right graph). Log2 ratios were normalized to have a standard deviation of 1 and a mean of 0 (z-score). Black lines indicate the optimal membership of 1, color-coding represents cluster membership values. Note that clusters were formed based on peptides that showed significant deregulation in at least one condition.

In order to identify which proteins were contained in these clusters, I next submitted the peptide lists obtained to GO-term enrichment analysis. Different processes showed highly significant enrichment in clones displaying CIN (Fig. 40 upper panel), polyploidy (Fig. 40 lower panel) and defined aneuploidy (Fig. 41). Analyses of clusters showing phospho-peptide up-regulations mostly identified enrichments of GO-terms related to cell cycle-, cytoskeleton (Fig. 40 upper and lower panel and Fig. 41 upper and lower panel green square). This finding is consistent with the hypothesis that, in general, aneuploidy can lead to increases in anaphase bridges, lagging chromosomes and micronuclei, as presented in the introduction [91](A. Janssen 2011 Science). As a consequence, an increased burden on the SAC or, generally, the cell cycle, can be detected. Moreover, from cluster analysis several GO terms associated with transcription could be identified in both PTAs and 4N (Fig. 40 light grey marked terms). As mentioned in the introduction, one of the effects commonly found in aneuloid cells is the presence of conserved gene expressions responses. This transcriptional response in aneuploid cells is associated with a characteristic enviromental stress and decreased cell proliferation [95,96](Sheltzer J.M. 2012 PNAS) (Durrbaum M. 2014 BMC Genomics). This concept is in line with the observation that PTAs and 4N cells up-regulate RNA-related pathways and show at the same time an increase in oxidative and proteolytic stress (Fig. 24) and innate immune-responses (Fig. 26 and 28).

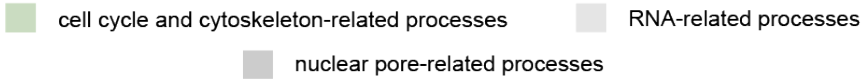

Enrichment analysis on cluster of up-regulations in PTA cells

GO.ID	Term	Significant	weight01Fisher
GO:0045944	positive reg. of transcription from RNA Poll II promoter	19	2.0e-11
GO:0016925	protein sumoylation	7	1.8e-07
GO:0007186	G-protein coupled receptor signaling	8	1.0e-06
GO:0045892	negative regulation of transcription	22	1.2e-06
GO:0008284	positive regulation of cell proliferation	10	1.9e-06
GO:0070527	platelet aggregation	4	5.6e-06
GO:0035329	hippo signaling	4	1.5e-05
GO:1904951	positive regulation of establ. of protein localizaition	10	1.7e-05
GO:0030261	chromosome condensation	4	2.6e-05
GO:0007267	cell-cell signaling	11	3.5e-05
GO:0000281	mitotic cytokinesis	4	7.6e-05
GO:0000122	negative reg. of transcription from RNA Poll II promoter	10	7.7e-05
GO:0031032	actomyosin structure organization	7	8.5e-05
GO:0006260	DNA replication	8	9.1e-05
GO:0060560	developmental growth involved in morphogenesis	6	0.00013
GO:0006999	nuclear pore organization	3	0.00013
GO:0043066	negative regulation of apoptotic process	12	0.00014
GO:0031047	gene silencing by RNA	7	0.00014
GO:0015031	protein transport	26	0.00016
GO:1902589	single-organism organelle organization	58	0.00017

Enrichment analysis on cluster of up-regulations in 4N and PTA cells

GO.ID	Term	Significant	weight01Fisher
GO:0051301	cell division	28	2.0e-14
GO:0000226	microtubule cytoskeleton organization	24	1.7e-10
GO:0030261	chromosome condensation	7	1.5e-09
GO:0006406	mRNA export from nucleus	10	4.5e-08
GO:0006355	regulation of transcription	54	5.2e-08
GO:0006325	chromatin organization	23	3.7e-07
GO:0000281	mitotic cytokinesis	6	5.4e-07
GO:0007077	mitotic nuclear envelope disassembly	6	1.2e-06
GO:0007018	microtubule-based movement	9	1.4e-06
GO:0045944	positive reg. of transcription from RNA Poll II promoter	15	2.2e-06
GO:0000070	mitotic sister chromatid segregation	11	4.2e-06
GO:0007049	cell cycle	62	6.3e-06
GO:0000381	regulation of alternative mRNA splicing	5	8.2e-06
GO:0006606	protein import into nucleus	12	1.2e-05
GO:0070925	organelle assembly	21	1.3e-05
GO:0030154	cell differentiation	51	2.0e-05
GO:0006998	nuclear envelope organization	10	2.1e-05
GO:1900034	regulation of cellular response to heat	6	2.2e-05
GO:0031047	gene silencing by RNA	7	2.4e-05
GO:0001764	neuron migration	5	2.5e-05

Figure 40 Tables listing the results of gene ontology (GO)-term enrichment analysis of phospho-peptides up-regulated across PTA clones (upper panel); and 4N plus PTAs (lower panel). Enrichment analysis was carried out for the 500 most deregulated phospho-peptides per condition ($p>0.05$), the 20 most significant enrichments are shown.

Remarkably, all these observations were made for cell lines that had undergone any kind of chromosome gain, notably 4N and PTAs (Fig. 40) as well as the trisomic clones (Fig. 41). Thus, I made the assumption that these

enriched processes are typical of aneuploidy or general increase in chromosome mass, rather than presence of chromosome instability.

cell cycle and cytoskeleton-related processes RNA-related processes

Enrichment analysis on cluster of up-regulations in trisomic cells

GO.ID	Term	Significant	weight01Fisher
GO:0045944	positive reg. of transcription from RNA Poll II promoter	14	1.7e-06
GO:0000902	cell morphogenesis	14	2.8e-05
GO:0031397	negative regulation of protein ubiquitination	5	6.1e-05
GO:0043065	positive regulation of apoptotic process	10	7.8e-05
GO:0006355	regulation of transcription	33	0.00019
GO:0008283	cell proliferation	21	0.00026
GO:0008285	negative regulation of cell proliferation	8	0.00045
GO:0007507	heart development	10	0.00060
GO:1902041	regulation of extrinsic apoptotic signaling	3	0.00073
GO:0030433	ER-assoc. ubiquitin-dependent protein breakdown	3	0.00073
GO:0001892	embryonic placenta development	4	0.00090
GO:0001510	RNA methylation	3	0.00092
GO:0035329	hippo signaling	3	0.00092
GO:0032990	cell part morphogenesis	6	0.00115
GO:2000045	regulation of G1/S transition of mitotic cell cycle	4	0.00136
GO:0051028	mRNA transport	6	0.00157
GO:0030216	keratinocyte differentiation	4	0.00163
GO:0043623	cellular protein complex assembly	8	0.00168
GO:0016925	protein sumoylation	4	0.00180
GO:0035023	regulation of Rho protein signal transdu...	4	0.00180

Enrichment analysis on cluster of up-regulations in 4N and trisomic cells

GO.ID	Term	Significant	weight01Fisher
GO:0042733	embryonic digit morphogenesis	3	2.5e-05
GO:0043266	regulation of potassium ion transport	3	3.5e-05
GO:0031532	actin cytoskeleton reorganization	4	3.5e-05
GO:0086003	cardiac muscle cell contraction	3	4.6e-05
GO:0071805	potassium ion transmembrane transport	3	4.6e-05
GO:0032663	regulation of interleukin-2 production	3	4.6e-05
GO:0086001	cardiac muscle cell action potential	3	6.0e-05
GO:0000281	mitotic cytokinesis	3	0.00012
GO:0016032	viral process	8	0.00015
GO:0043066	negative regulation of apoptotic process	7	0.00032
GO:0048589	developmental growth	5	0.00042
GO:0008283	cell proliferation	10	0.00073
GO:0007010	cytoskeleton organization	11	0.00131
GO:0030216	keratinocyte differentiation	3	0.00135
GO:1902305	regulation of sodium ion transmembrane transport	2	0.00161
GO:1903115	regulation of actin filament-based movement	2	0.00161
GO:0086065	cell communication involved in cardiac conduction	2	0.00161
GO:2000106	regulation of leukocyte apoptotic processes	2	0.00161
GO:0032456	endocytic recycling	2	0.00161
GO:0034766	negative regulation of ion transmembrane transport	2	0.00161

Figure 41: Tables listing the results of gene ontology (GO)-term enrichment analysis of phospho-peptides up-regulated across Trisomic clones (upper panel); and 4N plus Trisomic clones (lower panel). Enrichment analysis was carried out for the 500 most deregulated phospho-peptides per condition ($p>0.05$), the 20 most significant enrichments are shown.

Similar results were obtained by submitting clusters of phospho-peptide upregulations to STRING for functional protein network analysis. Firstly, I

observed a greater number of functional clusters in cells that had undergone major chromosome gains, including 4N and PTA clones (Fig. 42 & Fig. 43), when compared to trisomic clones (Fig. 44).

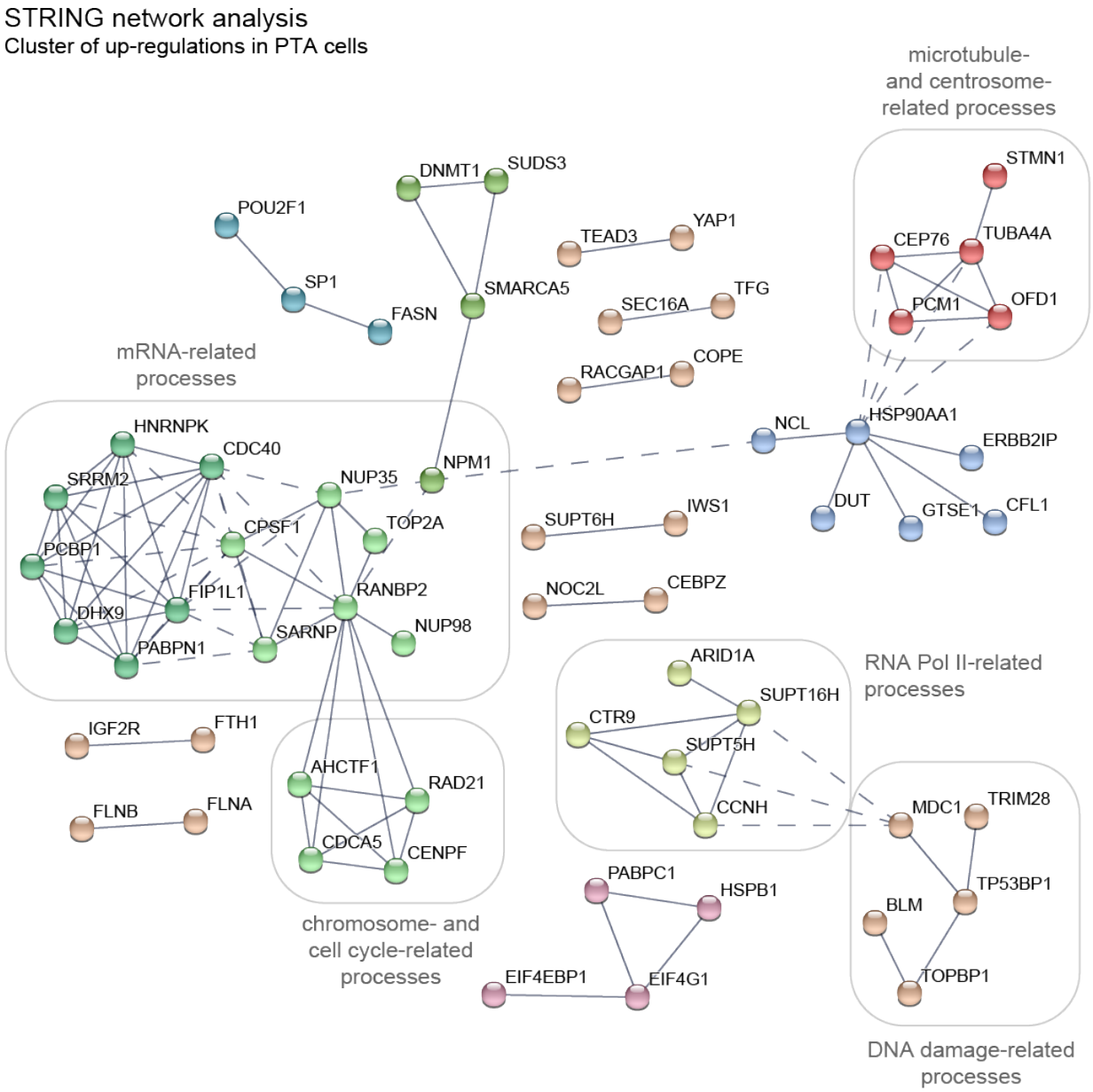

Figure 42: STRING functional network analysis of the phospho-peptides belonging to clusters shown in Figure 37 left panel. Nodal connections are based on a confidence value of 0.9 using experimental and database evidence. Solid lines indicate intra-network, dashed lines inter-network connections.

Secondly, the majority of the networks identified in clones of cells harboring both minor (trisomic clones) and major chromosome burdens (4N and PTA clones) was related to processes that are likely to be affected by an increase in

chromosome mass: replication, transcription and translation, transport through nuclear pores, DNA damage response, chromatin organization as well as microtubule- and centrosome-regulation (Fig. 42 & Fig. 43, Fig. 44).

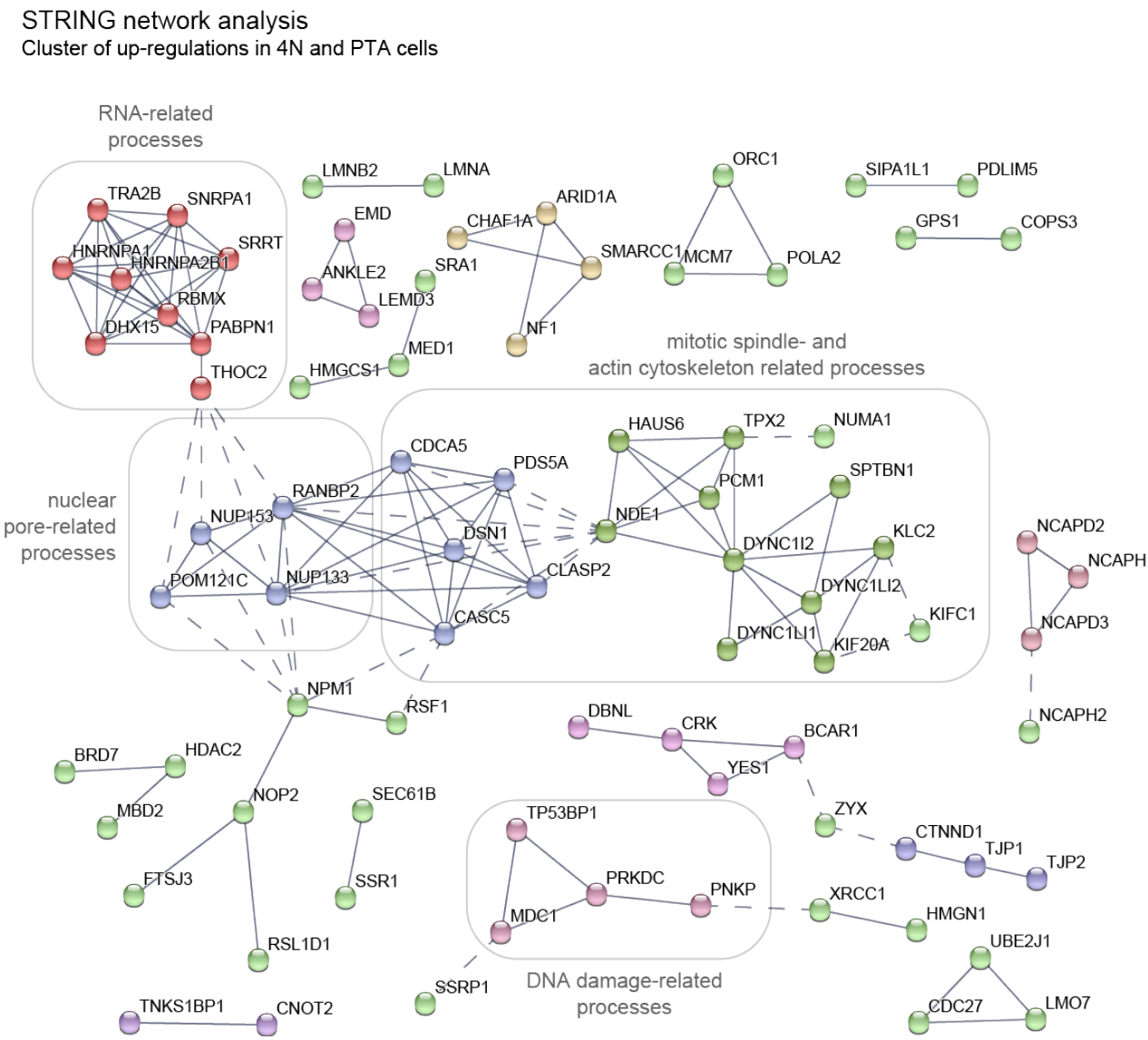

Figure 43: STRING functional network analysis of the phospho-peptides belonging to clusters shown in Figure 37 right panel. Nodal connections are based on a confidence value of 0.9 using experimental and database evidence. Solid lines indicate intra-network, dashed lines inter-network connections.

Thirdly, while networks for DNA- and/or RNA-related processes were identified in all clones (Fig. 42 & Fig. 43, Fig. 44), proteins regulating the mitotic apparatus and DNA damage response only formed networks in cells carrying a strongly increased chromosome mass, notably tetraploid and PTA clones (Fig. 42 and 43).

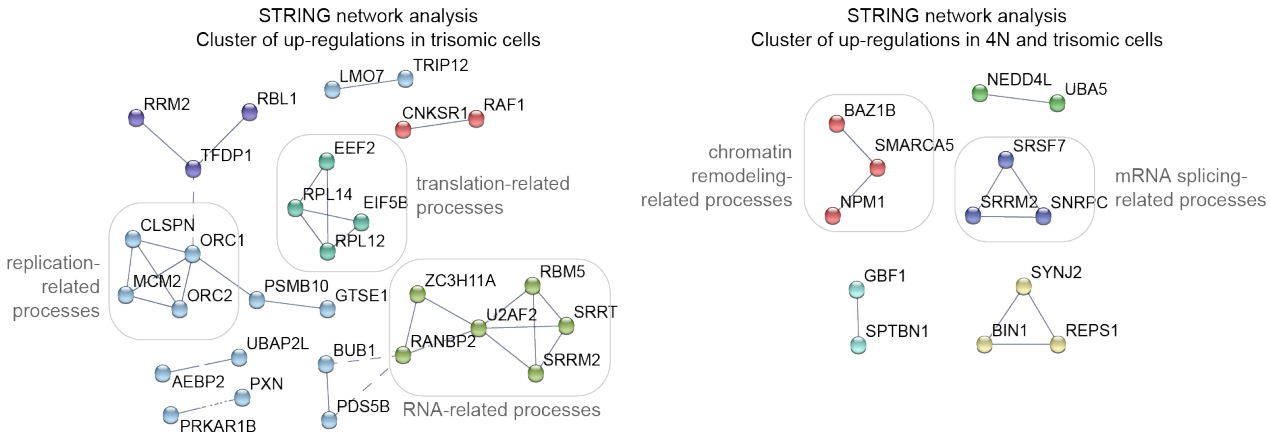

Figure 44: STRING functional network analysis of the phospho-peptides of fuzzy C-means algorithm clusters shown in Fig. 38. Nodal connections are based on a confidence value of 0.9 using experimental and database evidence. Solid lines indicate intra-network, dashed lines inter-network connections.

Taken together, these observations suggest that the most prominent changes in protein phosphorylation observed in this study correlate with a gain in chromosome number, rather than the presence of CIN. It is likely that a strong increase in chromosome mass imposes a stress on mitotic spindle organization and provokes a DNA damage response, while a numerically lower gain of chromosomes appears to elicit a response in DNA and RNA-related processes.

4.7. Targeted analysis of protein phosphorylation in DLD-1-derived cells.

As previously done for the protein abundance analysis, these un-biased analyses of the phosphoproteome dataset were also supported by targeted enrichment analysis using the CIN/cell division inclusion list, representing markers that have been already associated with CIN and mitotic cell division (Table S1). I identified enrichments of some phospho-peptides that were upregulated in both tetraploid and PTA clones, as well as in one trisomic clone (Fig. 45), whereas most clones did not show enrichments for down-regulated phospho-peptides (Fig. 45).

CIN/cell division inclusion list enrichment analysis
of the most deregulated phospho-peptides (500 phospho-peptides per condition)

phospho-peptides up-regulated in 4N and PTA cells

	signlList	totSign	nonSignlList	totNonSign	ftPValue
4N	80	324	2563	12305	0.1466766
PTA 1	94	322	2551	12317	0.0119480
PTA 3	79	260	2556	12312	0.0113770
PTA 4	62	214	2562	12306	0.0393165

phospho-peptides down-regulated in 4N and PTA cells

	signlList	totSign	nonSignlList	totNonSign	ftPValue
4N	14	82	2563	12305	0.7590456
PTA 1	12	72	2551	12317	0.7648565
PTA 3	32	139	2556	12312	0.8686990
PTA 4	33	191	2562	12306	0.8217455

phospho-peptides up-regulated in Tr7cells

	signlList	totSign	nonSignlList	totNonSign	ftPValue
4N	55	223	1326	7133	0.0735379
Tr7d1	57	204	1342	7117	0.5997863
Tr7d2	56	216	1319	7140	0.0405239

phospho-peptides down-regulated in Tr7cells

	signlList	totSign	nonSignlList	totNonSign	ftPValue
4N	37	185	1326	7133	0.3941695
Tr7d1	39	220	1342	7117	0.6436645
Tr7d2	43	185	1319	7140	0.1498234

Figure 45: Tables showing an enrichment analysis of the 500 most deregulated phospho-peptides per cell line using the CIN/cell division inclusion list. The numbers of inclusion list matches (signlList) and non-matches (totSign) were compared to random inclusion list matches (nonSignlList) and non-matches (totNonSign) in a human proteome background. Significance (ftPValue) was calculated using Fisher's exact test. Shaded areas highlight the most significant enrichments.

Filtering all phospho-peptides deregulated by at least 2-fold with the CIN/cell division inclusion list (Table S1), for closer inspection, revealed that no proteins included in the CIN/cell division inclusion list were exclusively observed to have altered phosphorylation states across all PTA clones. In contrast, I found phosphorylation for a number of proteins related to mitotic spindle and chromosome segregation to be commonly altered in both tetraploid as well as PTA clones (Fig. 46), and, to a lesser extent, in trisomic clones (Fig. 47).

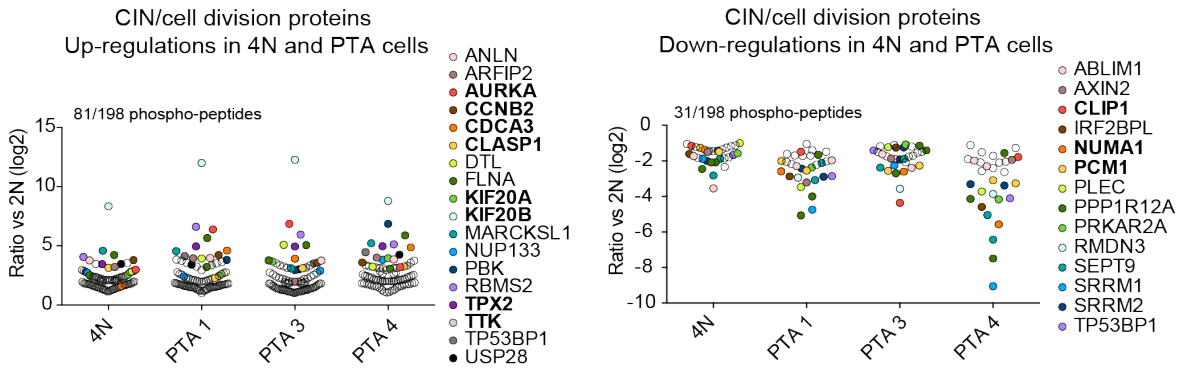

Figure 46: Dot plots showing the phospho-peptide ratios (versus parental 2N cells) of detected proteins belonging to the CIN/cell division inclusion list and showing at least 2-fold deregulation in 4N and PTAs. Dots represent significant (p≤0.05) phospho-peptide log2 ratios. Proteins related to mitotic spindle regulation and chromosome segregation are shown in bold.

These proteins included regulators of microtubule dynamics, kinetochore-microtubule interactions, centrosome function as well as spindle assembly checkpoint signaling (bold protein names in Fig. 46 and 47).

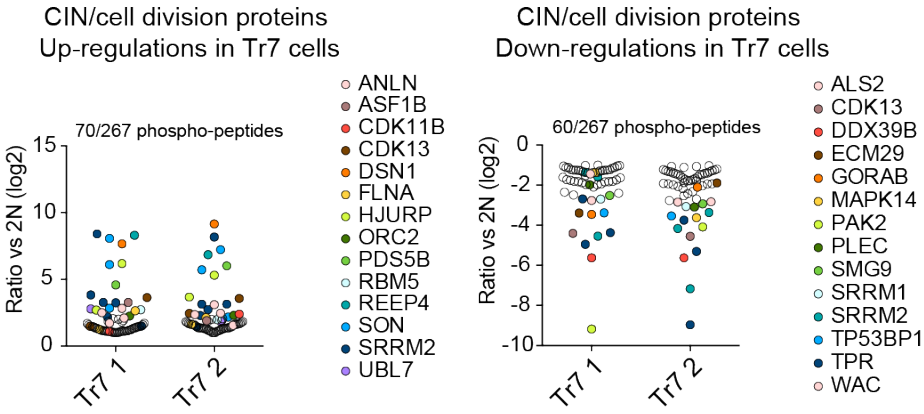

Figure 47: Dot plots showing the phospho-peptide ratios (versus parental 2N cells) of detected proteins belonging to the CIN/cell division inclusion list and showing at least 2-fold deregulation in 4N and Trisomic clones. Dots represent significant (p≤0.05) phospho-peptide log2 ratios. Proteins related to mitotic spindle regulation and chromosome segregation are shown in bold.

Network analysis of phospho-peptides jointly deregulated in 4N and PTA clones as well as in 4N and trisomic clones identified mitotic spindle- and chromatin-related processes, and, as expected for an increase in chromosome number, processes related to DNA replication and transcription (Fig. 48 lower and upper panels). Taken together, I conclude that a strong increase in

chromosome burden leads to changes in the phospho-proteome of pathways involved in chromosome segregation, possibly reflecting an increased burden on spindle formation and chromosome alignment.

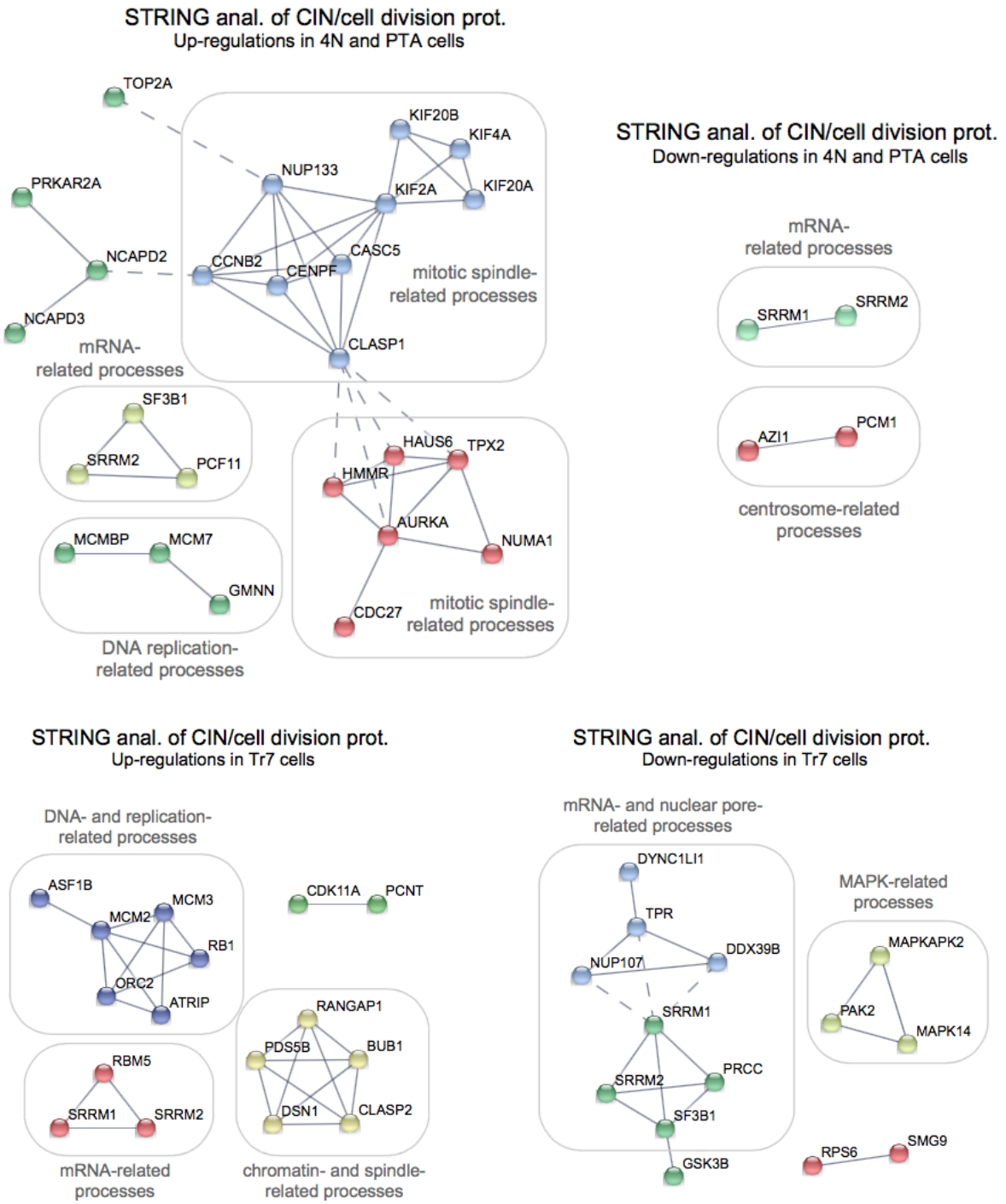

Figure 48: STRING functional network analysis of the data shown in 44 and 45. Nodal connections are based on a confidence value of 0.9 using experimental and database evidence. Solid lines indicate intra-network, dashed lines inter-network connections.

In line with the above interpretation, changes were predominantly observed in tetraploids as well as post-tetraploids and only to a lesser extent in cells carrying one additional chromosome.

As mentioned in the introduction, CIN has been observed to correlate with increased resistance to anti-cancer drugs, some of which are inhibitors of mitotic kinases [150,151](Kuznetsova AY 2015 Cell Cycle) (Lee AJ Cancer Res 2011). In a final set of experiments, I therefore asked whether inhibitors of spindle and cell cycle regulatory kinases would show a differential effect on cell survival that might be correlated with gains in chromosome number.

4.8. Drug sensitivity assays in cultures of DLD-1-derived cells.

Aneuploidy is generally associated with poor prognosis in solid tumors [9,11,151](Lee AJ Cancer Res 2011) (Walther A Gut 2008) (Carter SL Nat Genet 2006). Thus, the stratification of tumor responses according to CIN status should be considered within the context of clinical trials. With this context in mind, I used a panel of 38 well-annotated anti-cancer drugs largely targeting cell division-related protein kinases and performed drug-sensitivity assays. These assays measured intracellular ATP content as an indirect readout for cell survival [150](Kuznetsova AY, 2015, Cell Cycle). I oberserved several changes in drug resistance, which were common for tetraploid and PTA cultures (Fig. 49 and Table S3).

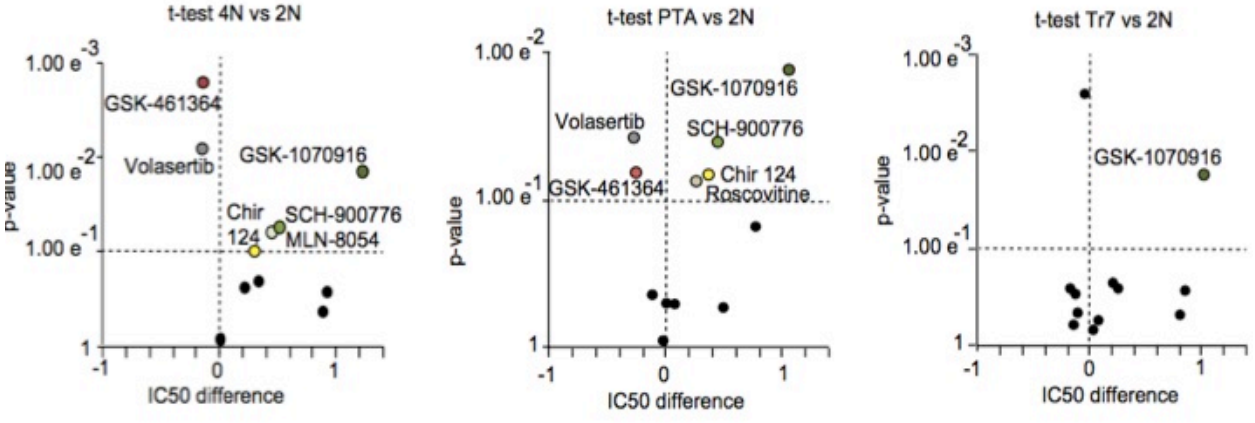

List of small-molecule inhibitors used in panels B and C

	CHIR 124	SCH 900776	GSK 1070916	MLN 8054	Roscovitine	GSK 461364	Volasertib
Target	Chk1	Chk1	AuroraB/C	Aurora A	CDK	Plk1	Plk1

Figure 49: Dot plots showing the significance (unpaired two-tailed t-test) and IC50 difference (relative to the parental diploid DLD-1 cell line, 2N) observed after applying the compounds shown in Table S3 to the indicated cell cultures. Dashed lines demark the quadrants of significant increases in sensitivity (upper left), significant decreases in sensitivity (upper right) and insignificant changes of IC50 values (lower quadrants). Data are from three biological replicates.

Specifically, I detected an increased drug resistance towards inhibitors of Aurora A kinase (GSK-1070916) [152](Adams ND J Med Chem 2010), Chk1 kinase (CHIR-124 and SCH-900776) [153,154](Tse AN Clin Cancer Res 2007) (Karp JE Clin Cancer Res 2012), and Cyclin-dependent kinases (Roscovitine) [155](Meijer L Acc CHem Res 2003) that correlated with a gain in chromosome mass in tetraploid and/or post-tetraploid aneuploidy clones. This trend was similar to a study that observed multi-drug resistance in response to aneuploidy [151](Lee et al Cancer Research 2011). Although I did not observe altered phosphorylation at phosphorylation sites regulated by Chk1 or Cdk1 [156,157](Smits VA FEBS J 2015) (M Malumbres 2014 Genome Biol) in our phospho-proteome analyses of tetraploid or PTA cells, I had observed increased phosphorylation of the Aurora A T-loop phosphorylation site [158](Evers P.A Curr Biol 2003) (Fig. 50).

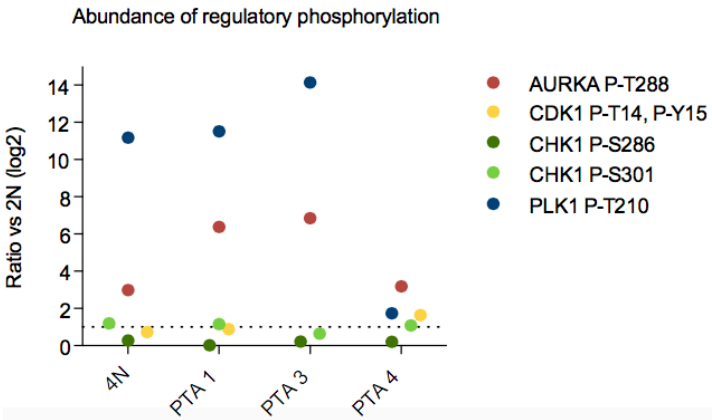

Figure 50: Dot plot showing selected detection ratios of regulatory phosphorylation sites of the centrosome and mitotic spindle kinase Aurora A (AURKA P-T288), the mitotic kinase Cdk1 (CDK1 P-T14, P-Y15), the cell cycle checkpoint kinase Chk1 (CHK1 P-S286, CHK1 P-S301) and the mitotic spindle kinase Plk1 (PLK1 P-T210). Dashed line indicated a 2-fold cutoff.

Aurora A is required for the phosphorylation and activation of the T-loop (on Thr210) of the essential spindle regulator Plk1, an important regulator of mitotic spindle formation and kinetochore function [159](von Schubert et al Cell

Rep 2015) (Fig. 49 and Fig. 52, Table S3). Most interestingly, I observed a trend towards increased Plk1 T-loop phosphorylation (at Thr210) in tetraploid and PTA clones even if this change was not always statistically significant (Fig. 50 and Fig. 51). In line with this observation, cells with strongly increased chromosome mass (4N and PTAs) showed a stronger sensitivity towards two inhibitors of Plk1 (GSK-461364 and volasertib) [160](Shin SB J Cell Physiol 2015), possibly reflecting a higher demand for Plk1 function in these cells, but not in trisomic cells.

p-values for selected phopho-peptides

Kinase, P-site	role of P-site	4N	PTA 1	PTA 3	PTA 4
AURKA P-T288	activating, T-loop	0.025	0.000	0.021	0.002
CDK1 P-T14/Y15	inhibitory	0.207	0.027	0.013	0.027
CHK1 P-S301	upon stalled replication and DNA damage	0.001	0.002	0.187	0.016
CHK1 P-S286	upon stalled replication and DNA damage	0.158	0.469	0.479	0.297
PLK1 P-T210	activating, T-loop	0.195	0.168	0.055	0.554

Figure 51: Table listing the p-values for phospho-peptide measurements shown in Figure 50.

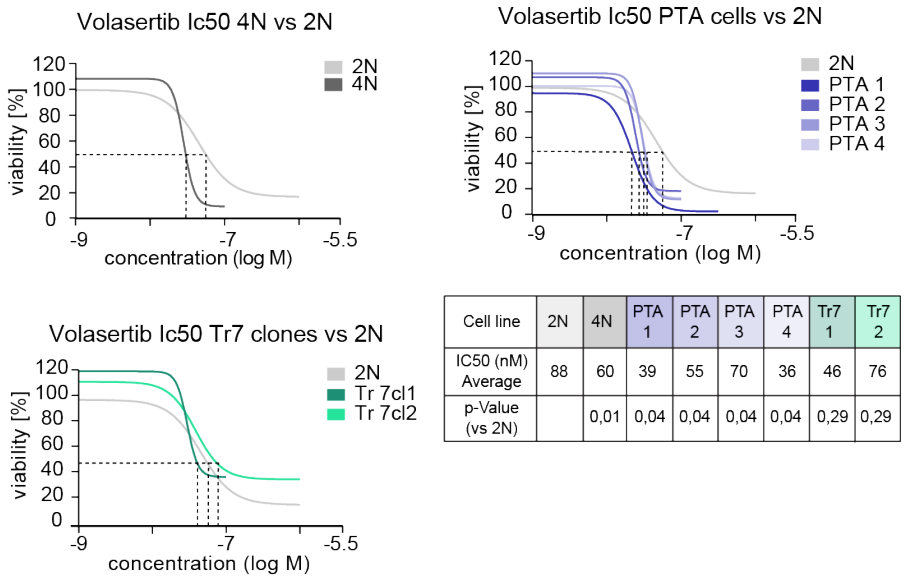

Cell line	2N	4N	PTA 1	PTA 2	PTA 3	PTA 4	Tr7 1	Tr7 2
IC50 (nM) Average	88	60	39	55	70	36	46	76
p-Value (vs 2N)		0,01	0,04	0,04	0,04	0,04	0,29	0,29

Figure 52: Graphs showing dose-response curves using the Plk1 inhibitor Volasertib on indicated cell cultures. Dashed lines indicate IC50 values. Table listing IC50 average from three biological replicates (see table S3) and p-values for indicated cell lines (unpaired two-tailed t-test).

This trend was also partially confirmed by a different approach, notably immunofluorescence microscopy (IFA) (Fig. 53). In particular, using a

phospho-specific antibody I observed a slightly higher phosphorylation at the Plk1 T-loop site in 4N and PTAs (even though this was always statistically significant), which was not accompanied by stronger staining for Plk1 protein.

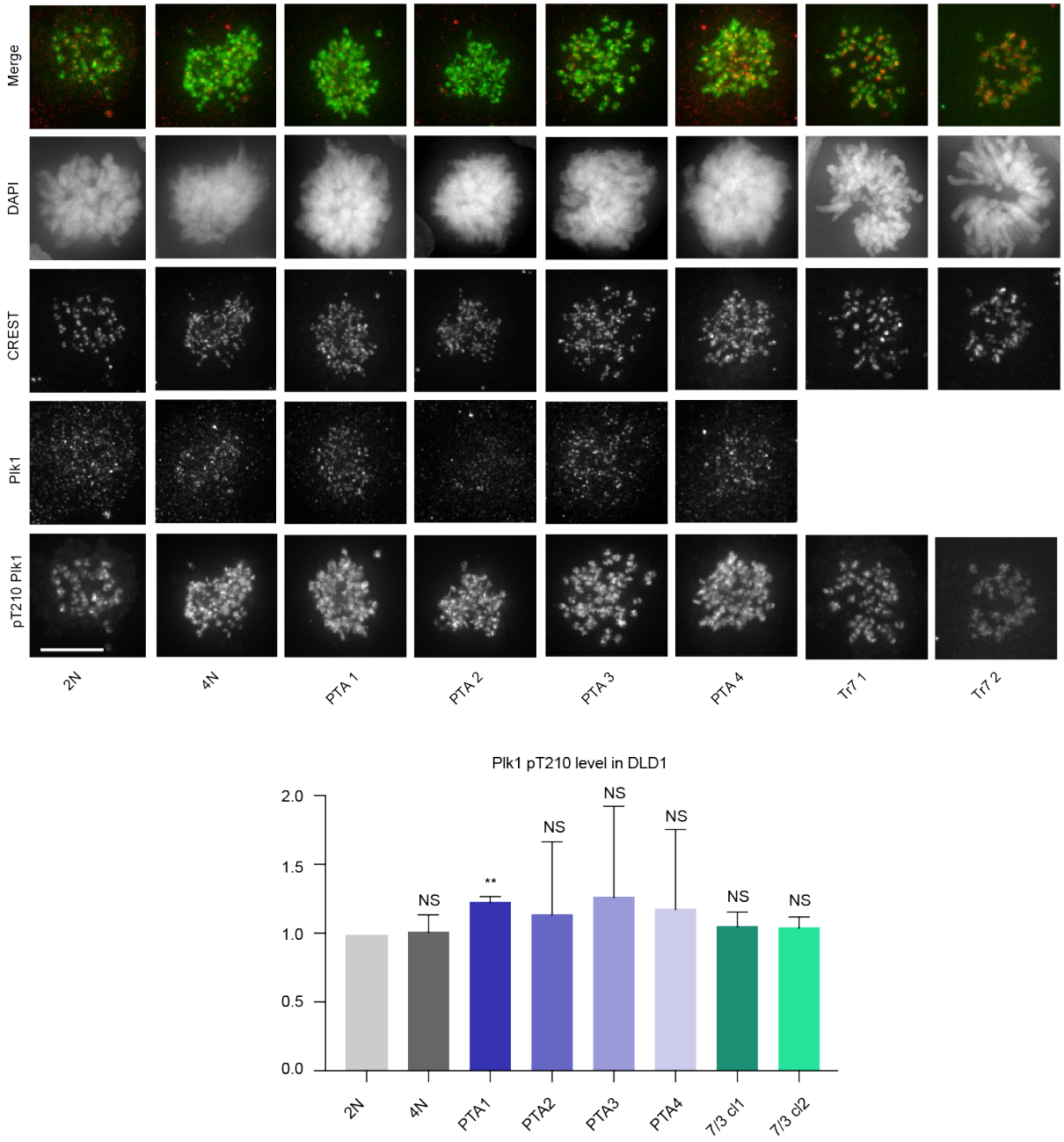

Figure 53: Upper panel: micrographs of cells stained with anti-Plk1, pT210 Plk1, CREST and DAPI. Note that in trisomic clones Plk1 staining could not be recorded, because these cells expressed histone H2B-GFP, blocking the fluorescein channel. Below panel: plot showing the quantification of pT210 Plk1 in all cell lines; normalization was done using CREST signal and ratios were calculated relative to the signals obtained for 2N cells (set to 1.0). Experiments were done in duplicates, bar represent 10 µm, two-tailed *t*-test: **P*<0.05, ***P*<0.01, ****P*<0.001 and *****P*<0.0001.

As discussed in the introduction, one factor triggering chromosomal instability is the presence of uncorrected, erroneus microtubule-kinetochore attachments, and this phenotype is linked to the presence of extra chromosomes. Higher levels of T-loop phosphorylated Plk1 could thus be explained by an increased need of the activated version of Plk1 to correct erroneous microtubule-kinetochore attachments.

In order to check whether I could detect increased merotelic attachments in cells that present an increase in chromosome mass, I also performed stainings on metaphase cells of diploid, tetraploid and PTA clones with α-tubulin and CREST antibodies (Fig. 54).

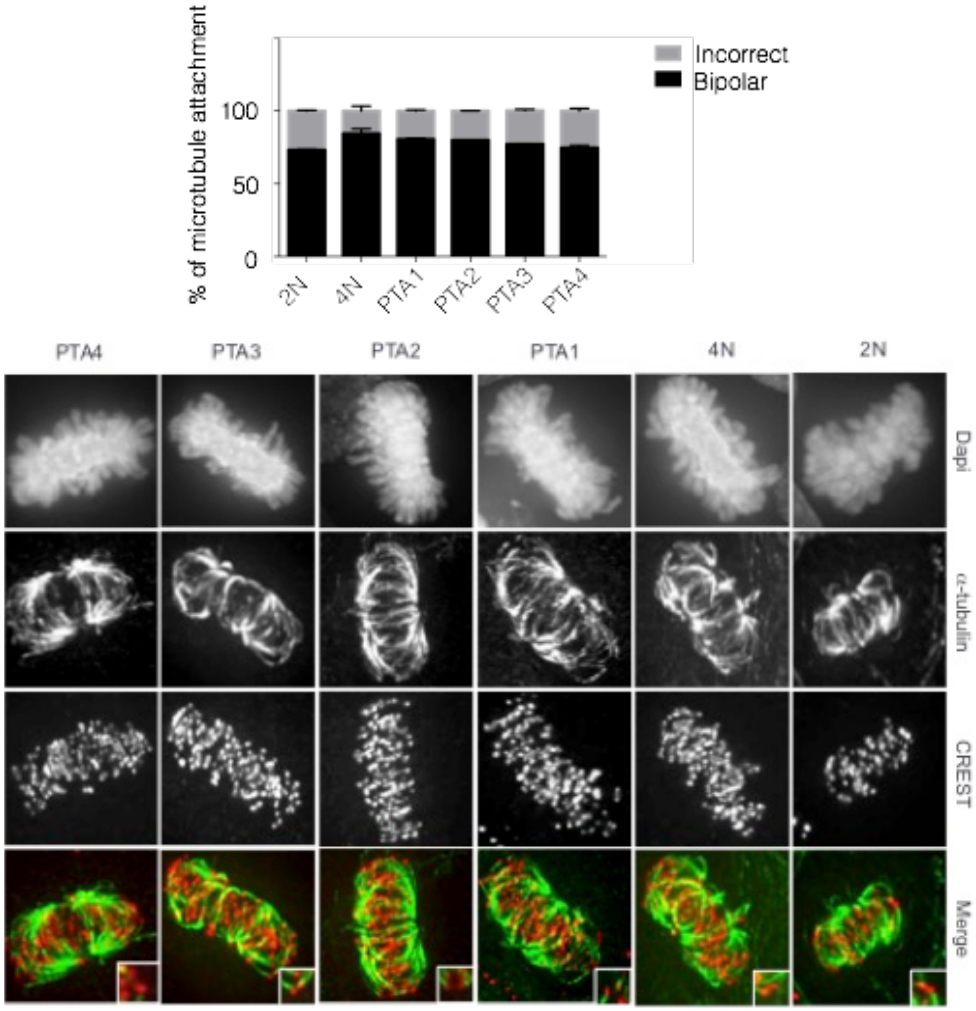

Figure 54: Upper panel: quantification of correct and incorrect attachments in non treated cells. Lower panel: micrographs of metaphase cells stained with anti- α-tubulin, CREST and DAPI.

Image analysis revealed indeed a small increase of uncorrect kinetochore-microtubule attachments, which could explain the presence of higher levels of

activated (T-loop phosphorylated) Plk1 at kinetochores. These observations suggest that the observed changes in the phosphorylation dynamics of the mitotic spindle phospho-proteome described in this study could potentially translate into differential responses to clinically used anti-cancer drugs.

5. Discussion.

The potential molecular causes triggering aneuploidy have been studied extensively, but most of the molecular mechanisms are still poorly understood. Moreover, even if the presence of aneuploidy in tumor cells has been extensively documented [116](Mitelman F. 2014 Chromosomes) (Beroukhim R. Nature 2010), it is still debated if aneuploidy fuels tumorigenesis [117,119-121](Storchova Z, et al. 2006 Nature) (Nicholson, et al. 2015) (Passerini, et al. 2016) (Santaguida and Amon 2015). Adding another level of complexity to the causality relation between aneuploidy and tumorigenesis, is CIN [15](Weaver B.A.A. Cancer cell 2007). It has indeed been proposed that CIN can both promote and suppress carcinogenesis [127,128](Jamal Hanjani 2017 N Engl J Med) (Murugaesu 2015 Cancer Discov). Thus, the relationship between aneuploidy, chromosomal instability and cancer has not yet been clarified.

In this study I aimed at distinguishing the effects of chromosome gains and CIN on protein expression and protein phosphorylation, with the hope that these studies might contribute to answer which molecular pathways are deregulated in cancer cells harboring aneuploidy and/or CIN, allowing these cells to survive. My results revealed that post-tetraploid aneuploidy cells and, to a lesser extent, trisomic aneuploid cells, displayed increased rates of mis-segregation, while tetraploid cells had a level of chromosome mis-segregation that was comparable to the diploid state. Second, in agreement with previous studies [98,99,102,105](Upender et al Cancer Res. 2004; Dephoure et al. eLife 2014; Stingele et al. Mol Syst Biol 2012; Sheltzer Cancer Research 2013), I have found that changes in chromosomal copy number had proportional effects on the levels of proteins encoded by the respective chromosomes, and that the stress resulting from extra chromosomes led to a deregulation of proteins involved in protein degradation, folding, oxidative stress response and innate immune response. Although I did not identify a proteomic signature attributable to a CIN-specific phenotype, phosphorylation data analysis revealed an increased phosphorylation of proteins related to cell cycle progression and mitosis, in all generated cell lines (PTAs, 4N and trisomic clones) *versus* parental diploid cells. Finally, in good agreement, I found two small molecule inhibitors of the key mitotic kinase Plk1 to reduce cell survival in tetraploid as well as post-tetraploid aneuploid cells. Notably, all these findings in protein expression and phosphorylation changes were not too

dissimilar in stable tetraploid and descendant unstable post-tetraploid aneuploid cells, suggesting that strong gain of chromosome mass is an important determinant of cellular response, regardless of gene balance. It could thus be that elevated chromosome number promotes adaptation, deregulation of proteomic and phospho-proteomic pathways in transformed cancer cells, regardless of the presence of CIN.

5.1. Inter cell line variation as a source of heterogeneity.

In order to pursue my purpose (and to establish proteomics methodology) I initially decided to compare a panel of 8 different cell lines showing distinct karyotype states and stability conditions [28](Gascoigne KE 2008 Cancer Cell). Proteomic analysis revealed a high level of complexity that did not allow to cluster CIN and non-CIN cell lines based on their proteome profiles. This result is in agreement with previous findings that had documented an extensive degree of interline variation [28] (Gascoigne KE 2008 Cancer Cell). This high inter-line variation, due to clonal, tissue origin or cancer type differences, could be expected to render the identification of protein expression patterns correlating with CIN difficult, at least at the experimental scale used in our pilot studies. Thus, by introducing different karyotype states in the same isogenic parental cell line I next aimed to decrease inter cell line variability and focus only on the differences caused by chromosome mass changes or the CIN phenotype.

5.2 Factors triggering of chromosomal instability.

5.2.1 Tetraploidization

In this study I used DLD-1colon cancer cells, which have essentially a diploid karyotype and show microsatellite instability (MIN). It has been previously shown that a tetraploidy state can be a source of chromosomal instability, inducing both aneuploidy and instability [83,161](Lv et al., 2012) (Sansregret et al., 2011). The data presented here supports these previously reported observations. Indeed, after one month of propagation in culture, posttetraploid cells displayed a broad variety of karyotypes. Observed karyotypes ranged from near-triploidy to hyper-triploidy, and median chromosome numbers varied between different posttetraploid isolates.

Therefore, transient passage through a tetraploid state can lead to variable aneuploidy.

It is important to consider that DLD-1 cells show a p53 deficient status – Ser241 ➔Phe– [135](Nanda R. Rodrigues Proc. Natl. Acad. Sci USA 1990), and a recent study supports the concept that the absence of a p53 response could favor the capacity of tetraploid clones to proliferate after chromosome mis-segregation. In particular, colon cancer microsatellite instable (MIN) HCT116, upon tetraploidization, exhibited a CIN positive phenotype [150](Kuznetsove AY et al 2015 Cell cycle). These considerations could explain the data from the time lapse experiments presented here, showing that PTAs have the capacity to proliferate, even after the completion of a cell division, showing a spontaneous chromosomal mis-segregation event. In contrast, I found that cells carrying small and defined chromosome mass gains, notably trisomic clones, showed a less pronounced CIN phenotype. This is in line with previous observations showing that the addition of single chromosomes can both drive and suppress the emergence of instability [120,162](Sheltzer JM Cancer Cell 2017) (Passerini V 2016 Nat Comm).

In conclusion, the emergence of a CIN phenotype after tetraploidization confirms previous observations showing that doubling of the genome can fuel chromosomal instability [80](Storchova Z 2008 Journal of cell science) and that loss of functional p53 favors the capacity of aneuploid cells to proliferate [150](Kuznetsove AY et al 2015 Cell cycle).

5.2.1 Erroneous mitosis is a source of CIN.

Defective mitosis is a frequent cause of CIN. Consistent with immunofluorescence experiments, I found that chromosome mis-segregation was elevated in post-tetraploid cells. Additionally, karyotype analyses indicated the presence of numerous aberrations in PTAs cells, in particular in PTA1 and PTA3; meanwhile in PTA2 and PTA4 less frequent copy number alterations were likely masked by clonal heterogeneity due to increased chromosome mis-segregation rates. Moreover, post-tetraploids displayed an increase in the frequency of lagging chromosomes. Anaphase lagging may serve as indirect evidence for an elevated frequency of merotelic attachments [163](Cimini et al., 2001). Importantly, merotelic attachments are not corrected by the SAC, and have thus been postulated to constitute a major cause of CIN in cancer cells [163] (Cimini et al., 2001; reviewed in Gregan et al., 2011). Therefore,

an increase in merotely, even in presence of a functional SAC, may lead to chromosome mis-segregation and aneuploidy. However, even if segregated to a proper daughter cell, the former lagging chromosome can be resolved into a micronucleus that then undergoes defective replication, resulting in the accumulation of DNA double- strand breaks in the subsequent interphase [92,121](Crasta et al., 2012) (S. Santaguida and A. Amon 2015 Nature Review). This can potentially cause fragmented chromosomes in the following mitosis. Taking together, the increased occurrence of lagging chromosomes in post-tetraploids is likely a manifestation of an increase in the frequency of merotelic attachments. Another mitotic defect prominently observed in our post-tetraploids, is occurrence of anaphase bridges. Similar to lagging chromosomes, anaphase bridges often break in mitosis and result in micronucleation; these micronuclei contain defective nuclear pore complexes and show deregulated gene transcription [164](Hoffelder et al., 2004). In support of this notion, I observed a significant increase of the formation of micronuclei, anaphase bridges and lagging chromosomes in PTAs and, less prominently, in Tr7. Numerous reasons can cause anaphase bridges: perturbed DNA replication [165,166](Chan et al., 2009) (Sofueva et al., 2011), defective homology-directed DNA repair [167,168](Acilan et al., 2007) (Laulier et al., 2011) and impaired sister chromatid cohesion [169](Wang et al., 2008). Notably, I detected the increase of UFBs positive for the marker BLM. UFBs originate either from DNA catenae or from replication or recombination intermediates that can be formed, for example, during double strand repair; thus, the occurrence of UFBs can be indicative of un-replicated or abnormal DNA structures [144](Chan, K 2011 Semin. Cell Dev. Biol). However, when I checked for alterations in the expression of proteins related to DNA replication, such as MCM and ORC complexes, I could not detect any significant deregulation (with the exception of one PTA clone). Altogether, it seems plausible that increased merotelic kinetochore attachments and/or defective DNA replication may be responsible for persistent chromosomal instability in these cells and the increase of mitotic errors in post-tetraploid cell lines.

5.3 Intra cell line heterogeneity influences cell proteome response to CIN.

By using a model where different cell lines share the same isogenic background, I aimed to eliminate the anticipated interline variation. However,

it was striking to see that although these karyotypically distinct cell lines were derived from a common ancestor, they could exhibit multiple proteome responses after CIN had occurred (Fig. 24). This is likely reflecting the presence of CIN itself, as CIN leads to gains, losses or rearrangements of (partial or entire) chromosomes during cell division, contributing to the constant evolution of karyotypes [7,125](Lengauer, et al. 1998) (McGranahan, et al. 2012).

5.3.1 Common "aneuploidy stress" proteome signature.

Previous comparative analyses of genomic, transcriptomic and proteomic profiles in aneuploidy cell lines yielded contradictory results [2,103,136,170](Torres at al 2007; William et al 2008; Kvitek et al 2008; Stenberg et al 2009). In particular, both positive and negative correlations between the presence of extra chromosomes and corresponding protein levels have been reported [98,106,131,137] (Torres et al 2010) (Pavelka et al 2010) (Stingele et al 2012 Mole Syst Biology) (Rebecca R. Beach Cell 2017). There is agreement, however, that levels of subunits of protein complexes are generally adjusted to maintain the correct stoichiometry [106](Torres et al 2010). In the present study, I have found that changes in chromosomal copy number exerted proportional effects on the levels of proteins encoded by the respective chromosomes, in line with the lack of a global dosage compensation system for autosomal aneuploidy in human cells. Notably, when I analyzed the relative abundance of protein complexes, such as MCM and ORC proteins, I noticed that all subunits of these complexes showed very similar relative abundances. These findings are in line with the conclusion that, in aneuploid cells, the stoichiometry of protein complex subunits is maintained. Every protein encoded by an unbalanced chromosome that functions in a protein complex and lacks its binding partner (or partners) risks to form aggregates and be insoluble; hence, such proteins are degraded [104](Tyedmers J. 2010 Nat. Rev. Mol. Cell.). In agreement, I found that the relative abundance of proteins functioning in protein proteolysis, protein folding and oxidative stress responses were upregulated in the presence of aneuploidy. Notably, this effect concerned only cell lines showing big chromosome mass gain, such as tetraploidy and PTAs, but not cells with minor chromosome gains (i.e. the trisomic lines).

An unbiased proteome analysis on generated cell lines revealed yet another change in the protein levels triggered by massive chromosome

increase, namely the deregulation of type I interferon-signaling components in tetraploid or post-tetraploid cells. Previous studies reported that the presence of chromosomal lesions leads to an increased abundance of cytoplasmic DNA fragments, which then trigger a DNA damage response and thereby the induction of type I interferon signaling [115,140,142,143](Samantha et al., Immunity, May 2016) (Erdal et al. Genes Dev March 2017) (Shen et al. Cell Reports 2015) (Karen J Mackenzie Nature 2017). This hypothesis has been further confirmed by BrdU staining, in non-denaturing conditions, that allowed me to detect an increased presence of cytoplasmic ssDNA. Moreover, a further observation tending to support this hypothesis was obtained by stainings with antibodies against BLM, revealing an increased frequency of UFBs in the trisomic, tetraploid and PTA cells, compared with controls, which could be indicative of double strand repair [142](Erdal et al. Genes Dev March 2017). Interestingly, one study suggested that an IFN-related DNA damage resistance signature (IRDS) is associated with resistance to DNA-damaging cancer therapy, due to a constitutive activation of the IFN pathway [141](Weichselbaum et al. PNAS Nov 2008). It could thus be that elevated chromosome numbers promote adaptation and immune evasion in transformed cancer cells. In favor of this interpretation, a recent study from the Amon laboratory shows that cells with complex karyotypes, raised after chromosome mis-segregation, produce pro-inflammatory signals that then promote their clearance by the immune system [86](Santaguida S. 2017 Dev Cell). Moreover, a link between the presence of micronuclei and innate immunity has recently been reported [115](Karen J Mackenzie Nature 2017). In particular, cGAS, a cytosolic sensor of double-stranded DNA, was shown to be activated by DNA damage and found to localize to micronuclei arising from lagging chromosomes or anaphase bridges. The presence of cytosolic dsDNA structures would thus lead to a proinflammatory response and stimulate the immune system [115] (Karen J Mackenzie Nature 2017). The observed IFN proteins overexpression in the generated PTAs and polyploidy cells, and as well in Hela S3, SW480, SW837, HT29, nicely correlate with the proposed model.

These data are in line with the current understanding of the immediate and long-term effects of chromosome mis-segregation and aneuploidy, in particular with the concept of *aneuploidy-associated stresses*. It has been proposed that a mixture of common features and traits, such as transcriptional and post-transcriptional responses and proteotoxic stress, are responsible for the effects of aneuploidy on cellular fitness [88-90](Santaguida S et al. Genes Dev.

2015) (Dominigues PH Cancer Res 2017) (Torres EM 2008 Genetics). Thus it could be that the stress resulting from strong increases in chromosome numbers leads to a deregulation of proteins involved in protein degradation and folding, as well as an oxidative stress response, and as shown recently, also to an IFN response.

5.3.2 Aneuploidy induces clonal heterogeneity in response to CIN

Since massive increases in chromosome numbers brought about a common proteome response, as discussed in the previous paragraph, I decided to check for the existence of common CIN-specific gene imbalances, through focus on a CIN-inclusion list (i.e. a list comprising proteins previously implicated in CIN). Unfortunately, however, I could not detect a common proteomic answer and/or the deregulation of CIN-specific genes in response to an increase in CIN phenotype. A possible explanation could be that a CIN signature is masked by the general deregulations that were triggered by an increase in ploidy, or due to clonal heterogeneity caused by elevated chromosome mis-segregation rates in CIN cells. Alternatively, changes may simply have been too small to detect. Importantly, however, the fact that the major changes observed in CIN cells were also characteristic of the tetraploid progenitor cell line suggest that strong gains of chromosome mass are an important determinant of cellular response, regardless of gene balance. In agreement with this hypothesis, I have found that changes in protein expression and phosphorylation (discussed below) are not very dissimilar in tetraploid and descendant post-tetraploid aneuploid cells.

5.4 Phospho-proteome changes in mitotic proteins might reflect response to massive chromosomes mass gain.

Since many of the proteins regulating mitosis are kinases I decided to also investigate possible phospho-proteomic alterations in the generated cell lines. In agreement with the previous conclusion emerging from this study, i.e. that chromosome mass increase is a stronger determinant of proteomic alterations than CIN, I found that changes in protein phosphorylation correlated primarily with the increase in ploidy. This suggests that readily detectable changes in protein phosphorylation occur in response to the challenges imposed by a large number of chromosomes, rather than by an increase in chromosome

mis-segregation rate. Notably, through unbiased phospho-proteome analysis I found that in PTAs and tetraploid cultures alterations in protein phosphorylation concerned processes directly associated with regulation of transcription and translation pathways. Previous work on aneuploid cells had identified several responses, such as the increase of oxidative and proteotoxic stress and DNA damage as well, and these were reflected in transcriptional responses [95,96](Sheltzer J.M. 2012 PNAS) (Durrbaum M. 2014 BMC Genomics). This concept is in line with the observations described in the unbiased proteome analysis showing the up-regulation of protein lysis, folding and oxidative stress.

Moreover, unbiased phospho-proteome analysis performed on the generated cell lines revealed yet another change in the mitotic spindle and, generally, in the cell cycle. Single chromosome gain in trisomic cells showed the same effect on the phospho-proteome even if less pronounced. This conclusion was further confirmed when I performed targeted analysis, using the CIN/cell cycle inclusion list. The significant enrichment of the above mentioned pathways in both tetraploid and PTAs cell lines leads me to the hypothesis that large chromosome mass gains significantly increase the burden on spindle check point proteins and mitotic proteins. This is in line with the increase, even if very subtle, of erroneous k-MT attachments observed in these cells.

It is important to notice that CIN/Cell cycle related proteins were affected only at the level of phosphorylation, while no corresponding deregulation was detected in the relative abundance of the corresponding proteins. This difference could also be confirmed by other techniques, notably IFA. Different explanations can be proposed for this interesting difference in responses. The changes in protein levels could be very subtle and weak, thus difficult to detect, but at the same time they could act in a synergistic fashion. On the other hand, changes in phosphorylation could exert major physiological effects. Plk1 levels, for example, were not detectably affected; on the other hand, increased phosphorylation of Plk1's T-loop suggested an increased activity, as shown by both IFA and proteomic data. Another possible explanation is that PTAs, as well as their tetraploid progenitor cells, preferentially regulate activation-deactivation of proteins previously associated with cell division, rather than their relative abundance.

Notably, between differentially phosphorylated proteins included in the CIN/Cell cycle list I observed a strongly increased phosphorylation of the mitotic protein TPX2, as well as the T-loops of the spindle kinases Aurora A and Plk1. TPX2 is an important regulator of the mitotic spindle, and it activates the mitotic kinase Aurora A (AURKA) through stimulation of autophosphorylation. It is interesting, therefore, that TPXw was reported to be frequently deregulated in aneuploid cancer cells [171](de Castro & Malumbres, Genes & Cancer 2012), showing strong correlation with CIN [9](Carter et al. Nat. Genet. 2006). Aurora-A, in turn, is required for the activation of the mitotic spindle regulator PLK1 [172](Erikson et al. PNAS 2002) (Macurek et al. Nature 2008) and both kinases are highly active in aneuploid cancer cells. These observations therefor, support the notion that increases of chromosome mass can lead to hyper-activation of key regulators of the mitotic spindle. This in turn could make cells sensitive to changes affecting spindle function and render them prone to subsequent elevation of chromosome mis-segregation rates.

5.5 Targeting CIN therapeutically.

The emergence of CIN can have important implications for the resistance of cancer cells to therapy, and this for three main reasons: first, innate resistance, perhaps reflecting a necessity of cancer cells to tolerate chromosomal instability and aneuploidy, may provide a higher threshold of tolerance to some therapeutic agents; second, acquired resistance, due to a high intra cell line variation (generated prior to treatment), provides a high probability that a sub-clone carrying protection against the therapeutic agent is already present in the tumor culture [173](Greaves and Maley 2012); finally adaptive resistance, where a resistant sub-clone may not exist before to treatment, but may be generated due to the selective pressure following therapy treatment.

At the same time, as already anticipated, CIN and aneuploidy can have a negative impact on cellular fitness. In particular, some studies analyzing CIN levels in relation to tumor outcome found that high levels of CIN were associated with better outcomes compared to intermediate levels of CIN [9,130](Carter SL. Nat Genet 2006) (Birbak NJ 2011 Cancer Res). However, as reported in the same study, examples of ovarian, gastric and lung cancers presented the poorest outcome, even though they also showed an

intermediate level of CIN, suggesting a complex relation between survival outcome and presence of instability [130](Birbak NJ 2011 Cancer Res). The idea that CIN can have an ambivalent role in cancer treatment finds a good agreement also with my findings. I showed that two small molecule inhibitors of Plk1 reduced cell survival in tetraploid as well as post-tetraploid aneuploid cells, when compared to diploid parental cells, but not in trisomic clones. These data suggest that a pronounced increase in chromosome number imposes a stress on cell that is already present in tetraploid progenitor cells and that is permissive towards CIN in descendant aneuploid cells. On the other hand, additionon of a single chromosome in the trisomic lines brought about a less pronounced CIN phenotype and also a reduced survival rate upon cancer drug treatments.

In conclusion, the relation between CIN and prognosis after drug treatments is not yet clear. Thus, much further work will be required to fully understand the mechanisms behind CIN, and to decipher how CIN contributes to cancer progression. The hope remains that a better understanding of these processes will eventually lead to better cancer treatment.

6. Materials & Methods

6.1 Experimental approaches.

6.1.1 Culturing of cell lines.

Colon carcinoma lines HCT116, RKO, HT29, SW480, SW837 (a gift from Dr. Steven Taylor, The University of Manchester, UK) were cultured as previously described [28](Gascoigne KE 2008 Cancer Cell). HeLa S3 cells, were grown in DMEM-Glutamax medium (Invitrogen, CA, USA), supplemented with 10% heat-inactivated fetal calf serum (FCS) (PAN Biotech, Aidenbach, Germany) and penicillin-streptomycin (Pen-Strep; 100 IU/ml and 100 mg/ml, Gibco Life Technologies, Zug, Switzerland). hTERT-RPE1 cells and were cultured in F12 DMEM (Sigma Aldrich, MO, USA) supplemented with 10% heat-inactivated FCS, L-glutamine (2 mM; PAN Biotech, Aidenbach, Germany), sodium bicarbonate (0.35%; Sigma-Aldrich, MO, USA) and Pen-Strep. DLD-1 2N and 4N were kindly provided by Dr. Spiros Linardopoulos and maintained according to the supplier's recommendations [63](Drosopoulos K. 2014 Nature Communications). H2B-GFP cultures were generated by retrovirus transduction, the plasmid was pLPCX based, a gift from Dr. Steven Taylor [28](Gascoigne et al. Cancer Cell 2008), selected in presence of 2 μg/ml puromycin for 72 hours and maintained after in presence of 0.5 μg/ml puromycin. All lines were grown at 37°C in a humidified 5% CO_2 incubator. DLD-1 PTA and trisomic clones were generated as described below.

6.1.2. Generation of trisomic and PTA clones

To generate DLD-1 containing an additional chromosome 7, microcell fusion was performed by microcell-mediated chromosome transfer, in collaboration with Dr. Zuzana Storchova, as previously described [120](Passerini V. 2016 Nat Commun.). Clonal populations arising from single cells after chromosome transfer were isolated and further expanded in presence of 2 μg/ml puromycin and G418 0.2 mg/ml.

Tetraploid DLD-1 populations were kindley provided by Dr. S. Linardopoulos and generated as indicated previously [63] (Drosopoulos K. 2014 Nature Communications). Spontaneously arising posttetraploid aneuploidy (PTA) clones were derived from a tetraploid DLD-1 parental culture by sorting

according to DNA content, using a BD FACS Aria cell sorter. 4N cells were harvested in trypsin, washed in phosphate-buffered saline (PBS), and resuspended for 30 min at 37° in 50 mg/ml RNase A and 1 mg/ml propidium iodine. After sorting, single cells were placed into three 96-well plates and cultured in medium without antibiotics. After visual inspection to ensure the presence of single cells and 1 mo of clonal expansion, multiple clones were obtained and four could be validated, by FACS, aCGH, and chromosome spreads, as PTA clones. (see below).

6.2 Cell line characterization

6.2.1. Chromosome spreads

The cells were treated with 50ng/ml colchicine (Sigma-Aldrich) for 5 hours to depolymerize microtubule. Cells were then collected and swollen in 75 mM KCl in a 37°C water bath for 15 minutes, fixed drop by drop with iced cold Carnoy solution (75% methanol and 25% acetic acid) and spread on a glass slide. The slides were dried at 42°C and stained with DAPI dye (Life Technologies) or further stained by whole chromosome FISH.

6.2.2. Whole chromosome FISH

Multicolor FISH was performed with a DNA probe mixture according to the manufacture (Chromosome specific painting probe kit, ChromBios GmbH, Nussdorf, Germany). We used probes directly label with red fluorochrome for chromosome 3 and 5 and probes label with digoxin for chromosome 4 and 7. In brief after chromosome spread cells were incubated with probe mixture (1ml each probe and HybMix buffer up to 10ml), coverslip was applied and sealed. After denaturation at 72° for 6 minutes slides were kept at 37° in a humid chamber over night. Coverslip was then sucked off and slides were washed for 5 minutes in 2X SSC solution, then for 1 minute in prewarm 70° 0.4X SSC 0.1%Tween solution and finally to 4X SSC 0.1% Tween solution for 5 minutes at room temperature. The slides were then incubated at least 30 minutes at 37° with 100ml FITC Mouse Anti-Digoxin (Jackson ImmunoResearch) solution (1:300 in 4X SSC/0.1% Tween). Slides were finally washed twice in 45° prewarm 4X SSC/0.1% Tween solution for 5-10 minutes.

Finally DAPI staining was performed. The analysis was carried out using Fiji for visual inspection of the images.

6.2.3. Fluorescent microscopy, image processing, quantification and live cell imaging.

Cells were grown on coverslips and fixed in PTEMF buffer (20 mM PIPES, pH 6.8, 0.2% Triton X-100, 10 mM EGTA, 1 mM MgCl2, 4% formaldehyde). Z-stacks of randomly selected cells were acquired using a DeltaVision microscope (GE Healthcare) on an Olympus IX71 base (Applied Precision, WA, USA), equipped with a Plan Apochromat N 60x/NA1.42 oil immersion objective (Olympus) and a CoolSNAP HQ2 camera (Photometrics). Deconvolution and projection were done using SoftWorx software (GE Healthcare). Statistical analysis, were done from 2-3 independent experiments and parametric t-test two tails was done with GraphPad Prism software. Standard deviation (SD) is represented by error bars.
For time-lapse imaging, cells were imaged using a Nikon ECLIPSE Ti microscope equipped with a CoolLED pE-1 illumination system and a 20x/NA0.75 air Plan Apochromat objective (Nikon) in a climate-controlled environment. Images were acquired every 9 minutes for 72hs. MetaMorph 7.7 software (MDS Analytical Technologies, Sunnyvale, CA, USA) was used for acquisition and processing of data.

6.2.4. Array-comparative genomic hybridization

Array-comparative genomic hybridization (aCGH) was performed as previously described (Juskevicius, D. et al 2016 Leukemia) (Ruiz, C Proc Natl Acad 2011), with minor modifications. In brief, 1 µg of sample DNA (cell lines DLD1 2N, 4N, PTA and trisomic clones) and equal amounts of female reference genomic DNA (Promega 46/XX, Madison, WI, USA) were digested with DNaseI to a size range of 200-500bp. Subsequent labelling of sample and reference DNA with Cy3-dUTP and Cy5-dUTP, respectively, was performed with the BioPrime® Array CGH Genomic Labeling System (Invitrogen, Carlsbad, CA, USA). Labelling efficiency was quantified by measuring the specific activity of the incorporated dyes with a Nanodrop (Thermo Fischer Scientific, Waltham, MA, USA). Reference and sample DNA were mixed and hybridized to 180k CGH arrays (Agilent Technologies, Santa Clara, CA, USA) for 24 hours in a rotating

oven at 67ºC. Microarray slides were scanned with the Agilent 2565C DNA scanner and images were analysed with Agilent's Feature Extraction using default settings. Feature extracted array CGH data were evaluated using Agilent's CytoGenomics software v3.0.1.1. Aberrations were called with the aberration detection algorithm ADM2 set to a threshold of 12.0, with Fuzzy Zero and GC-content (window size: 2kb) correction. A minimum of three probes was necessary to call an aberration.

6.2.5. Cell proliferation assay

All the compounds were dissolved in 100% DMSO. Cells were dispensed in a 384-well plate at optimal density. Compound diluition series was performed using Biomek FX Lab Auomation Workstation, the concentration range of 0.32 nm to 32 µM, and 5 µl of compound dilution was added to the cells after 24hours. After 72 hours 25 µl of ATPlite 1Step™ (PerkinElmer, Groningen, The Netherlands) solution was added to each well. Luminescence read out was performed on an Envision™ multimode reader (PerkinElmer, Waltham, MA, USA). IC50s were fitted by non-linear regression using XLfit™5. A two-tailed Student's t-test was performed to determine whether differences in sensitivity (ΔpIC50) were statistically significant (pValue < 0.1).

6.3 Proteome and phosphoproteome analysis.

6.3.1. Sample preparation and Tandem Mass Tag labeling

Cells were cultured as described before and synchronized in G2/M phase incubating cells 24 hours with thymidine 2mM and subsequentially with STLC 10mM for 12 hours. Cells were collected by mitotic shake off and lysate in 8M Urea (Sigma), 0,1M ammonium bicarbonate in presence of phosphatase inhibitors (Sigma P5726&P0044). From each cell 1 mio cells were collected by mitotic shake off, centrifugate and cell pellets were washed twice with PBS. Cells were lysed in 200 µl lysis buffer (2% sodium deoxycholate (SDC), 0.1 M ammoniumbicarbonate) using strong ultra-sonication (two cycles of sonication S3 for 10 seconds, Hielscher Ultrasonicator). Protein concentration was determined by BCA assay (Thermo Fisher Scientific) using a small sample aliquot. 50µg of proteins were digested as described previously [138](Ahrné E. 2016 J. Proteome Research). TMT 10 plex labeling procedure, protein

identification and relative abundance calculation were extensively already described [138] (Ahrné E. 2016 J. Proteome Research). In brief protein relative quantification was performed using the in- house developed SafeQuant R package. This analysis included adjustment of reporter ion intensities, global data normalization by equalizing the total reporter ion intensity across all channels, summation of reporter ion intensities per protein and channel, calculation of protein abundance ratios and testing for differential abundance using empirical Bayes moderated t-statistics. Finally the calculated p-values were corrected for multiple testing using the Benjamini–Hochberg method.

6.3.2. Phosphopeptide enrichment

Phosphorylated peptides were selectively enriched by titanium dioxide beads. Cells were cultured and synchronized as described in previous section. 2mg of proteins were lysate, digested and clean up with C18 column before the following phosphopeptide enrichment. A piece of C18 material was plugged at the constricted end of a Mobicol columns (Mobitec) tip, and an equivalent amount of 2 mg of titanium dioxide resin (Sachtopore) was transferred to each of the microcolumns for 2mg of peptides. The microcolumns were washed with 200 µl of HPLC water (Chemie Brunswick), subsequentially in Methanol (Sigma) and finally Buffer A (mixture of 80% Acetonitrile (Thermo Scienitfic) and 2.5% trifluoroacetic acid (Pierce) saturated with phtalic acid 100mg/ml) freshly prepared. Digested peptides were redissolved in 300µl Buffer A and incubate to resin for 35 minutes using head rotator, allowing phosphorylated peptides to bind to the titanium dioxide beads. The beads were spin-down, the flow-trough containing non phosphopeptide was kept, and after several washing with Buffer A, Buffer B (mixture of 80% Acetonitrile and 0.1% trifluoroacetic acid) and Buffer C (0.1% trifluoroacetic acid), phosphopeptide were elute with 0.3M ammoniumhydroxide. Elute was acidified at pH below 2.5 with 2M HCl and 5% trifluoroacetic acid). Before LC-MS analysis sample were further purified with C18 column.

6.3.3. Enrichment analysis

Relative protein quantification was performed, as described above, for all cell-lines, using the DLD-1 2N cell-line as control. The quantified proteins were sorted by increasing p-value and the 300 most significantly deregulated

proteins for each cell-line were subject to functional enrichment analysis. To this end, Biological Process Gene Ontology (GO) (Ashburner et al.) annotations were mapped to all identified proteins using the R package *GO.db* v.3.4.1. Next, GO-term enrichment was investigated for each set of 300 deregulated proteins with respect to the set of non-deregulated proteins. Here, the R package *topGO* was used, setting the nodeSize filter to 10 and calculating enrichment p-values for each GO-term using a one-sided Fisher's exact test [174](Alexa et al.).
Similarly, enrichment of CIN/Cell cycle INCLUSI0N LIST, OGs and TSGs amongst deregulated proteins, with respect to the set of non-deregulated proteins, was assessed using a one-sided Fisher's exact test. CIN/Cell cycle inclusion list was created compiling protein hits identified from previous studies. In particular it included the protein identifier from CIN70 gene expression list [9](Carter SL Nat Genet 2006); 572 validated mitotic genes from mitocheck consortium http://www.mitocheck.org [146](Neumann B 2010 Nature); and finally all the identifiers corresponding to mitotic and cell cycle related GO terms (Included GO identifiers: GO:0007094; GO:0007051; GO:0005828; GO:0005813; GO:0007059; GO:0005813; GO:0007049; GO:1905115. Annotation source http://www.uniprot.org. OGs and TSGs list (550 in total) was previously published in Davoli T 2017 Science.

7. Supplementary material

7.1. Supplementary table

Supplementary table S1: Tumor suppressor (TSG), oncogene (OG) and Chromosomal instable inclusion list

TSGs

TP53	NAA25	CSDE1	RNF43	SOX21	SRSF11	ID3
PTEN	MLLT4	PRRC2C	ARHGAP35	CCDC144NL	MKRN1	SMAD2
CDKN2A	PHF6	HLA-DRB1	ZC3H13	LUC7L3	TYRP1	NOTCH2
ARID1A	TCF12	SESTD1	RASA1	RPL5	VPS13A	TBL1XR1
APC	KMT2A	CD58	STK11	AMBRA1	PRKRA	ZFP36L1
PBRM1	DNER	ZNF319	CDKN1A	CSNK2A1	NCOR2	SMARCB1
RB1	MGA	PTPRK	EP300	ZMYM4	DAAM1	RBMX
VHL	CYLD	CHD3	CDKN1B	AXIN1	PUS7	AJUBA
NF1	TMCO2	RPL18	ARID1B	FAS	BTG3	TET2
MAP3K1	HS6ST1	PPM1D	B2M	INPPL1	PRPF40A	CDK12
SMAD4	GIGYF2	BRE	KDM5C	EPHA2	NIPBL	ELF3
KDM6A	TP53BP1	SPCS1	IL32	HERC1	SLC23A2	WT1
GATA3	CCDC88A	SPSB2	FUBP1	DACH1	CDC27	KEAP1
ARID2	EIF2AK3	TMPO	TGFBR2	PTCH1	KCNT2	PLEKHA6
SETD2	USP9X	ZNF750	KANSL1	CNOT3	MOAP1	HLA-B
KMT2D	GSE1	TMEM30A	BCOR	CTDNEP1	GAPVD1	NF2
NPM1	JMJD1C	SPRED2	GPS2	EXO5	RBM15	RBM10
ATRX	CBFB	RXRB	SMARCA4	ATAD2	SMC4	CHD8
FBXW7	FANCM	BRWD3	LARP4B	RGS12	SCRN3	ZC3H18
KMT2C	IWS1	PCDH7	NSD1	SPRED1	UBR5	CEBPA
PIK3R1	FOXA1	ZBTB18	HLA-A	PLAC4	RNF111	DDX3X
CASP8	ZNF292	DEPDC5	CRIPAK	AMOT	WDR47	MYO6
CDH1	ZNRF3	BTBD7	AOAH	ARHGAP5	DOPEY1	ZNF318
CTCF	BRCA1	BCL10	CREBBP	DENND6A	WBP1	MBD6

ATM	TCF7L2	GNPTAB	TNRC6B	RUFY2	MAGED1	COL4A2
CIC	CHD2	PLEKHM3	ACVR1B	ZMYM3	TCEB3	TRIP12
RUNX1	SOX9	TAOK1	DNMT3A	MED23	ZNF234	KMT2B
RPL22	WDR33	DIP2C	ACVR2A	ASXL2	GLTSCR1	CCAR1
STAG2	EMG1	NFATC4	RERE	RAD21	FAM58A	SEC22A
FAT1	MTFR1L	ADAMTS19	ASXL1	GGCT	KIAA0907	ERRFI1
NOTCH1	TRAF3	TTC18	NCOR1	HNF1A	BRD7	MORC4
MAP2K4	AMER1	CERK	USP28	LIMCH1	PPP3CC	MEN1
BAP1	SIN3A	IFNGR2	THRAP3	CTNND1	FOSL2	TBX3
ZFP36L2	MBD1	PEX2	STX7	LDB1	THUMPD3	MAP3K4
CPEB2	HGF	MYO1B	COQ9	PHACTR4	CLGN	INO80
HMCN1	SNRPN	TBC1D10C	LEMD2	BRCA2	BMPR2	CUL3
NUP98	YLPM1	SPATA6	ATR	AFF4	BIRC6	RIMS2
IDH2	HAUS8	SMARCA1	COL8A2	INO80	CCDC38	PSIP1
EPB41L4A	SIK3	BAX	DYRK1A	CUL3	RAPGEF6	DUSP16
ANKRD46	KDM3B	PNISR	UGT2A2	RIMS2	SUZ12	UPF3B
ANO3	CCDC120	WAC	PABPC3	PSIP1	WWC2	ATG5
RBBP6	TEX11	C2CD5	GPR174	DUSP16	GGNBP2	SFPQ
NEK9	B3GNT5	CCDC38	WWC2	UPF3B	TNIK	APPBP2
RBM26	KBTBD7	RAPGEF6	GGNBP2	DPY19L4	CACUL1	KBTBD7
HDAC2	HNRNPD	SUZ12	TNIK	ABCA10	KBTBD7	

OGs

BRAF	MYCN	TOR1A	EBPL	FMNL3	HIST1H3B	UGT8
KRAS	MEF2B	HGF	IFITM1	HARS2	SLC35G3	RIMS2
PIK3CA	MB21D2	HIST1H2BF	MFF	STXBP6	TLL1	CDC73
IDH1	HRAS	PDE7B	GABRG1	MDGA2	PDYN	TXNRD1
CTNNB1	CARM1	ZNF117	CUL1	CACNG3	ABI1	C16orf80
AKT1	DKK2	MAGI2	EPHA6	IRF2	DICER1	CCND3
IDH2	MBOAT2	RIT1	MYOT	SMARCA2	ZFR	KLK8
NRAS	ERBB3	BTBD11	KLHL5	MLLT11	UBE2QL1	GRIA2
RAC1	EEF1B2	NSMCE1	PRRX1	BCLAF1	TLL2	SAP30
EGFR	GNAS	UBQLN2	CPB1	PRPF8	FGFR3	SMOC2
NFE2L2	NUTM2F	DCLK1	NRAP	ARHGEF33	STXBP1	MRPL49
EZH2	TAF1	MFAP5	ZNF181	NBPF10	PSMC3IP	SRC

U2AF1	RHOA	COL5A2	RGPD3	BRWD3	GTF2I	BZW2
SF3B1	PTN	ABCB1	RBM39	GPR141	MICU3	IREB2
PGM5	ALK	TUSC3	GNG4	MECOM	ASCC3	ENAH
PPP6C	PTPN11	KCNQ5	HMCN1	PTPRF	IL5RA	NBPF1
PPP2R1A	ACADS	SKAP2	GRIA3	XPOT	GNA15	MAPK8IP 2
MAPK1	MED12	INTS7	NSFL1C	ALDH1L2	JUN	SEC63
FGFR2	SULT1C4	METTL14	SEMG2	LPA	ITM2C	CCDC132
AQP2	ZNF799	XYLT1	CRISPLD1	STAT3	POLE	RHBDL3
MTOR	LHFPL1	FAM8A1	HLF	PLCL1	TM2D3	SOS1
KRT15	ARF4	JAKMIP2	CMAS	OR4M2	ZNF479	TKTL2
MEF2BNB	KCND3	SOX17	CCDC36	TMEM11	CDH7	NNMT
CHD4	MYC	LSM11	SMO	PIK3CB	REXO2	LPHN3
MAP2K1	CAPRIN2	GRXCR1	SEPT14	PSPH	GK2	MYO3A
TRIM48	MFGE8	GRID1	EIF1AX	WNT11	ZFP2	OPRM1
ERBB2	LUM	OR5I1	SIAH2	STRIP2	CSNK1E	C3orf27
SPOP	TBX18	GRM5	AK8	MAPK8	KAT8	TOX
KRTAP4-11	TRIM23	MYF5	MRPL32	POTEG	CD163	PPP1R9A
FLT3	MS4A8	MYH2	C16orf45	MARCO	GRID2	WDR17
MYD88	PRKCI	CSMD3	WBSCR17	SPPL3	IL21	PTPRU
RRAS2	GOT2	PLK2	NRG3	NENF	BRSK1	PIK3R5
MAX	LZTR1	ZNF844	LIN9	DTX1	SOCS5	CADPS
KRTAP4-5		ACBD3	C16orf87	GABRA5	SCN3A	CIZ1
ZBTB7A	ZNF559	SBNO1	NDUFS5	PCMTD1	GABRA2	SHB
COL9A1	GJB3	TES	TBX15	ZNF878	TRPC6	

CIN

ATAD2	GRPE1	CROCC	PKN2	VPS4A	PHP14	THOC5	ARP8
STK26	CTCF	F177A	RAB9A	PCF11	PELO	MIER1	TOP2B
CK5P3	CEP83	CHMP5	ABLM1	PDS5B	RIC8B	RBMX2	MAEA
UBL5	NMNA1	MAPK2	CKAP2	CBP	PCNA	LCOR	NEDD1
PIEZ1	KAP2	NDE1	NU133	SPAST	SC23A	ATRIP	CCNB2
ASCC3	EVI5	RL36L	ANCHR	CDK2	CENPH	MACC1	DLG1
SPG20	CLAP1	CHD3	CHK1	NDUC2	NEUA	NSUN2	TOPK
ARL8B	USP9X	ODPB	K1161	HAUS4	RM18	SIR3	CLPB
DLRB1	CDCA3	NPM3	U2AF2	CLIC4	KI18A	MIPT3	KIF3A
PKHA7	PB1	KDM1B	PP1B	IL18	MYPT1	DCK	TPX2
TIPRL	LZIC	RBM5	RS20	ANLN	SPAG5	GNA13	MMS19
DLDH	SPF27	KIF15	MEN1	BECN1	AKT1	XRCC3	TAOK2
ECM29	MGLL	RMD3	CAPG	HOOK3	KIF2C	CND3	RD23A
BRCA1	WDR81	CHM2B	RABL6	TBCC	CD81	PML	PAR6B
DDB1	CI114	PP1G	DC1I2	CCND1	DDX18	KI13A	CCDB1
UBP16	RAB8A	ZWINT	CHRD1	NUBP1	CASC5	SF3A1	LIMD1
TACC3	RNH2B	XPC	CDK7	MK14	CTDP1	REEP4	PRC1
IST1	CDC7	SAHH3	LIS1	MET15	PPP5	IFT81	TAGL2
H15	GTR1	GALT7	PIGS	ZW10	YETS4	CCNK	2AAA

REQU	NOC3L	DPH7	COTL1	PP1A	APC5	RBMS2	NH2L1
CE350	RM14	CD123	PTN11	C1QBP	SMC1A	MARE3	MYCBP
UBP1	CDC5L	FA64A	CSK22	APC	APC4	HNRH1	CLPX
PDK1	UB2E1	NTF2	MD1L1	NEMP1	SRSF1	RS6	COG7
AXIN2	GOGA2	HEXA	SNUT1	RL32	CISY	CUL3	TBB5
UXT	SDC1	RAB3I	CEP76	CND1	RFA2	PSMG2	CHD4
ENSA	B3GLT	BUB3	ARL3	NIT2	USF1	HAUS6	TYW1
GORAB	XYLK	F136A	RGAP1	NUMA1	CDK1	WDR61	NEB2
MOT1	PCID2	SAS6	SSA27	CCNT1	NKAPL	CCAR2	CD11B
CP250	DI3L2	PAPD5	GNAI3	TCPQ	SMC4	GSK3B	NU107
DHYS	CKS2	MCMBP	TKFC	CSN3	RMD1	PSMD6	ST14
CENPI	SENP6	PCGF5	MYD88	ELYS	B2L15	KIFC1	SSRG
DDX41	PDC6I	UBP33	CUL7	U5S1	MRE11	BUB1B	SGT1
AL9A1	TBG1	QORX	CATA	SRP14	RED	UBP28	SNW1
ACAD9	GWL	NDC80	THOC1	SETMR	EMAL3	BRCC3	NUDC
PGTB2	AR2BP	RIOK3	TCPE	TXND9	MLH1	MARE2	RUVB2
TOPB1	APEX1	AURKB	CENPF	MCCB	HAUS1	SNP29	TEST
NOL3	NED4L	TS101	CA109	SF3B1	KIF3B	FANCJ	TXN4A
NUDC2	CHAP1	FBX30	ZN511	ORC2	GTF2I	GTPB1	TBC17
RL24	MSH2	VPS4B	EAF6	ARPC2	TPR	NUSAP	CTF18
ARHG2	FEN1	PHF6	DTL	RAGP1	EHD1	SUMO3	ASUN
CSK21	TP53B	PCH2	GCP3	I2BPL	IGSF8	RBGP1	SYNE2
CCNA2	MRP	RBM10	TRIM2	CUL4A	PIGU	ULA1	HAUS3
ARFP2	G6PD	CC124	IFT25	DJB11	ITA11	PSN1	TOP1
MCM2	UIMC1	PARD3	APC1	ACTZ	CHM4B	PIGG	MSH6
PRP8	ZN207	NDK7	ETHE1	AAAS	NSL1	BOREA	ANM1
BRE	IFT27	RB	PSMD8	BUB1	TIM	ECT2	CCNB1
IL18	SGO2	DCAM	FZR	SART3	NTM1A	ARMX3	PCBP1
CPSF5	KIF14	SEM3C	CHM2A	CNDD3	ELAV1	NU205	RFC4
DC1L2	BIRC5	DICER	PRCC	CIAO1	AURKA	DYLT1	HMGA2
TMUB1	RS3	RO52	SKAP	PDS5A	TOP2A	DIAP3	MB12A
HOOK1	SMAD4	HJURP	TIM44	PAF15	FA83D	TRUB1	CHM1A
STK39	GL8D1	CDC27	E41L5	KIF11	KMT5A	MDHC	DOK1
NDUBA	UBQL2	SMC5	BABA1	PLEC	CEP41	PSMD6	NDK6
KMT2C	NHRF1	APC10	F173A	DYHC1	AKP8L	ADT2	CEP55
BLM	ESPL1	RFA1	KAPCA	CCNY	UBE2C	IMP3	ECSIT
PSRC1	HAUS8	ASPM	XPO1	GCP4	PTER	ACL6A	EPCR
INO80	ZC3H4	WAC	CETN2	ARP2	IDH3B	GNAI2	CFDP1
RRAS2	DHX9	HPSE	OBSL1	UB2G1	BCAR1	DNLI4	ATM
PALMD	DCMC	NU214	ACPM	B2L13	RFWD3	KIF23	PRP19
ZHX2	SMC3	TBA1C	RECQ5	UBL7	TTYH3	INT3	PSB5
SDCG8	UGDH	MZT1	MARE1	UBC9	KNTC1	ERP44	MYL6B
RUVB1	SPC25	MCM3	EXOC3	APC7	CDC23	SLU7	KIF2A
TOIP1	CEP44	SPDLY	KI20A	U119A	KC1A	KC1D	DSN1
PTTG1	CDC20	NUP37	CDK5	TYW1	RPGP2	NXT1	FR10
STAG1	CETN3						

Supplementary table S2: Protein membership to the Venn diagram in PTA clones and 4N

NF1	OSBPL11	CRK	TLE3	ACIN1	NUP153	TP53BP1	HTT
SLC12A2	PDLIM5	ASPM	MKI67	DDX24	MDC1	PHF6	CHAMP1
AHNAK	KIF20A	NUP98	TCOF1	NUCKS1	NCAPH2	HNRNPA1	TOP2A
MSF	NUSAP1	PPP1R12A	LARP4	GTSE1	RANBP2	HSP90AA1	FLNB
ZC3H13	ANLN	HNRNPM	NUMA1	CENPF	LAD1	MAP4	ARID1A
DPF2	FTSJ3	TJP2	FLNA	MAP2	NUP133	FAM83H	NCL
MARCKS	PCYT1A	HMGN4	DYNC1LI1	ADD3	PCM1	SPAG9	SCRIB
KDM3B	TPX2	NPM1	NOLC1	ATRX	SRRM2	DENND4	

Protein membership to the Venn diagram in Trisomic clones and 4N

RSRC2	SHROOM3	SVIL	PDCD4	AKAP11	ADAR	AFDN	TPR
CGN	IWS1	AHNAK	SCRIB	ZNF185	NUCKS1	TCOF1	LMO7
SRSF10	C17orf75	MARCKS	TRIP12	UNG	YAP1	HMGA1	SRFBP1
ZC3H13	MAPK1	SNX1	GPATCH8	SRRM2	HIST1H1E	MCM2	PROSER2
RTN4	PPP1R12A	SND1	TP53BP1	TACC2	FAM83H	PDAP1	RRP1B
REEP4	SON	SRRM1	MAP2	CUX1	RBM27	RRM2	
LRRFIP1	BAZ1B	CEP170B	TRA2A	RBL1	COIL	PLEC	
CLSPN	MICALL2	MAP1S	PHACTR4	TMX1	MAPK3	TBC1D4	
ZRANB2	EEF2	MARCKSL1	FLNA	PTPN14	TJP2	EIF2AK2	
CHERP	CTNND1	SERBP1	OXSR1	BIN1	ACIN1	MTA1	

Supplementary table S3: List of compounds tested in diploid, tetraploid, aneuploidy and trisomic DLD-1 clones

Name	Target	Pathway	Highest concentration in assay (mM)	Incub time (days)
5-fluorouracil	thymidylate synthase	DNA-RNA Synthesis	10	3
ABT-737	Bcl-2	Apoptosis	10	5
actinomycin-D	interfering with mRNA synthesis	DNA-RNA Synthesis	0,316	3
afatinib	EGFR/HER2	Cell growth	10	3
AMG-900	pan Aurora	SAC	10	3
AT-7519	multi-CDK inhibitor for CDK1, 2, 4, 6 and 9	Cell cycle progression	10	3
BI-2536	Plk1	SAC	1	3
BIIB021	HSP90	Protein folding	1	3
bortezomib	Proteasome	Protein folding	1	3
CHIR-124	Chk1	Cell cycle progression	1	3
cobimetinib	MEK1	Cell growth	10	3
danusertib	panAurora inhibitor	SAC	10	3

daunorubicin	DNA and RNA synthesis	DNA-RNA Synthesis	1	3
dinaciclib	CDK inhibitor for CDK2, CDK5, CDK1 and CDK9	Cell cycle progression	0,316	3
docetaxel	microtubule	Microtubule Assembly	1	5
epothilone B	microtubule	Microtubule Assembly	0,0316	3
fasudil	ROCK-II, PKA, PKG, PKC, MLCK	Energy stress	10	3
GSK-1070916	Aurora B/C	SAC	10	3
GSK-461364	Plk1	SAC	10	3
KU-60019	ATM	DNA repair	10	3
MK-1775	Wee	Cell cycle progression	10	3
MK-5108	Aurora A	SAC	10	3
MLN-8054	Aurora A	SAC	10	3
MPI-0479605	TTK/MPS1	SAC	10	3
MPS1-IN-1	TTK	SAC	10	3
NMS-P715	TTK	SAC	1	3
olaparib	PARP1/2	DNA repair	10	3
paclitaxel	microtubule	Microtubule Assembly	10	5
palbociclib	CDK4, CDK6	Cell cycle progression	10	3
PHA-793887	CDK2, CDK5 and CDK7	Cell cycle progression	10	3
roscovitine	CDK	SAC	10	3
SCH-900776	Chk1	SAC	10	3
venetoclax	Bcl-2	Apoptosis	10	3
vincristine	tubulin	Microtubule Assembly	3,16	3
volasertib	Plk1	SAC	3,16	3
VX-680	pan-Aurora	SAC	10	3
BAY 320	Bub1	SAC	10	3
doxorubicin	topoisomerase II	DNA-RNA Synthesis	3,16	5

7.2. Figure legends

Figure 1: mechanisms that generate aneuploidy (from Bernardo Orr, Aneuploidy 2015 current Biol).

Figure 2: the mitotic checkpoint: a safeguard to protect against aneuploidy (from [1]Andrew J. Holland and Don W. Cleveland July 2009 Nature Reviews).

Figure 3: scheme showing different attachment configurations between chromosomes and microtubules from [175]

Figure 41: gene ontology (GO)-term enrichment analysis of phospho-peptides up-regulated across Trisomic clones (upper panel); and 4N plus Trisomic clones

Figure 42: STRING functional network analysis of the phospho-peptides up-regulated in PTAs

Figure 43: STRING functional network analysis of the phospho-peptides in PTAs and 4N

Figure 44: STRING functional network analysis of the phospho-peptides in trisomic clones and trisomic plus 4N

Figure 45: tables showing an enrichment analysis of the 500 most deregulated phospho-peptides per cell line using the CIN/cell division inclusion list.

Figure 46: dot plots showing the phospho-peptide ratios of detected proteins belonging to the CIN/cell division inclusion list deregulation in 4N and PTA

Figure 47: dot plots showing the phospho-peptide ratios of detected proteins belonging to the CIN/cell division inclusion list deregulation in 4N and Trisomic clones

Figure 48: STRING functional network analysis ofphospho peptide deregulated in 4N, 4N plus PTAs, Trisomic clones and Trisomic clones plus 4N

Figure 49: dot plots showing the significance and IC50 difference obtained using the kinase drugs listed in table S7

Figure 50: dot plot showing selected detection ratios of regulatory phosphorylation sites of the centrosome and mitotic spindle kinase Aurora A (AURKA P-T288), the mitotic kinase Cdk1 (CDK1 P-T14, P-Y15), the cell cycle checkpoint kinase Chk1 (CHK1 P-S286, CHK1 P-S301) and the mitotic spindle kinase Plk1 (PLK1 P-T210)

Figure 51: table listing the p-values for phospho-peptide measurements shown in Figure 49.

Figure 52: graphs showing dose-response curves using the Plk1 inhibitor Volasertib on generated cell cultures

Figure 53: micrographs of cells stained with anti-Plk1, pT210 Plk1, CREST and DAPI.

Figure 54: micrographs of metaphase cells stained with anti- α-tubulin, CREST and DAPI.

7.3 Table legends

Table 1: frequent impairment of the mitotic checkpoint in human cancers (From Beth AA Weaver, Don W Cleveland Current Opinion in Cell Biology 2006)

Table S1: inclusion list of tumor suppressor genes (TSGs), oncogenes (OGs) and chromosomal instable genes (CIN) considered during the targeted analysis. These inclusion lists were generated as described in material and method section.

Table S2: Venn diagram analyses. List of proteins common in PTAs and 4N or 4N plus trisomic clones. Venn diagrams were obtained by selecting the 500 most deregulated phospho-peptides per cell line (based on an FDR of <10%, yielding a total of 1410 phospho-peptides from 807 proteins). Note that this experiment was performed in biological triplicates.

Table S3: Drug screening assay spreadsheet. List of targets, incubation time and concentrations for each of the tested compounds.

8. Abbreviations

ABC	Array comparative genomic hybridization
aCGH	Anaphase-promoting complex/cyclosome
APC/C	American type culture collection
ATCC	Ataxia telangiectasia mutated
ATM	Budding uninhibited by benzimidazoles 1
Bub1	Budding uninhibited by benzimidazoles 3
Bub3	budding uninhibited by benzimidazoles-related 1
BubR1	Cell division cycle protein 20
CDC20	cyclin-dependent kinase 1
CDK1	Centromere protein A
CENP A	Centromere protein E
CENP E	Centromere protein F
CENP F	Checkpoint kinase 1
CHK1	chromosome passenger complex
CPC	calcinosis, Raynaud's syndrome, esophageal
CREST	dysmotility, sclerodactyly, telangiectasia
	Chromosome Instability
CIN	dihydrocytochalasin B
DCB	Dukes’s Type C, colorectal adenocarcinoma
DLD-1	Dulbecco's modified Eagle's medium
DMEM	Double strand break
DSB	Fluorescence hybridization in situ
FISH	Green fluorescent protein
GFP	Human papilloma virus
HPV	Heat shock factor 1
HSF1	Heat shock protein 90
HSP90	Immunofluorescente assay
IFA	Inner centromeric protein
INCENP	Kinetochore microtubule
k-MT	Kinetochore null protein 1
KNL1	Kinetochire
KT	Mitotic arrest-deficient 1
MAD1	Mitotic arrest-deficient 2
MAD2	MAPs
ATP binding cassette	MCC

MEF	Mitotic checkpoint complex
MIN	Murine embryonic fibroblast
MT	Microsatellite instability
PI	Microtubule
PP2A	Propidium iodide
PT	Serine/threonine protein phosphatese 2A
PVDF	Post Tetraploid
PTA	Polyvinylidene disluoride membrane
PLK1	Posttetraploid aneuploid
RPE1 hTERT	Polo like kinase 1
ROS	Retinal pigment epithelium cell line
SAC	reactive oxygen species
SD	Spindle assembly checkpoint
SEM	Standard deviation
TMT	Standard error of mean
Microtubule associated proteins	Tandem mass tag labeling

9. Acknowledgements

I would like to thank my Ph.D. thesis supervisor Prof. Dr. Erich Nigg, for allowing me to perform research in his group at the Biozentrum. I am heartfelt grateful for his support and guidance, advices and as well as for the excellent working conditions in the lab.

I also thank Prof. Dr. Michael Hall for kindly accepting to co-referee my work. I am grateful to Prof. Dr. Lukas Bubendorf and Prof. Dr. Dirk Bumann for being in my thesis committee.

I wish express my gratitude to Prof Dr. Zuzana Storchova and Dr. Guido Zaman for their helpful advice and collaborations on my project.

I would like to express a deep sense of gratitude to many other people I had a chance to work with. I thank Dr. Conrad von Schubert for the project discussion and guidance; Dr. Erik Ahrné and Dr. Alex Schmidt for their willingness to answer all the questions and the tremendous help on data analysis, and Dr. Thomas Lorber for the significative amount of work on aCGH analysis. Tons of thanks go to Aline Campos Sparr and Judith de Venner for excellent technical support and all their patience.

I thank all members of Nigg lab: Dr. Olivier Ganier, Dr. Christian Arquint and Dr. Fabien Cubizolles for useful comments on my writing, daily scientific (and not) discussions and suggestions. A special thank to Elena Nigg for the expert lab help. I am grateful to the all past members of the Nigg lab, Ana A., Patrick, Ana B., Dominik, Anna-Maria and Lukas for generating a stimulating a joyful environment. A huge thank as well to the special guest that we have hosted in the last months: Emmanuel and Chantal.

A special appreciation goes to all PloidyNet members for the support, all the advices, discussions and fun during our meetings.

I would like to express my sincere gratitude to my parents and my family, grazie per avermi trasmesso tutta la vostra educazione e affetto, senza questi non sarei la persona che sono oggi. Last but not least I would like to thank my husband Daniele for all his support during this long journey, the help and the constant patient. Non vedo l'ora di iniziare questa nostra avventura insieme.

10. Bibliography

1. Holland, A. J. & Cleveland, D. W. Boveri revisited: chromosomal instability, aneuploidy and tumorigenesis. *Nat Rev Mol Cell Biol* **10,** 478–487 (2009).
2. Torres, E. M. *et al.* Effects of aneuploidy on cellular physiology and cell division in haploid yeast. *Science* **317,** 916–924 (2007).
3. Williams, B. R. *et al.* Aneuploidy affects proliferation and spontaneous immortalization in mammalian cells. *Science* **322,** 703–709 (2008).
4. McCoy, E. E., Segal, D. J., Bayer, S. M. & Strynadka, K. D. Decreased ATPase and increased sodiun content of platelets in Down's syndrome. Relation to decreased serotonin content. *N Engl J Med* **291,** 950–953 (1974).
5. Lauren Heller, C. S. H. L. P. Symposium 75_Nuclear Organization and Function. 1–8 (2011).
6. Haruki, N. *et al.* Persistent Increase in Chromosome Instability in Lung Cancer. *The American Journal of Pathology* **159,** 1345–1352 (2001).
7. Lengauer, C., Kinzler, K. W. & Vogelstein, B. Genetic instability in colorectal cancers. *Nature* **386,** 623–627 (1997).
8. Yoon, D.-S. *et al.* Variable Levels of Chromosomal Instability and Mitotic Spindle Checkpoint Defects in Breast Cancer. *The American Journal of Pathology* **161,** 391–397 (2002).
9. Carter, S. L., Eklund, A. C., Kohane, I. S., Harris, L. N. & Szallasi, Z. A signature of chromosomal instability inferred from gene expression profiles predicts clinical outcome in multiple human cancers. *Nat Genet* **38,** 1043–1048 (2006).
10. Duesberg, P., Stindl, R. & Hehlmann, R. Explaining the high mutation rates of cancer cells to drug and multidrug resistance by chromosome reassortments that are catalyzed by aneuploidy. *Proc Natl Acad Sci USA* **97,** 14295–14300 (2000).
11. Walther, A., Houlston, R. & Tomlinson, I. Association between chromosomal instability and prognosis in colorectal cancer: a meta-analysis. *Gut* **57,** 941–950 (2008).
12. Birkbak, N. J. *et al.* Paradoxical Relationship between Chromosomal Instability and Survival Outcome in Cancer. *Cancer Research* **71,** 3447–3452 (2011).
13. Silk, A. D. *et al.* Chromosome missegregation rate predicts whether aneuploidy will promote or suppress tumors. *Proc. Natl. Acad. Sci. U.S.A.* **110,** E4134–41 (2013).
14. Weaver, B. A. & Cleveland, D. W. The Aneuploidy Paradox in Cell Growth and Tumorigenesis. *Cancer Cell* **14,** 430–433 (2008).
15. Weaver, B. A. A., Silk, A. D., Montagna, C., Verdier-Pinard, P. & Cleveland, D. W. Aneuploidy Acts Both Oncogenically and as a Tumor Suppressor. *Cancer Cell* **11,** 25–36 (2007).
16. Orr, B., Godek, K. M. & Compton, D. Aneuploidy. *Current Biology* **25,** R538–R542 (2015).
17. DeLuca, J. G. & Musacchio, A. Structural organization of the kinetochore–microtubule interface. *Current Opinion in Cell Biology* **24,** 48–56 (2012).
18. Musacchio, A. & Salmon, E. D. The spindle-assembly checkpoint in space and time. *Nat Rev Mol Cell Biol* **8,** 379–393 (2007).
19. Weaver, B. A. & Cleveland, D. W. Does aneuploidy cause cancer? *Current Opinion in Cell Biology* **18,** 658–667 (2006).
20. Babu, J. R. *et al.* Rae1 is an essential mitotic checkpoint regulator that cooperates with Bub3 to prevent chromosome missegregation. *J. Cell Biol.* **160,** 341–353 (2003).
21. Baker, D. J. *et al.* BubR1 insufficiency causes early onset of aging-associated phenotypes

and infertility in mice. *Nat Genet* **36,** 744–749 (2004).
22. Sotillo, R. *et al.* Mad2 Overexpression Promotes Aneuploidy and Tumorigenesis in Mice. *Cancer Cell* **11,** 9–23 (2007).
23. Kabeche, L. & Compton, D. A. Checkpoint-Independent Stabilization of Kinetochore-Microtubule Attachments by Mad2 in Human Cells. *Current Biology* **22,** 638–644 (2012).
24. Ryan, S. D. *et al.* Up-regulation of the mitotic checkpoint component Mad1 causes chromosomal instability and resistance to microtubule poisons. *Proc. Natl. Acad. Sci. U.S.A.* **109,** E2205–14 (2012).
25. Janssen, A., Kops, G. J. P. L. & Medema, R. H. Elevating the frequency of chromosome mis-segregation as a strategy to kill tumor cells. *Proc. Natl. Acad. Sci. U.S.A.* **106,** 19108–19113 (2009).
26. Thompson, S. L. & Compton, D. A. Proliferation of aneuploid human cells is limited by a p53-dependent mechanism. *J. Cell Biol.* **188,** 369–381 (2010).
27. Tighe, A., Johnson, V. L., Albertella, M. & Taylor, S. Aneuploid colon cancer cells have a robust spindle checkpoint. *EMBO reports* 1–6 (2001).
28. Gascoigne, K. E. & Taylor, S. S. Cancer Cells Display Profound Intra- and Interline Variation following Prolonged Exposure to Antimitotic Drugs. *Cancer Cell* **14,** 111–122 (2008).
29. Earnshaw, W. C. Discovering centromere proteins: from cold white hands to the A, B, C of CENPs. *Nat Rev Mol Cell Biol* **16,** 443–449 (2015).
30. Akiyoshi, B. & Biggins, S. Reconstituting the kinetochore–microtubule interface: what, why, and how. *Chromosoma* **121,** 235–250 (2012).
31. Musacchio, A. & Desai, A. A Molecular View of Kinetochore Assembly and Function. *Biology* **6,** 5–47 (2017).
32. Godek, K. M., Kabeche, L. & Compton, D. A. Regulation of kinetochore–microtubule attachments through homeostatic control during mitosis. *Nature Publishing Group* **16,** 57–64 (2014).
33. Ruchaud, S., Carmena, M. & Earnshaw, W. C. The Chromosomal Passenger Complex: One for All and All for One. *Cell* **131,** 230–231 (2007).
34. Welburn, J. P. I. *et al.* Aurora B Phosphorylates Spatially Distinct Targets to Differentially Regulate the Kinetochore-Microtubule Interface. *Molecular Cell* **38,** 383–392 (2010).
35. Liu, D., Vader, G., Vromans, M. J. M., Lampson, M. A. & Lens, S. M. A. Sensing Chromosome Bi-Orientation by Spatial Separation of Aurora B Kinase from Kinetochore Substrates. *Science* **323,** 1350–1353 (2009).
36. Wang, E., Ballister, E. R. & Lampson, M. A. Aurora B dynamics at centromeres create a diffusion-based phosphorylation gradient. *J. Cell Biol.* **194,** 539–549 (2011).
37. Martin-Lluesma, S. Role of Hec1 in Spindle Checkpoint Signaling and Kinetochore Recruitment of Mad1/Mad2. *Science* **297,** 2267–2270 (2002).
38. Lin, Z.-Z. *et al.* Significance of Aurora B overexpression in hepatocellular carcinoma. Aurora B Overexpression in HCC. *BMC Cancer* **10,** 461 (2010).
39. Giet, R., Petretti, C. & Prigent, C. Aurora kinases, aneuploidy and cancer, a coincidence or a real link? *Trends in Cell Biology* **15,** 241–250 (2005).
40. Michaelis, C., Ciosk, R. & Nasmyth, K. Cohesins: chromosomal proteins that prevent premature separation of sister chromatids. *Cell* **91,** 35–45 (1997).
41. Gruber, S., Haering, C. H. & Nasmyth, K. Chromosomal cohesin forms a ring. *Cell* **112,** 765–777 (2003).
42. Nasmyth, K. & Haering, C. H. Cohesin: Its Roles and Mechanisms. *Annu. Rev. Genet.* **43,** 525–558 (2009).
43. Waizenegger, I. C., Hauf, S., Meinke, A. & Peters, J. M. Two distinct pathways remove

mammalian cohesin from chromosome arms in prophase and from centromeres in anaphase. *Cell* **103,** 399–410 (2000).
44. Losada, A., Hirano, M. & Hirano, T. Cohesin release is required for sister chromatid resolution, but not for condensin-mediated compaction, at the onset of mitosis. *Genes Dev.* **16,** 3004–3016 (2002).
45. Sumara, I. *et al.* The Dissociation of Cohesin from Chromosomes in Prophase Is Regulated by Polo-like Kinase. *Molecular Cell* **9,** 515–525 (2002).
46. Giménez-Abián, J. F. *et al.* Regulation of Sister Chromatid Cohesion between Chromosome Arms. *Current Biology* **14,** 1187–1193 (2004).
47. Oliveira, R. A. & Nasmyth, K. Getting through anaphase: splitting the sisters and beyond. *Biochm. Soc. Trans.* **38,** 1639–1644 (2010).
48. Clift, D. & Marston, A. L. The Role of Shugoshin in Meiotic Chromosome Segregation. *Cytogenet Genome Res* **133,** 234–242 (2011).
49. Tanno, Y. *et al.* The inner centromere-shugoshin network prevents chromosomal instability. *Science* **349,** 1237–1240 (2015).
50. Yamada, H. Y. *et al.* Haploinsufficiency of SGO1results in deregulated centrosome dynamics, enhanced chromosomal instability and colon tumorigenesis. *Cell Cycle* **11,** 479–488 (2014).
51. Solomon, D. A. *et al.* Mutational inactivation of STAG2 causes aneuploidy in human cancer. *Science* **333,** 1039–1043 (2011).
52. Djos, A., Fransson, S., Kogner, P. & Martinsson, T. Aneuploidy in neuroblastoma tumors is not associated with inactivating point mutations in the STAG2 gene. *BMC Medical Genetics* **14,** 1–1 (2013).
53. Morrison, C., Vagnarelli, P., Sonoda, E., Takeda, S. & Earnshaw, W. C. Sister chromatid cohesion and genome stability in vertebrate cells. *Biochm. Soc. Trans.* **31,** 263–265 (2003).
54. Nigg, E. A. & Stearns, T. The centrosome cycle: Centriole biogenesis, duplication and inherent asymmetries. *Nature Publishing Group* **13,** 1154–1160 (2011).
55. Basto, R. *et al.* Flies without Centrioles. *Cell* **125,** 1375–1386 (2006).
56. Nigg, E. A. Reviews and comment from the nature publishing group. *Nat Rev Genet* **3,** 815–815 (2002).
57. Ganem, N. J. & Pellman, D. Limiting the Proliferation of Polyploid Cells. *Cell* **131,** 437–440 (2007).
58. Ganem, N. J., Godinho, S. A. & Pellman, D. A mechanism linking extra centrosomes to chromosomal instability. *Nature* **460,** 278–282 (2009).
59. Kwon, M. *et al.* Mechanisms to suppress multipolar divisions in cancer cells with extra centrosomes. *Genes Dev.* **22,** 2189–2203 (2008).
60. Gisselsson, D. *et al.* Generation of trisomies in cancer cells by multipolar mitosis and incomplete cytokinesis. *Proc. Natl. Acad. Sci. U.S.A.* **107,** 20489–20493 (2010).
61. Sansregret, L. & Swanton, C. The Role of Aneuploidy in Cancer Evolution. *Cold Spring Harb Perspect Med* **7,** a028373–18 (2017).
62. Brinkley, B. R. Managing the centrosome numbers game: from chaos to stability in cancer cell division. *Trends in Cell Biology* **11,** 18–21 (2001).
63. Drosopoulos, K., Tang, C., Chao, W. C. H. & Linardopoulos, S. APC/C is an essential regulator of centrosome clustering. *Nature Communications* **5,** 3686 (2014).
64. Basto, R. *et al.* Centrosome Amplification Can Initiate Tumorigenesis in Flies. *Cell* **133,** 1032–1042 (2008).
65. Silkworth, W. T., Nardi, I. K., Scholl, L. M. & Cimini, D. Multipolar Spindle Pole Coalescence Is a Major Source of Kinetochore Mis-Attachment and Chromosome Mis-

Segregation in Cancer Cells. *PLoS ONE* **4,** e6564–9 (2009).
66. Godinho, S. A. & Pellman, D. Causes and consequences of centrosome abnormalities in cancer. *Philos. Trans. R. Soc. Lond., B, Biol. Sci.* **369,** 20130467–20130467 (2014).
67. Nigg, E. A. & Raff, J. W. Centrioles, Centrosomes, and Cilia in Health and Disease. *Cell* **139,** 663–678 (2009).
68. Nigg, E. A. Origins and consequences of centrosome aberrations in human cancers. *Int. J. Cancer* **119,** 2717–2723 (2006).
69. Telentschak, S., Soliwoda, M., Nohroudi, K., Addicks, K. & Klinz, F.-J. Cytokinesis failure and successful multipolar mitoses drive aneuploidy in glioblastoma cells. *Oncol Rep* **33,** 1–8 (2015).
70. Fukasawa, K., Choi, T., Kuriyama, R., Rulong, S. & Vande Woude, G. F. Abnormal centrosome amplification in the absence of p53. *Science* **271,** 1744–1747 (1996).
71. Tarapore, P., Horn, H. F., Tokuyama, Y. & Fukasawa, K. Direct regulation of the centrosome duplication cycle by the p53-p21Waf1/Cip1 pathway. *Oncogene* **20,** 3173–3184 (2001).
72. Borel, F., Lohez, O. D., Lacroix, F. B. & Margolis, R. L. Multiple centrosomes arise from tetraploidy checkpoint failure and mitotic centrosome clusters in p53 and RB pocket protein-compromised cells. *Proc Natl Acad Sci USA* **99,** 9819–9824 (2002).
73. Marthiens, V. *et al.* Centrosome amplification causes microcephaly. *Nature Cell Biology* **15,** 731–740 (2013).
74. Korzeniewski, N., Treat, B. & Duensing, S. The HPV-16 E7 oncoprotein induces centriole multiplication through deregulation of Polo-like kinase 4 expression. *molecular cancer* **10,** 61 (2011).
75. Li, J. *et al.* SAK, A New Polo-Like Kinase, Is Transcriptionally Repressed by p53 and Induces Apoptosis upon RNAi Silencing. *Neoplasia* **7,** 312–323 (2005).
76. Aleza, P. *et al.* Tetraploidization events by chromosome doubling of nucellar cells are frequent in apomictic citrus and are dependent on genotype and environment. *Annals of Botany* **108,** 37–50 (2011).
77. Kellis, M., Birren, B. W. & Lander, E. S. Proof and evolutionary analysis of ancient genome duplication in the yeast Saccharomyces cerevisiae. *Nature* **428,** 617–624 (2004).
78. Gallardo, M. H., Bickham, J. W., Honeycutt, R. L., Ojeda, R. A. & Kohler, N. Discovery of tetraploidy in a mammal. *Nature* **401,** 341–341 (1999).
79. Guidotti, J.-E. *et al.* Liver cell polyploidization: a pivotal role for binuclear hepatocytes. *J. Biol. Chem.* **278,** 19095–19101 (2003).
80. Storchova, Z. & Kuffer, C. The consequences of tetraploidy and aneuploidy. *Journal of Cell Science* **121,** 3859–3866 (2008).
81. Zack, T. I. *et al.* Pan-cancer patterns of somatic copy number alteration. *Nature Publishing Group* 1–10 (2013). doi:10.1038/ng.2760
82. Fujiwara, T. *et al.* Cytokinesis failure generating tetraploids promotes tumorigenesis in p53-null cells. *Nature* **437,** 1043–1047 (2005).
83. Lv, L. *et al.* Tetraploid cells from cytokinesis failure induce aneuploidy and spontaneous transformation of mouse ovarian surface epithelial cells. *Cell Cycle* **11,** 2864–2875 (2014).
84. Stukenberg, P. T. Triggering p53 after cytokinesis failure: Figure 1. *J. Cell Biol.* **165,** 607–608 (2004).
85. Soto, M. *et al.* p53 Prohibits Propagation of Chromosome Segregation Errors that Produce Structural Aneuploidies. *CellReports* **19,** 2423–2431 (2017).
86. Santaguida, S. *et al.* Chromosome Mis-segregation Generates Cell- Cycle-Arrested Cells with Complex Karyotypes that Are Eliminated by the Immune System. *Developmental*

Cell **41,** 638–651.e5 (2017).
87. Uetake, Y. & Sluder, G. Cell cycle progression after cleavage failure. *J. Cell Biol.* **165,** 609–615 (2004).
88. Santaguida, S., Vasile, E., White, E. & Amon, A. Aneuploidy-induced cellular stresses limit autophagic degradation. *Genes Dev.* **29,** 2010–2021 (2015).
89. Domingues, P. H. *et al.* Cellular Prion Protein PrP Cand Ecto-5′-Nucleotidase Are Markers of the Cellular Stress Response to Aneuploidy. *Cancer Research* **77,** 2914–2926 (2017).
90. Torres, E. M., Williams, B. R. & Amon, A. Aneuploidy: Cells Losing Their Balance. *Genetics* **179,** 737–746 (2008).
91. Janssen, A., van der Burg, M., Szuhai, K., Kops, G. J. P. L. & Medema, R. H. Chromosome Segregation Errors as a Cause of DNA Damage and Structural Chromosome Aberrations. *Science* **333,** 1895–1898 (2011).
92. Crasta, K. *et al.* DNA breaks and chromosome pulverization from errors in mitosis. *Nature Publishing Group* **482,** 53–58 (2012).
93. Liu, P. *et al.* Chromosome Catastrophes Involve Replication Mechanisms Generating Complex Genomic Rearrangements. *Cell* **146,** 889–903 (2011).
94. Gasch, A. P. *et al.* Genomic expression programs in the response of yeast cells to environmental changes. *Molecular Biology of the Cell* **11,** 4241–4257 (2000).
95. Sheltzer, J. M., Torres, E. M., Dunham, M. J. & Amon, A. Transcriptional consequences of aneuploidy. *Proc. Natl. Acad. Sci. U.S.A.* **109,** 12644–12649 (2012).
96. Durrbaum, M. *et al.* Unique features of the transcriptional response to model aneuploidy in human cells. *BMC Genomics* 1–14 (2014). doi:10.1186/1471-2164-15-139
97. Foijer, F. *et al.* Chromosome instability induced by Mps1 and p53 mutation generates aggressive lymphomas exhibiting aneuploidy-induced stress. *Proc Natl Acad Sci USA* **111,** 13427–13432 (2014).
98. Stingele, S. *et al.* Global analysis of genome, transcriptome and proteome reveals the response to aneuploidy in human cells. *Mol Syst Biol* **8,** 608–19 (2012).
99. Upender, M. B. *et al.* Chromosome transfer induced aneuploidy results in complex dysregulation of the cellular transcriptome in immortalized and cancer cells. *Cancer Research* **64,** 6941–6949 (2004).
100. Selmecki, A., Forche, A. & Berman, J. Aneuploidy and Isochromosome Formation in Drug-Resistant Candida albicans. *Science* **313,** 367–370 (2006).
101. Makarevitch, I., Phillips, R. L. & Springer, N. M. Profiling expression changes caused by a segmental aneuploid in maize. *BMC Genomics* **9,** 7–13 (2008).
102. Sheltzer, J. M. A transcriptional and metabolic signature of primary aneuploidy is present in chromosomally unstable cancer cells and informs clinical prognosis. *Cancer Research* **73,** 6401–6412 (2013).
103. Balch, W. E., Morimoto, R. I., Dillin, A. & Kelly, J. W. Adapting proteostasis for disease intervention. *Science* **319,** 916–919 (2008).
104. Tyedmers, J., Mogk, A. & Bukau, B. Cellular strategies for controlling protein aggregation. *Nature Publishing Group* **11,** 777–788 (2010).
105. Dephoure, N. *et al.* Quantitative proteomic analysis reveals posttranslational responses to aneuploidy in yeast. *eLife* **3,** 36–27 (2014).
106. Torres, E. M. *et al.* Identification of Aneuploidy- Tolerating Mutations. *Cell* **143,** 71–83 (2010).
107. Oromendia, A. B., Dodgson, S. E. & Amon, A. Aneuploidy causes proteotoxic stress in yeast. *Genes Dev.* **26,** 2696–2708 (2012).
108. Donnelly, N., Passerini, V., Dürrbaum, M., Stingele, S. & Storchová, Z. HSF1 deficiency and impaired HSP90-dependent protein folding are hallmarks of aneuploid human cells. *The*

EMBO Journal **33,** 2374–2387 (2014).
109. Tang, Y.-C., Williams, B. R., Siegel, J. J. & Amon, A. Identification of Aneuploidy-Selective Antiproliferation Compounds. *Cell* **144,** 499–512 (2011).
110. Gordon, D. J., Resio, B. & Pellman, D. Causes and consequences of aneuploidy in cancer. *Nature Publishing Group* **13,** 189–203 (2012).
111. Niwa, O., Tange, Y. & Kurabayashi, A. Growth arrest and chromosome instability in aneuploid yeast. *Yeast* **23,** 937–950 (2006).
112. Burds, A. A., Lutum, A. S. & Sorger, P. K. Generating chromosome instability through the simultaneous deletion of Mad2 and p53. *Proc Natl Acad Sci USA* **102,** 11296–11301 (2005).
113. Guerrero, A. A. *et al.* Centromere-localized breaks indicate the generation of DNA damage by the mitotic spindle. *Proc Natl Acad Sci USA* **107,** 4159–4164 (2010).
114. Li, M. *et al.* The ATM-p53 pathway suppresses aneuploidy-induced tumorigenesis. *Proc. Natl. Acad. Sci. U.S.A.* **107,** 14188–14193 (2010).
115. Mackenzie, K. J. *et al.* cGAS surveillance of micronuclei links genome instability to innate immunity. *Nature Publishing Group* 1–22 (2017). doi:10.1038/nature23449
116. Beroukhim, R. *et al.* The landscape of somatic copy-number alteration across human cancers. *Nature Publishing Group* **463,** 899–905 (2010).
117. Storchová, Z. *et al.* Genome-wide genetic analysis of polyploidy in yeast. *Nature* **443,** 541–547 (2006).
118. Li, R. *et al.* Aneuploidy correlated 100% with chemical transformation of Chinese hamster cells. *Proc Natl Acad Sci USA* **94,** 14506–14511 (1997).
119. Nicholson, J. M. *et al.* Chromosome mis-segregation and cytokinesis failure in trisomic human cells. *eLife* 1–23 (2015). doi:10.7554/eLife.05068.001
120. Passerini, V. *et al.* The presence of extra chromosomes leads to genomic instability. *Nature Communications* **7,** 1–12 (2016).
121. Santaguida, S. & Amon, A. Short- and long-term effects of chromosome mis-segregation and aneuploidy. *Nat Rev Mol Cell Biol* **16,** 473–485 (2015).
122. Hasle, H. Pattern of malignant disorders in individuals with Down's syndrome. *The Lancet Oncology* **2,** 429–436 (2001).
123. Sussan, T. E., Yang, A., Li, F., Ostrowski, M. C. & Reeves, R. H. Trisomy represses ApcMin-mediated tumours in mouse models of Down's syndrome. *Nature* **451,** 73–75 (2008).
124. Paulsson, K. & Johansson, B. Trisomy 8 as the sole chromosomal aberration in acute myeloid leukemia and myelodysplastic syndromes. *Pathologie Biologie* **55,** 37–48 (2007).
125. McGranahan, N., Burrell, R. A., Endesfelder, D., Novelli, M. R. & Swanton, C. Cancer chromosomal instability: therapeutic and diagnostic challenges. *EMBO reports* **13,** 528–538 (2012).
126. Swanton, C. & Caldas, C. Molecular classification of solid tumours: towards pathway-driven therapeutics. *Br. J. Cancer* **100,** 1517–1522 (2009).
127. Jamal-Hanjani, M. *et al.* Tracking the Evolution of Non–Small-Cell Lung Cancer. *N Engl J Med* **376,** 2109–2121 (2017).
128. Murugaesu, N. *et al.* Tracking the Genomic Evolution of Esophageal Adenocarcinoma through Neoadjuvant Chemotherapy. *Cancer Discovery* **5,** 821–831 (2015).
129. Rutledge, S. D. *et al.* Selective advantage of trisomic human cells cultured in non-standard conditions. *Sci. Rep.* **6,** 22828 (2016).
130. Birkbak, N. J. *et al.* Paradoxical Relationship between Chromosomal Instability and Survival Outcome in Cancer. *Cancer Research* **71,** 3447–3452 (2011).
131. Beach, R. R. *et al.* Aneuploidy Causes Non-genetic Individuality. *Cell* **169,** 229–242.e21

(2017).
132. McGranahan, N. & Swanton, C. Clonal Heterogeneity and Tumor Evolution: Past, Present, and the Future. *Cell* **168,** 613–628 (2017).
133. Galipeau, P. C. *et al.* 17p (p53) allelic losses, 4N (G2/tetraploid) populations, and progression to aneuploidy in Barrett's esophagus. *Proc Natl Acad Sci USA* **93,** 7081–7084 (1996).
134. Dodgson, S. E. *et al.* Chromosome-Specific and Global Effects of Aneuploidy in Saccharomyces cerevisiae. *Genetics* **202,** 1395–1409 (2016).
135. Rodrigues, N. R. *et al.* p53 mutations in colorectal cancer. *Proc Natl Acad Sci USA* **87,** 7555–7559 (1990).
136. Kvitek, D. J., Will, J. L. & Gasch, A. P. Variations in Stress Sensitivity and Genomic Expression in Diverse S. cerevisiae Isolates. *PLoS Genet* **4,** e1000223–11 (2008).
137. Pavelka, N. *et al.* Aneuploidy confers quantitative proteome changes and phenotypic variation in budding yeast. *Nature* **468,** 321–325 (2010).
138. Ahrné, E. *et al.* Evaluation and Improvement of Quantification Accuracy in Isobaric Mass Tag-Based Protein Quantification Experiments. *J. Proteome Res.* **15,** 2537–2547 (2016).
139. Donnelly, N. & Storchová, Z. Aneuploidy and proteotoxic stress in cancer. *Molecular & Cellular Oncology* **2,** e976491–11 (2014).
140. Ho, S. S. W. *et al.* The DNA Structure-Specific Endonuclease MUS81 Mediates DNA Sensor STING-Dependent Host Rejection of Prostate Cancer Cells. *Immunity* **44,** 1177–1189 (2016).
141. Weichselbaum, R. R. *et al.* An interferon-related gene signature for DNA damage resistance is a predictive marker for chemotherapy and radiation for breast cancer. *Proc. Natl. Acad. Sci. U.S.A.* **105,** 18490–18495 (2008).
142. Erdal, E., Haider, S., Rehwinkel, J., Harris, A. L. & McHugh, P. J. A prosurvival DNA damage-induced cytoplasmic interferon response is mediated by end resection factors and is limited by Trex1. *Genes Dev.* **31,** 353–369 (2017).
143. Shen, Y. J. *et al.* Genome-Derived Cytosolic DNA Mediates Type I Interferon-Dependent Rejection of B Cell Lymphoma Cells. *CellReports* **11,** 460–473 (2015).
144. Chan, K. L. & Hickson, I. D. New insights into the formation and resolution of ultra-fine anaphase bridges. *Seminars in Cell and Developmental Biology* **22,** 906–912 (2011).
145. Davoli, T. *et al.* Cumulative Haploinsufficiency and Triplosensitivity Drive Aneuploidy Patterns and Shape the Cancer Genome. *Cell* **155,** 948–962 (2013).
146. Neumann, B. *et al.* Phenotypic profiling of the human genome by time-lapse microscopy reveals cell division genes. *Nature* **464,** 721–727 (2010).
147. McIntosh, D. & Blow, J. J. Dormant Origins, the Licensing Checkpoint, and the Response to Replicative Stresses. *Cold Spring Harbor Perspectives in Biology* **4,** a012955–a012955 (2012).
148. Hills, S. A. & Diffley, J. F. X. DNA Replication and Oncogene-Induced Review Replicative Stress. *Current Biology* **24,** R435–R444 (2014).
149. Futschik, M. E. & Carlisle, B. Noise-robust soft clustering of gene expression time-course data. *J Bioinform Comput Biol* **3,** 965–988 (2005).
150. Kuznetsova, A. Y. *et al.* Chromosomal instability, tolerance of mitotic errors and multidrug resistance are promoted by tetraploidization in human cells. *Cell Cycle* **14,** 2810–2820 (2015).
151. Lee, A. J. X. *et al.* Chromosomal instability confers intrinsic multidrug resistance. *Cancer Research* **71,** 1858–1870 (2011).
152. Adams, N. D. *et al.* Discovery of GSK1070916, a Potent and Selective Inhibitor of Aurora B/C Kinase. *J. Med. Chem.* **53,** 3973–4001 (2010).

153.Tse, A. N. *et al.* CHIR-124, a Novel Potent Inhibitor of Chk1, Potentiates the Cytotoxicity of Topoisomerase I Poisons In vitro and In vivo. *Clinical Cancer Research* **13,** 591–602 (2007).
154.Karp, J. E. *et al.* Phase I and Pharmacologic Trial of Cytosine Arabinoside with the Selective Checkpoint 1 Inhibitor Sch 900776 in Refractory Acute Leukemias. *Clinical Cancer Research* **18,** 6723–6731 (2012).
155.Meijer, L. & Raymond, E. Roscovitine and Other Purines as Kinase Inhibitors. From Starfish Oocytes to Clinical Trials. *Acc. Chem. Res.* **36,** 417–425 (2003).
156.Smits, V. A. J. & Gillespie, D. A. DNA damage control: regulation and functions of checkpoint kinase 1. *FEBS J* **282,** 3681–3692 (2015).
157.Malumbres, M. Cyclin-dependent kinases. *Genome Biol.* **15,** 1–10 (2014).
158.Eyers, P. A., Erikson, E., Chen, L. G. & Maller, J. L. A Novel Mechanism for Activation of the Protein Kinase Aurora A. *Current Biology* **13,** 691–697 (2003).
159.Schubert, von, C. *et al.* Plk1 and Mps1 Cooperatively Regulate the Spindle Assembly Checkpoint in Human Cells. *CellReports* **12,** 66–78 (2015).
160.Shin, S.-B., Woo, S.-U. & Yim, H. Differential Cellular Effects of Plk1 Inhibitors Targeting the ATP-binding Domain or Polo-box Domain. *J. Cell. Physiol.* **230,** 3057–3067 (2015).
161.Sansregret, L. & Nepveu, A. Gene signatures of genomic instability as prognostic tools for breast cancer. *Future Oncology* **7,** 591–594 (2011).
162.Sheltzer, J. M. *et al.* Single-chromosome Gains Commonly Function as Tumor Suppressors. *Cancer Cell* **31,** 240–255 (2017).
163.Cimini, D. *et al.* Merotelic Kinetochore Orientation Is a Major Mechanism of Aneuploidy in Mitotic Mammalian Tissue Cells. *J. Cell Biol.* **153,** 517–528 (2001).
164.Hoffelder, D. *et al.* Resolution of anaphase bridges in cancer cells. *Chromosoma* **112,** 1–9 (2004).
165.Chan, K. L., Palmai-Pallag, T., Ying, S. & Hickson, I. D. Replication stress induces sister-chromatid bridging at fragile site loci in mitosis. *Nature Cell Biology* **11,** 753–760 (2009).
166.Sofueva, S. *et al.* Ultrafine anaphase bridges, broken DNA and illegitimate recombination induced by a replication fork barrier. *Nucleic Acids Research* **39,** 6568–6584 (2011).
167.Acilan, C., Potter, D. M. & Saunders, W. S. DNA repair pathways involved in anaphase bridge formation. *Genes Chromosom. Cancer* **46,** 522–531 (2007).
168.Laulier, C., Cheng, A. & Stark, J. M. The relative efficiency of homology-directed repair has distinct effects on proper anaphase chromosome separation. *Nucleic Acids Research* **39,** 5935–5944 (2011).
169.Wang, L. H.-C., Schwarzbraun, T., Speicher, M. R. & Nigg, E. A. Persistence of DNA threads in human anaphase cells suggests late completion of sister chromatid decatenation. *Chromosoma* **117,** 123–135 (2007).
170.Stenberg, P. *et al.* Buffering of Segmental and Chromosomal Aneuploidies in Drosophila melanogaster. *PLoS Genet* **5,** e1000465–10 (2009).
171.Perez de Castro, I. & Malumbres, M. Mitotic Stress and Chromosomal Instability in Cancer: The Case for TPX2. *Genes & Cancer* **3,** 721–730 (2013).
172.Macůrek, L. *et al.* Polo-like kinase-1 is activated by aurora A to promote checkpoint recovery. *Nature* **455,** 119–123 (2008).
173.Greaves, M. & Maley, C. C. Clonal evolution in cancer. *Nature* **481,** 306–313 (2012).
174.Alexa, A., Rahnenfuhrer, J. & Lengauer, T. Improved scoring of functional groups from gene expression data by decorrelating GO graph structure. *Bioinformatics* **22,** 1600–1607 (2006).
175.Maiato, H., Rieder, C. L. & Khodjakov, A. Kinetochore-driven formation of kinetochore fibers contributes to spindle assembly during animal mitosis. *J. Cell Biol.* **167,** 831–840 (2004).